4-15-2009

Investigation of Interactions of the Rubella Virus P150 Replicase Protein with Host Cell Proteins in Infected Cells

Suganthi Suppiah
Georgia State University

INVESTIGATION OF INTERACTIONS OF THE RUBELLA VIRUS P150 REPLICASE PROTEIN WITH HOST CELL PROTEINS IN INFECTED CELLS

by

SUGANTHI SUPPIAH

Under the Direction of Dr Teryl K Frey

ABSTRACT

Due to their simplicity, viruses require the assistance of host factors for various aspects of their replication cycle. This study investigated the interaction of one of the two non-structural replicase proteins of rubella virus (RUBV), P150, with cell proteins. RUBV forms replication complexes for replicating its RNA in association with membranes of endosomes and lysosomes; the thusly modified endosomes/lysosomes are termed cytopathic vacuoles or CPVs. In the first study, a RUBV expressing a FLAG epitope-tagged P150 was used to co-immunoprecipitate putative interacting cell proteins from an infected cell lysate fraction enriched for CPVs using differential centrifugation. However, the only interacting protein identified was the companion RUBV replicase protein P90. Thus, cell proteins do not bind with either sufficient affinity or in stoichiometric amounts to be detected by this method and may not be a component of the virus holoenzyme. In the second study, a proline-rich region within P150 with three PxxPxR

consensus SH3 domain-binding motifs was investigated for its ability to bind cell proteins. Substitution mutations (to alanine) of the two prolines were made in each of these motifs with the finding that mutations in the first two motifs led to lower viral titers and a small plaque phenotype with reversion to the wt sequence within one passage. Mutations in the third motif had a wt phenotype and did not revert. However, these mutations did not affect viral RNA synthesis, suggesting that the importance of these motifs is in a later stage of viral life cycle, e.g. virion assembly and release. To extend these findings, the proline hinge region with either the wt or mutant sequence was expressed as a GST-fusion in human cells. Pulldown experiments revealed specific binding with human p32 protein (gC1qR), which was previously shown to interact with the RUBV capsid protein. Binding of p32 with P150 was confirmed. The function of p32 in the RUBV replication cycle is unclear, but could involve virion assembly and release or induction of apoptosis.

INDEX WORDS: Rubella virus, Proteomics, SH3 domain, Protein-protein interaction, Cytopathic vacuole, Virus replication, P32

INVESTIGATION OF INTERACTIONS OF THE RUBELLA VIRUS P150 REPLICASE PROTEIN WITH HOST CELL PROTEINS IN INFECTED CELLS

by

SUGANTHI SUPPIAH

A Dissertation Submitted in Partial Fulfillment of the Requirements for the Degree of

Doctor of Philosophy

in the College of Arts and Sciences

Georgia State University

2009

INVESTIGATION OF INTERACTIONS OF THE RUBELLA VIRUS P150 REPLICASE PROTEIN WITH HOST CELL PROTEINS IN INFECTED CELLS

by

SUGANTHI SUPPIAH

Committee Chair: Dr. Teryl K. Frey

Committee: Dr. Margo A. Brinton
Dr. Phang C. Tai
Dr. Susanna F. Greer
Dr. Tom C. Hobman

Electronic Version Approved:

Office of Graduate Studies
College of Arts and Sciences
Georgia State University
May 2009

DEDICATION

My deepest gratitude goes to my parents, Paremiswary and Suppiah, to whom I would like to dedicate this dissertation to. It is their encouragement, support and dedication their whole lives towards my education that allowed me to pursue my dreams and achieve my goal in a science career. I would also like to thank my brother (Nithi), sister (Santhea) and my husband (Matthew) for their endless moral support. Work done in the lab was also made easier with the help of the members of the Frey lab (Wen Pin Tzeng, Heather, Jason and Yu Mei), who were always there to help with the work itself and also being there for me as friends. I would like to thank my mentor, Dr Frey, for giving me the opportunity to pursue my PhD in his lab, and also believing in me and my work. Special thanks also go to the members of my committee (Dr Brinton, Dr Tai, Dr Greer and Dr Hobman) who were willing to spend their time in helping me achieve this degree.

TABLE OF CONTENTS

LIST OF TABLES

LIST OF FIGURES

CHAPTER 1

Introduction

History and clinical manifestations

Rubella, the disease, was first described in the 1700s by two German physicians, de Bergan in 1752 and Orlow in 1758, the reason behind the synonym for the disease "German measles" [1]. Rubella was initially not recognized as a separate disease entity; rather it was associated with both scarlet fever and measles until 1814, when it was finally recognized as a distinct disease and named "rothëln". The physician who made this discovery was George de Maton and subsequently the disease was renamed rubella by the Englishman Henry Veale in 1866, who described the original term, "rothëln", as "foreign to the ears"

Rubella was thought to be a benign disease until an important discovery in 1941 by Norman Gregg, an Australian ophthalmologist. He found that there was a correlation between teratogenecity in newborn infants and contraction of RUBV by their mothers during pregnancy. Specifically, this hypothesis was based on case studies collected by himself and his colleagues showing a significant incidence of cataracts in babies born to mothers who were infected with the virus during their pregnancy. The clinical manifestations of congenital rubella were more extensive than the occurrence of cataracts. Some of the other manifestations that were recognized were cardiac defects, deafness, retarded development leading to low birth weight and microcephaly.

A rubella epidemic in the United States between 1964 and 1965, led to the recognition of a variety of other congenital rubella defects. Approximately 20,000 cases of congenital rubella syndrome (CRS) were recorded during those years and this vast number of CRS cases contributed to the recognition of a variety of other defects that occurred as a result of congenital

infection [2]. The occurrence of multiple defects was seen primarily when infection took place during the first eight weeks of pregnancy. The fetus is at risk for congenital defects for up to about twelve weeks of pregnancy and this includes an increased risk of death and stillbirths [3]. Some of the other complications associated with congenital rubella are purpura and thrombocytopenia, enlarged liver and spleen, bone defects and central nervous system damage.

In contrast, complications are rare in children and adults who are infected by the virus. The complications that do occur most usually involve arthritis and arthralgia, two forms of joint complications that primarily affect adult women [4]. It is believed that the virus persists in synovial cells and fluids of the joints. The live attenuated vaccine virus causes transient arthritis in ~10% of adult female vaccinees. Why and how arthritis occurs, and primarily in women, is a point of interest that has not been explored. Acute rubella can also lead to a post-infectious encephalitis, which is rarely fatal [5]. As for the disease in infected children and adults, the incubation period varies between 14 and 22 days. The earliest sign of infection is lymphadenopathy [6] and, in some cases, fever. Rash appears after this incubation period and typically lasts for three days (leading to another synonym for the disease, “three day measles”). Rash usually starts on the face and spreads to the neck and trunk. Patients are a risk to naïve individuals for about a week after the onset of rash. Serum antibodies appear at the time of rash and virus can be isolated from nasopharyngeal washing from four to seven days after appearance of the rash [6]. The route of horizontal transmission is respiratory, whereas vertical transmission to the unborn fetus is due to a systemic infection of the mother, spreading through the placenta and establishing a chronic infection in the fetus.

Thus far, immunization before pregnancy is the only preventive measure to counter the occurrence of CRS. The successful development of rubella vaccines began when permissive cell

culture systems used to isolate the virus were established in 1962 [7]. Two groups independently identified cell lines that permitted the growth and isolation of rubella virus (RUBV); one was a primary African green monkey kidney cell line developed by the Parkman group (Walter Reed Army Institute of Research) and the other was a human amnion cell line developed by the Weller and Neva group (Harvard School of Tropical Health). However, Parkman's group was the first to develop a live attenuated vaccine, HPV-77, in 1966 [8]. A derivative of vaccine (HPV-77/DE-5) was the first RUBV vaccine licensed for usage in the United States in 1969. It was later replaced with the RA27/3 vaccine strain when the vaccine program was expanded in 1979.

Rubella virus (RUBV) and teratogenicity

The exact mechanism by which congenital RUBV infection leads to CRS is unknown and has been a point of contention. We do know that infection by the virus in the developing fetus is persistent, facilitated by the undeveloped fetal immune system at the time of infection. Virus penetration in the developing fetus is widespread, affecting many organs; however, the percentage of infected cells in affected organs is low, on the order of 1 in 10,000 [9]. Necrotic lesions are detectable, but not widespread, and immunopathological damage is nonexistent. The primary observation is aborted fetuses with small organs or tissues size due to a reduced number of cells.

As for the mechanisms that cause this pathology, there are several ideas stemming from observations made from a variety of studies involving the effect of RUBV on infected culture cells. Several studies have shown that cell lines infected by RUBV grow more slowly or stop growing altogether after a few passages. This has been attributed to mitotic inhibition and chromosomal breakage leading to disruptions in cell growth [10, 11] and/or the presence of an uncharacterized protein in the supernatant of infected cells [12]. Another study showed that

infection of Vero (African green monkey kidney) cells by RUBV led to the progressive disintegration of actin microfilaments [13] a finding that would lend support to mitotic inhibition as a possible mechanism for cell cycle disruption because actin microfilaments are the basis for the development of mitotic spindle.

Aside from the physical disruption of cell division, other studies pointed to the possible role of interaction of RUBV proteins with host cell proteins as a contributing factor to the occurrence of CRS. In particular, it was shown that one of the RUBV nonstructural replicase proteins, P90, interacts with two host proteins, retinoblastoma (pRB) [14] and Citron-k Kinase (CK) [15], which function in growth and differentiation and cell cycle regulation, respectively. Either RUBV infection or over-expression of P90 [15] led to cell cycle arrest and the presence of cells in the population exhibiting tetraploidy. Since it is known that the symptoms of CRS are associated with retardation of organ development and genetic damage, it was speculated that disruption of cell cycle by RUBV P90 may be a mechanism of the disruption of organogenesis.

A series of studies done by several different labs showed that RUBV induces apoptosis in a variety of cell lines, pointing to the possible role of apoptosis in organ underdevelopment. RUBV-induced apoptosis appears to be through both p53-dependent and independent pathways [16-20]. In one cell line, overexpression of the virus capsid protein promoted induction of apoptosis while in another cell line, overexpression of one of the replicase proteins, P150 appeared to be the inducer. Thus, the phenomenon of induction of apoptosis by RUBV is complicated and likely cell line dependent. In this regard, Adamo and Zapata found that RUBV does not induce apoptosis in primary human embryo fibroblasts (undifferentiated and proliferating cells), but does so in human normal-term placenta chorionic villi explants [21]. The finding was confirmed in a follow up study that used a line of primary fetal fibroblasts in

comparison with a line of adult lung cells [22]. In this study, it was found that the adult cells were programmed for apoptosis while in the fetal cells apoptosis was supressed. This finding could potentially explain the persistence of RUBV in infected fetuses, but seems to rule out apoptosis as a mechanism for the pathogenesis of CRS.

RUBV genomic coding strategy and replication cycle

RUBV virus is the sole member of the genus RUBV within the Family *Togaviridae*. The single-strand RNA viral genome is 9,762 nt in length and encodes two open reading frames (ORF's) [23]. The genome has a 5' cap structure [24], a 5' open reading frame and a 3' poly-A tail [5], features that allow it to act as a messenger RNA when released into the host cell. The genome is thus considered to be of "positive" or "plus-sense" polarity. The genome RNA also has 5' and 3' cis acting elements (CAE) which have been shown to be important for virus replication [25, 26]. A diagram of the RUBV replication cycle is shown in Fig. 1.1. Upon entry of the virus into a host cell, which is thought to occur via receptor mediated endocytosis [27], cell-viral membrane fusion followed by release of the genome from the capsid occurs. Once released into the cytoplasm, the genome serves as an mRNA from which the ORF at its 5' end is translated to produce the viral nonstructural protein (NSP) precursor, P200, that is cleaved to generate two mature nonstructural proteins (NSPs), P150 and P90. P150 and P90 are located at the N- and C-terminal ends of P200, respectively. The protease that cleaves the P200 precursor lies at the C-terminus of P150. This nonstructural (NS) protease is a cysteine protease, with residues Cys-1151 and His-1272 as the catalytic dyad [28, 29], that catalyzes the cleavage of P200 at a single site, between the Gly-1301 and Gly-1302 residues. The protease domain is the only domain within P150 whose function has been experimentally proven. The other domains within RUBV P150 are the methyl/guanylyltransferase domain, the proline rich or hypervariable

domain, and the X-domain, which shares homology with adenosylribose phosphatases (ADP-ribose-1-phosphatase) of cells and other RNA viruses [30] (see Fig. 1.2 for non-structural protein predicted motifs). The P90 nonstrucural protein contains the virus helicase domain [31] and the RNA dependent RNA polymerase (RDRP) domain [32]. The helicase domain has been shown to have ATPase activity while mutagenesis of the catalytic GDD domain characteristic of RDRP's abrogates infectivity.

In the infected cells, the plus strand genomic RNA serves a dual purpose. First, it serves as a messenger RNA as discussed above; and second, it serves as the template for the synthesis of a minus-strand genomic complement. The minus-strand RNA is the template from which more genomic RNA is synthesized (40S) and from which a subgenomic mRNA is transcribed. The subgenomic RNA contains sequences from the 3' end of the genomic RNA, which encode the 3' proximal ORF. The RUBV structural proteins are translated from this subgenomic RNA to produce a p110 polyprotein containing the viral capsid and glycoproteins E2 and E1, in that order [24, 33]. During translation of the polyprotein, translocation into the ER occurs mediated via signal peptides present in the amino termini of E2 and E1, and cleavage ensues within the ER lumen to produce the mature structural proteins [34, 35]. Cleavage of the structural polyprotein is mediated cotranslationally by cellular signalase [35] present in the lumen of ER, so that the p110 precursor is not observed in infected cell lysates.

P200 appears to catalyze synthesis of the minus strand RNA from the genomic RNA while P150 and P90 catalyze synthesis of the genomic and subgenomic plus strand RNAs [36]. Thus, proteolytic cleavage controls RNA replication. RNA replication occurs in so-called replication complexes (RCs) contained in spherules that appear on the inner surface of endosomes and lysosomes in infected cells [37, 38] (see Fig. 1.3). These modified endosomes

and lysosomes in infected cells have been termed cytopathic vacuoles or CPVs. CPVs are approximately 0.6-2.0 μm in diameter and the membrane spherules that line the CPVs at regular intervals are 50 nm in diameter. The presence of active RCs in these spherules has been demonstrated using antibodies against double stranded RNA, an intermediate in the replication process, via immuno-electron microscopy [39, 40]. Biogenesis of CPVs leads to a redistribution of some of the organelles in the infected cell. Specifically, the RER, Golgi, and mitochondria are recruited to the area surrounding the CPV. The subgenomic RNA is translated in association with the RER and the direct translation of this RNA following its synthesis is supported by the observation that thread-like ribonucleoproteins structures extend from the base of the CPV spherules and form connections with RER [41, 42]. Virion budding occurs into this Golgi and therefore the presence of Golgi at the location of viral genome synthesis would facilitate the packaging of mature virions in a compartmentalized region of the infected cell. The reason for the recruitment of mitochondria is less clear, although they could provide a localized supply of ATP.

Virus and host protein interactions

Viruses require the assistance of host factors in general for various aspects of their replication cycles. This is because the simplicity of the viral genome does not allow for the coding of large numbers of complex proteins and as obligate intracellular parasites, viruses take advantage of what the cell has to offer. For example, RNA viruses that replicate in the cytoplasm and use viral encoded RNA dependent RNA polymerase (RdRp), have to modify the host cytoplasmic environment as normal eukaryotic RdRp functions occurs in the nucleus. As a result, host factors such as those involved in translation may be used as part of the viral replicative machinery. Examples of such interactions will be discussed later.

There are different ways in which host cellular factors play a role in virus RNA replication. Some of these interactions will be described in more detail later. Host cellular factors have been shown to bind to both the viral genome as well as to the enzymatic replication complex to promote template recognition, template switching from translation to replication as well as promoting proper assembly of the replication complex. Intracellular membranes and the cytoskeleton also play important roles in helping to target virus proteins to the appropriate sites of replication and RNA replication of all plus-strand RNA viruses occurs in association with membranes [43-45]. Virus components could also interact with host cellular factors involved in signaling pathway. Some of these signaling pathways affect the cell cycle as well as the innate immune response of the host cell. Since our work is on RUBV, which is a positive sense RNA virus, some examples of host cellular factors interacting with other positive strand RNA viruses will be further discussed as some of these interactions might have functional parallels in RUBV infected cells.

The classic example of virus-host interaction is that of host proteins combining with the RDRP subunit of bacteriophage Qβ to comprise the complete enzyme complex [46]. Studies found that three host proteins EF-Tu, EF-Ts and ribosomal protein S1 were a part of the bacteriophage holoenzyme. These host components are part of the translation machinery of the cell. These host cellular factors function in the holoenzyme by conferring specificity to template binding. Studies involving bacteriophage Qβ replicase protein have shown that subunits S1, EF-Tu and EF-Ts. enable template recognition of positive and negative strand RNA during the process of replication [47]. Additionally, a fourth host protein, HF1 (ribosome-associated protein) binds to the 3' end of the genome to direct the synthesis of negative strand RNA [48].

This is a good example of how a virus uses host cellular factors to compensate for the lack of virus factors important for its replication.

Subsequently, appropriation of host cellular factors involved in host cell translation has been found to be quite a common theme among different viruses. For example, the binding of eIF-3 (translation elongation factor 3) to both the RDRP and the 5' and 3' untranslated regions (UTRs) of the genomes of positive strand RNA viruses has been found to occur [49,50]. Studies done with brome mosaic virus (BMV) RDRP purified from infected barley cells [49] reported the copurification and enrichment of eIF-3. Addition of eIF-3 to BMV RdRp led to a 3-fold increase of minus strand RNA synthesis *in vitro*. eIF-3 has also been shown to associate with the RDRP complex of poliovirus (3AB-3CD^{pro}) [50]. This interaction was hypothesized to be important for the binding of the replication complex to the 5' cloverleaf of the genome in the replicative intermediate to facilitate the synthesis of genomic RNA from the minus strand template. In a study of host proteins binding to West Nile virus (WNV) RNA, it was found that the host translation factor eEF1α bound to the 3' stem loop of the genomic RNA [51]. Mutational analysis of this binding site caused a decrease in production of minus strand RNA, strongly pointing to the role of eEF1α in facilitating minus strand synthesis [52]. In another study involving the non-structural protein NS5A of bovine viral diarrhea virus (BVDV) that has a role in BVDV replication, interaction with translation elongation factor eEF1α was demonstrated [53]. This interaction was shown to be specific for BVDV NS5A protein and occurred consistently among the different BVDV isolates. This finding was relevant because the NS5A protein of BVDV is the most variable among the many BVDV isolates [54] and the conserved interaction of eEF1α with NS5A was highly indicative of the role of eEF1α in BVDV replication.

Techniques employed in investigating virus and host factor interactions

The preceeding discussion of some studies on the identification of host proteins involved in virus RNA replication reveals that three main techniques have been employed: isolation of pairing partners of expressed virus replicase proteins or domains of virus replicase proteins, use of viral RNA sequences as bait for binding of cell proteins in cell lysates, and isolation of replication complexes and replicase proteins from infected cells to identify cell proteins which co-purify. With the expansion of the sequence database, bioinformatics tools have been developed to predict specific interactions. For example, the interaction of pRB and P90, described above [14], was originally predicted by bioinformatics algorithms using consensus sequences. Finally, gene deletion libraries in yeast and genome wide siRNA knockdown techniques have been employed to identify cell proteins essential for virus replication. Representative examples will be used to illustrate the use of each of these techniques, concentrating on studies that utilized RUBV or an alphavirus, the nearest relatives of RUBV.

1) Detection of protein pairing partners through expression of proteins and/or protein domains. The yeast two-hybrid system has been used extensively for the identification of protein pairing partners. In this system, the protein of interest is expressed in yeast as a bait to identify pairing partners. The interaction of the bait protein with a binding partner (prey) expressed from a library leads to the transcription of a reporter gene downstream of an activating sequence resulting in colony selection and identification. In one such study, the interaction of RUBV capsid with the mitochondrial p32 protein was discovered [55]. RUBV capsid was used as bait to screen a CV1 (monkey cell) cDNA library and a strong interaction of capsid protein with p32 was found. The interaction of these two proteins were confirmed through co-immunoprecipitation (both in-vitro and in-vivo) and immunofluorescence assays (IFA). A

follow up of this work confirmed that p32 bound to RUBV capsid through two clusters of arginine present at the capsid's N-terminus. Studies also showed that over-expression of capsid led to the clustering of mitochondria in the perinuclear region of cells. Mutations introduced in the p32 binding sites on capsid led to decreased mitochondrial clustering, implying that the p32-capsid interaction is important for this phenomenon to occur. Virus induced mitochondrial clustering is a hallmark of RUBV infection [1] and this study suggested that p32 was directing the clustering of mitochondria to sites of virus production in association with capsid. The researchers also found that mutation of the p32 binding site on capsid led to a decrease in subgenomic RNA production, lower viral titers and altered plaque morphology. The P90-citron K kinase interaction discussed above was also discovered by the yeast two hybrid system using P90 as bait [15]**.**

In another study done to identify binding partners of RUBV capsid, the capsid protein was over-expressed as a GST fusion protein from a mammalian expression vector (pEBG expression vectors) [56]. The GST-capsid fusion protein expressed in transfected COS cells were isolated with its binding partners on gluthathione-agarose beads and high abundance cell proteins were identified by gel electrophoresis and mass-spectrometry analysis. Using this method, researchers identified poly (A)-binding protein (PABP) as a binding partner of capsid protein. This interaction once again was verified via both in-vitro and in-vivo methods. PABP is a host protein that plays an important role in the regulation of translation [57]. The researchers postulated that the interaction of capsid protein and PABP may be important in the regulation of host translation by RUBV. By sequestering PABP, researchers hypothesized that translation would be inhibited and that this would favor the transition of viral genome from viral translation to packaging.

2). Identification of cell proteins interacting with viral RNA sequences. This technique is based on the hypothesis that binding of host proteins to the *cis*-acting elements in viral RNA species facilitates specific binding of the viral RDRP to its template. Host proteins act as a bridge to recruit viral RNA to the RdRp and possibly are part of the enzymatically active ribonucleoprotein complex. In addition, host proteins that bind to different cis-acting elements (i.e at different ends of the same strand or on different strands) can regulate template switching. Using radiolabelled RNAs corresponding to *cis*-acting elements as probes, the binding of host proteins to 5' and 3' cis-acting elements of genomic and anti-genomic RNA have been detected and confirmed using gel mobility shift and UV crosslinking assays. Subsequently, using sequential chromatography or RNA affinity columns followed by mass spectrometry, host proteins that interact with specific RNA sequences can be identified.

These techniques were used in the studies mentioned above that demonstrated that eEF-1α binds to the 3' *cis*-acting element of the West Nile virus (WNV) genomic RNA [51], similar techniques led to the identification of TIA-1 and TIAR binding to the 3' stem loop of the WNV minus strand RNA [58, 59]. TIA-1 and TIAR are multifunctional RNA binding proteins that shuttle between the nucleus and cytoplasm and have roles in translation and RNA splicing. The effect of these host proteins on WNV replication was evaluated in TIAR and TIA-1 knockout murine embryo fibroblast cell lines. Results showed that WNV replication was impaired in the TIAR knockout cell line but not in the TIA-1 knockout cell line. Later studies showed that mutations of TIAR/TIA-1 binding sites made in the 3' stem loop of the WNV minus strand in an infectious clone negatively affected plaque size, genomic RNA levels and virus production [60]. It was concluded that the binding of TIAR/TIA-1 to the 3' stem loop of the WNV minus strand played an important role in the synthesis of genomic RNA and it was hypothesized that this

binding promoted RDRP specific recognition of the 3' end of the minus strand template and also stabilization of the replication complex. The interaction of the 3' stem loop of WNV minus strand RNA with TIAR/TIA-1, which are components of stress granules [61], was found to confer resistance to the formation of stress granules in infected cells. This study suggested that the interaction of the WNV negative strand 3' stem loop with TIAR facilitated virus genome synthesis and inhibited the formation of stress granules, causing host translation machinery not to be shut down.

In RUBV, several host proteins have been found to associate with stem-loops at the 5' and 3' ends of the genome strand. Calreticulin, a calcium binding protein was found to associate with a stem loop at the 3' end of the genome RNA [62]. Only the phosphorylated form of calreticulin bound to the viral RNA. However, a subsequent mutagenesis study failed to confirm that calreticulin binding to this stem-loop was important for replication [25]. In another study, the La autoantigen was found to interact with the 5' stem loop of RUBV genome RNA [63]. La antigen is an RNA binding protein that is important for initiation and termination of RNA polymerase III [64] and is involved in autoimmune disease as a target of the immune system. The specificity of the RNA-protein interaction between the 5' stem loop (+) of RUBV and the La autoantigen in samples that were positive for endogenous La antigen or recombinant La antigen together with the observed inhibition of this complex formation in serum containing anti-La antibody, demonstrated the functional relevance of this binding. Also, patients who were infected with RUBV had an increase in anti-La antibody. This increase is thought to be a contributing factor to the arthritis and arthralgia seen in adult female patients.

3). Isolation of host proteins binding to viral proteins in virus infected cells

Isolation of viral replicase proteins from infected cells by immunoprecipitation and identification of co-immunoprecipitating host proteins that interact with virus proteins of interest is an alternate technique. This approach has been used in three recent studies on interaction of host proteins with the replicase proteins of Sindbis virus (SINV), a member of the alphavirus genus. These studies used virus that expressed a GFP-tagged nonstructural replicase protein nsP3; the presence of this tag did not interfere with virus replication. In one study, isolation was done following a time course from 2 to 10 hours post-infection and interacting host proteins over the time course were identified [65]. The control used for this experiment was free GFP that was expressed from a subgenomic RNA. Using this method, cellular redistribution that would occur as a result of virus infection was taken into account. Immunoaffinity purification from cell lysates was done with magnetic beads coated with polyclonal anti-GFP antibody and co-purifying cell proteins were resolved by one dimensional SDS-PAGE and then identified by mass-spectrometry analysis. Once the identities of these proteins were determined, their interaction with nsP3 was confirmed using additional methods such as reciprocal co-immunoprecipitation and co-localization. Candidate interacting proteins were identified that interacted with nsP3 throughout the time course of infection (G3BP proteins) and as well as only during the late infection period (14-3-3 proteins). G3BP proteins have been shown to be involved in a variety of cellular processes including RNA metabolism, translation and assembly of stress granules. They also have a role in transport of RNA in and out of the nucleus [66-68]. Since SINV shuts down endogenous cell translation and redirects the translation machinery to the production of virus proteins, it was postulated that G3BP proteins may a play a role in the regulation of SINV translation possibly including sequestering host RNA in order to facilitate

virus translation. The 14-3-3- proteins consist of a group of proteins that are known phosphoserine-binding adapter proteins involved in cellular signaling. Since this interaction occurs later during virus infection, it was suggested that a phosphorylation event involved in host translation shutoff, shutoff of minus strand synthesis or other signaling cascades could be a functional result of this interaction.

Two additional studies were done to investigate host proteins that interacted with the nonstructural replicase proteins of Sindbis virus. In one of these studies, nsP3 protein tagged with GFP expressed from a Sindbis replicon (without structural proteins) was employed to study the localization of nsP3 and its association with host cell proteins [69]. In this study, the interaction of nsP3 with host proteins was studied in both mosquito cells (mosquitoes are vectors for this virus) and vertebrate cells (hosts that are acutely infected). Rather than immunoprecipitation as in the previously described study, control and nsP3-GFP expressing cells were homogenized and sedimented on sucrose gradients to fractionate cells components. Fractions containing different membranes were clearly separated and nsP3 was found in both nuclear and plasma membranes as well as in endosome-like vesicles suggesting multiple roles for nsP3: one function that is associated with replication complexes found in conjunction with the other non-structural proteins in the plasma as well as endosomal membranes, and another function that is possibly related to regulatory processes associated with its presence near the nuclei. Using this fractionation method, the researchers were also able to identify interactions between the G3BP1 and G3PB2 proteins, as well of other cell proteins (including two other stress reponse proteins, YBX1 and HSC70), with nsP3 by co-immunoprecipitation in both the membrane and nuclear fractions. The researchers were also able to identify the presence of dsRNA in the membrane associated fraction using Western blot analysis, indicating that

replication occurred in association with membranous structures as previously reported. In mosquito cells, Rasputin, an insect homolog of G3BP protein, interacted with nsP3 associated with a membrane fraction (endosome, microsome and plasma membrane). This finding indicated the conserved nature of this interaction in both vertebrate and invertebrate cells.

In the third study on the interaction of host cell proteins with the SINV replication complex, differential expression of proteins in cytoplasmic membrane fractions of infected and uninfected cells was compared [70]. Two-dimensional difference in-gel electrophoretic (2D-DIGE) analysis was performed using Cy3 and Cy5 labelled proteins from membrane fractions of infected and uninfected cells. This study led to the identification of the heterogenous nuclear ribonuclear protein K (hnRNP K) as a cell protein enriched in cyoplasmic membrane fractions from infected cells. It was subsequently shown that hnRNP K co-immunoprecipitated with the SINV nonstructural proteins and the subgenomic (but not the genomic) RNA and it was hypothesized that it was part of the RC and played a role as in regulating the ratio of genomic and subgenomic RNA synthesis and subsequent subgenomic RNA translation. While this method was a good method for identifying host proteins that were enriched in certain cellular fractions during infection, it was not a good way to identify interacting proteins that did not change in abundance at a specific location as a result of infection.

4). Genomic scans. A cell genome wide mutation approach to identify host genes involved in virus replication was done in yeast cells which were found to accommodate the replication of brome mosaic virus (BMV), a plant virus. In this study, using a single-gene deletion mutant library, the effects of many host proteins on BMV replication were rapidly analyzed [71]. It was found that the absence of approximately 100 genes either inhibited or stimulated BMV RNA replication and gene expression by 3 to more than 25 fold. One observation worth noting was

that deletion of the gene encoding an acyl-CoA binding factor involved in membrane sphingolipid biosynthesis inhibited BMV replication by 25 fold. Such an observation gives validation to the data because of the importance of cellular membranes as virus replication complex formation sites. While fibroblast lines from mouse knock out lines can be used for the same end, recently siRNA knockdown libraries have been used to identify genes important in virus replication in commonly used cell culture lines. For example, an siRNA screen was used to identify 305 genes in human cells that affect WNV replication [72]. Although this strategy is powerful, it identifies genes that function in any aspect of the virus life cycle, including some with epistatic rather than direct effects.

Goals of the dissertation

The focus of my dissertation research was to continue the research on virus-host interactions in RUBV-infected cells, specifically interactions that involve binding of host factors to the RUBV P150 non-structural replicase protein, a protein that had not previously been investigated in this regard.

Specific Aim 1. To identify host cell proteins interacting with P150 in RUBV-infected cells by co-immunprecipitation.

Recently, a RUBV infectious clone expressing a P150 tagged with epitopes such as FLAG, HA, or c-myc became available in our lab allowing us to use commercially available reagents to immunoprecipitate tagged P150 from infected cells and to co-immunoprecipitate interacting cellular proteins. Therefore, the initial goal of this Specific Aim was to identify co-immunoprecipitating cell proteins with the subsequent goal of characterizing their role in RUBV replication.

Specific Aim 2. To determine if the binding of cell proteins with the P150 proline rich region plays a role in virus replication.

A proline rich region was previously identified in the P150 non-structural replicase protein that extends from residues 716 to 782 (out of 1301 amino acids). Proline rich domains in cell proteins often function as adaptor regions that mediate protein-protein association and are often involved in interactions between intermediates in cellular signaling cascades. Commonly, these interactions are via SH3 domains and the P150 proline rich region contains three putative Class II SH3 binding motifs with the consensus sequence PxxPxR. To test the hypothesis that protein-protein interactions mediated by these motifs were important during virus infection, mutations to disrupt putative binding were introducted into a RUBV infectious cDNA clone to see if a change in phenotype resulted and to characterize that phenotype.

Specific Aim 3. To investigate the cell proteins bound by the P150 proline rich region.

The P150 proline rich region was expressed as a GST fusion protein and used to specifically isolate interacting cell proteins in transfected 293-T human kidney cells. Mutations predicted to interrupt the interactions mediated by the PxxPxR motifs were introduced into the fusion protein to ascertain the specificity of the interaction. Proteins which specifically bound to wt P150 and not the mutant were to be identified by mass spec, their interaction with P150 confirmed and their importance in virus replication to be analyzed.

References

1. Lee, J.Y. and D.S. Bowden, *Rubella virus replication and links to teratogenicity.* Clin Microbiol Rev, 2000. **13**(4): p. 571-87.
2. Cooper, L.Z., et al., *Neonatal thrombocytopenic purpura and other manifestations of rubella contracted in utero.* Am J Dis Child, 1965. **110**(4): p. 416-27.
3. Dudgeon, J.A., *Maternal rubella and its effect on the foetus.* Arch Dis Child, 1967. **42**(222): p. 110-25.
4. Tingle, A.J., et al., *Rubella-associated arthritis. I. Comparative study of joint manifestations associated with natural rubella infection and RA 27/3 rubella immunisation.* Ann Rheum Dis, 1986. **45**(2): p. 110-4.
5. Frey, T.K., *Molecular biology of rubella virus.* Adv Virus Res, 1994. **44**: p. 69-160.
6. Green, R.H., et al., *Studies on the Experimental Transmission, Clinical Course, Epidemiology and Prevention of Rubella.* Trans Assoc Am Physicians, 1964. **77**: p. 118-25.
7. Parkman, P.D., E.L. Buescher, and M.S. Artenstein, *Recovery of rubella virus from army recruits.* Proc Soc Exp Biol Med, 1962. **111**: p. 225-30.
8. Parkman, P.D., et al., *Attenuated rubella virus. I. Development and laboratory characterization.* N Engl J Med, 1966. **275**(11): p. 569-74.
9. Rawls, W.E., *Viral persistence in congenital rubella.* Prog Med Virol, 1974. **18**(0): p. 273-88.
10. Boue, J.G. and A. Boue, *Effects of rubella virus infection on the division of human cells.* Am J Dis Child, 1969. **118**(1): p. 45-8.
11. Hoskins, J.M. and S.A. Plotkin, *Behaviour of rubella virus in human diploid cell strains. II. Studies of infected cells.* Arch Gesamte Virusforsch, 1967. **21**(3): p. 296-308.
12. Plotkin, S.A. and A. Vaheri, *Human fibroblasts infected with rubella virus produce a growth inhibitor.* Science, 1967. **156**(3775): p. 659-61.
13. Bowden, D.S., et al., *Distribution by immunofluorescence of viral products and actin-containing cytoskeletal filaments in rubella virus-infected cells.* Arch Virol, 1987. **92**(3-4): p. 211-9.
14. Forng, R.Y. and C.D. Atreya, *Mutations in the retinoblastoma protein-binding LXCXE motif of rubella virus putative replicase affect virus replication.* J Gen Virol, 1999. **80 (Pt 2)**: p. 327-32.
15. Atreya, C.D., S. Kulkarni, and K.V. Mohan, *Rubella virus P90 associates with the cytokinesis regulatory protein Citron-K kinase and the viral infection and constitutive expression of P90 protein both induce cell cycle arrest following S phase in cell culture.* Arch Virol, 2004. **149**(4): p. 779-89.
16. Pugachev, K.V. and T.K. Frey, *Rubella virus induces apoptosis in culture cells.* Virology, 1998. **250**(2): p. 359-70.
17. Megyeri, K., et al., *Involvement of a p53-dependent pathway in rubella virus-induced apoptosis.* Virology, 1999. **259**(1): p. 74-84.
18. Duncan, R., et al., *Rubella virus capsid protein induces apoptosis in transfected RK13 cells.* Virology, 2000. **275**(1): p. 20-9.
19. Duncan, R., et al., *Rubella virus-induced apoptosis varies among cell lines and is modulated by Bcl-XL and caspase inhibitors.* Virology, 1999. **255**(1): p. 117-28.

20. Hofmann, J., M.W. Pletz, and U.G. Liebert, *Rubella virus-induced cytopathic effect in vitro is caused by apoptosis.* J Gen Virol, 1999. **80 (Pt 7)**: p. 1657-64.
21. Adamo, P., et al., *Rubella virus does not induce apoptosis in primary human embryo fibroblast cultures: a possible way of viral persistence in congenital infection.* Viral Immunol, 2004. **17**(1): p. 87-100.
22. Adamo, M.P., M. Zapata, and T.K. Frey, *Analysis of gene expression in fetal and adult cells infected with rubella virus.* Virology, 2008. **370**(1): p. 1-11.
23. Dominguez, G., C.Y. Wang, and T.K. Frey, *Sequence of the genome RNA of rubella virus: evidence for genetic rearrangement during togavirus evolution.* Virology, 1990. **177**(1): p. 225-38.
24. Oker-Blom, C., *The gene order for rubella virus structural proteins is NH2-C-E2-E1-COOH.* J Virol, 1984. **51**(2): p. 354-8.
25. Chen, M.H. and T.K. Frey, *Mutagenic analysis of the 3' cis-acting elements of the rubella virus genome.* J Virol, 1999. **73**(4): p. 3386-403.
26. Pogue, G.P., et al., *5' sequences of rubella virus RNA stimulate translation of chimeric RNAs and specifically interact with two host-encoded proteins.* J Virol, 1993. **67**(12): p. 7106-17.
27. Petruzziello, R., et al., *Pathway of rubella virus infectious entry into Vero cells.* J Gen Virol, 1996. **77 (Pt 2)**: p. 303-8.
28. Marr, L.D., C.Y. Wang, and T.K. Frey, *Expression of the rubella virus nonstructural protein ORF and demonstration of proteolytic processing.* Virology, 1994. **198**(2): p. 586-92.
29. Chen, J.P., et al., *Characterization of the rubella virus nonstructural protease domain and its cleavage site.* J Virol, 1996. **70**(7): p. 4707-13.
30. Eriksson, K.K., et al., *Mouse hepatitis virus liver pathology is dependent on ADP-ribose-1''-phosphatase, a viral function conserved in the alpha-like supergroup.* J Virol, 2008. **82**(24): p. 12325-34.
31. Gros, C. and G. Wengler, *Identification of an RNA-stimulated NTPase in the predicted helicase sequence of the Rubella virus nonstructural polyprotein.* Virology, 1996. **217**(1): p. 367-72.
32. Wang, X. and S. Gillam, *Mutations in the GDD motif of rubella virus putative RNA-dependent RNA polymerase affect virus replication.* Virology, 2001. **285**(2): p. 322-31.
33. Oker-Blom, C., et al., *Rubella virus contains one capsid protein and three envelope glycoproteins, E1, E2a, and E2b.* J Virol, 1983. **46**(3): p. 964-73.
34. Frey, T.K. and L.D. Marr, *Sequence of the region coding for virion proteins C and E2 and the carboxy terminus of the nonstructural proteins of rubella virus: comparison with alphaviruses.* Gene, 1988. **62**(1): p. 85-99.
35. Clarke, D.M., et al., *Expression of rubella virus cDNA coding for the structural proteins.* Gene, 1988. **65**(1): p. 23-30.
36. Liang, Y. and S. Gillam, *Mutational analysis of the rubella virus nonstructural polyprotein and its cleavage products in virus replication and RNA synthesis.* J Virol, 2000. **74**(11): p. 5133-41.
37. Peranen, J. and L. Kaariainen, *Biogenesis of type I cytopathic vacuoles in Semliki Forest virus-infected BHK cells.* J Virol, 1991. **65**(3): p. 1623-7.

38. Froshauer, S., J. Kartenbeck, and A. Helenius, *Alphavirus RNA replicase is located on the cytoplasmic surface of endosomes and lysosomes.* J Cell Biol, 1988. **107**(6 Pt 1): p. 2075-86.
39. Magliano, D., et al., *Rubella virus replication complexes are virus-modified lysosomes.* Virology, 1998. **240**(1): p. 57-63.
40. Lee, J.Y., J.A. Marshall, and D.S. Bowden, *Characterization of rubella virus replication complexes using antibodies to double-stranded RNA.* Virology, 1994. **200**(1): p. 307-12.
41. Fontana, J., et al., *Novel replication complex architecture in rubella replicon-transfected cells.* Cell Microbiol, 2007. **9**(4): p. 875-90.
42. Risco, C., J.L. Carrascosa, and T.K. Frey, *Structural maturation of rubella virus in the Golgi complex.* Virology, 2003. **312**(2): p. 261-9.
43. Netherton, C., et al., *A guide to viral inclusions, membrane rearrangements, factories, and viroplasm produced during virus replication.* Adv Virus Res, 2007. **70**: p. 101-82.
44. Novoa, R.R., et al., *Virus factories: associations of cell organelles for viral replication and morphogenesis.* Biol Cell, 2005. **97**(2): p. 147-72.
45. Denison, M.R., *Seeking membranes: positive-strand RNA virus replication complexes.* PLoS Biol, 2008. **6**(10): p. e270.
46. Blumenthal, T. and G.G. Carmichael, *RNA replication: function and structure of Qbeta-replicase.* Annu Rev Biochem, 1979. **48**: p. 525-48.
47. Brown, D. and L. Gold, *RNA replication by Q beta replicase: a working model.* Proc Natl Acad Sci U S A, 1996. **93**(21): p. 11558-62.
48. Barrera, I., et al., *Different mechanisms of recognition of bacteriophage Q beta plus and minus strand RNAs by Q beta replicase.* J Mol Biol, 1993. **232**(2): p. 512-21.
49. Quadt, R., et al., *Characterization of a host protein associated with brome mosaic virus RNA-dependent RNA polymerase.* Proc Natl Acad Sci U S A, 1993. **90**(4): p. 1498-502.
50. Harris, K.S., et al., *Interaction of poliovirus polypeptide 3CDpro with the 5' and 3' termini of the poliovirus genome. Identification of viral and cellular cofactors needed for efficient binding.* J Biol Chem, 1994. **269**(43): p. 27004-14.
51. Blackwell, J.L. and M.A. Brinton, *Translation elongation factor-1 alpha interacts with the 3' stem-loop region of West Nile virus genomic RNA.* J Virol, 1997. **71**(9): p. 6433-44.
52. Davis, W.G., et al., *Interaction between the cellular protein eEF1A and the 3'-terminal stem-loop of West Nile virus genomic RNA facilitates viral minus-strand RNA synthesis.* J Virol, 2007. **81**(18): p. 10172-87.
53. Johnson, C.M., et al., *The NS5A protein of bovine viral diarrhoea virus interacts with the alpha subunit of translation elongation factor-1.* J Gen Virol, 2001. **82**(Pt 12): p. 2935-43.
54. Deng, R. and K.V. Brock, *Molecular cloning and nucleotide sequence of a pestivirus genome, noncytopathic bovine viral diarrhea virus strain SD-1.* Virology, 1992. **191**(2): p. 867-9.
55. Beatch, M.D. and T.C. Hobman, *Rubella virus capsid associates with host cell protein p32 and localizes to mitochondria.* J Virol, 2000. **74**(12): p. 5569-76.
56. Ilkow, C.S., et al., *Rubella virus capsid protein interacts with poly(a)-binding protein and inhibits translation.* J Virol, 2008. **82**(9): p. 4284-94.
57. Imataka, H., A. Gradi, and N. Sonenberg, *A newly identified N-terminal amino acid sequence of human eIF4G binds poly(A)-binding protein and functions in poly(A)-dependent translation.* EMBO J, 1998. **17**(24): p. 7480-9.

58. Shi, P.Y., W. Li, and M.A. Brinton, *Cell proteins bind specifically to West Nile virus minus-strand 3' stem-loop RNA.* J Virol, 1996. **70**(9): p. 6278-87.
59. Li, W., et al., *Cell proteins TIA-1 and TIAR interact with the 3' stem-loop of the West Nile virus complementary minus-strand RNA and facilitate virus replication.* J Virol, 2002. **76**(23): p. 11989-2000.
60. Emara, M.M., et al., *Mutation of mapped TIA-1/TIAR binding sites in the 3' terminal stem-loop of West Nile virus minus-strand RNA in an infectious clone negatively affects genomic RNA amplification.* J Virol, 2008. **82**(21): p. 10657-70.
61. Kedersha, N.L., et al., *RNA-binding proteins TIA-1 and TIAR link the phosphorylation of eIF-2 alpha to the assembly of mammalian stress granules.* J Cell Biol, 1999. **147**(7): p. 1431-42.
62. Singh, N.K., C.D. Atreya, and H.L. Nakhasi, *Identification of calreticulin as a rubella virus RNA binding protein.* Proc Natl Acad Sci U S A, 1994. **91**(26): p. 12770-4.
63. Pogue, G.P., et al., *Autoantigens interact with cis-acting elements of rubella virus RNA.* J Virol, 1996. **70**(9): p. 6269-77.
64. Craig, A.W., et al., *The La autoantigen contains a dimerization domain that is essential for enhancing translation.* Mol Cell Biol, 1997. **17**(1): p. 163-9.
65. Cristea, I.M., et al., *Tracking and elucidating alphavirus-host protein interactions.* J Biol Chem, 2006. **281**(40): p. 30269-78.
66. Irvine, K., et al., *Rasputin, more promiscuous than ever: a review of G3BP.* Int J Dev Biol, 2004. **48**(10): p. 1065-77.
67. Prigent, M., et al., *IkappaBalpha and IkappaBalpha /NF-kappa B complexes are retained in the cytoplasm through interaction with a novel partner, RasGAP SH3-binding protein 2.* J Biol Chem, 2000. **275**(46): p. 36441-9.
68. Tourriere, H., et al., *The RasGAP-associated endoribonuclease G3BP assembles stress granules.* J Cell Biol, 2003. **160**(6): p. 823-31.
69. Gorchakov, R., et al., *Different types of nsP3-containing protein complexes in Sindbis virus-infected cells.* J Virol, 2008. **82**(20): p. 10088-101.
70. Burnham, A.J., L. Gong, and R.W. Hardy, *Heterogeneous nuclear ribonuclear protein K interacts with Sindbis virus nonstructural proteins and viral subgenomic mRNA.* Virology, 2007. **367**(1): p. 212-21.
71. Kushner, D.B., et al., *Systematic, genome-wide identification of host genes affecting replication of a positive-strand RNA virus.* Proc Natl Acad Sci U S A, 2003. **100**(26): p. 15764-9.
72. Krishnan, M.N., et al., *RNA interference screen for human genes associated with West Nile virus infection.* Nature, 2008. **455**(7210): p. 242-5.

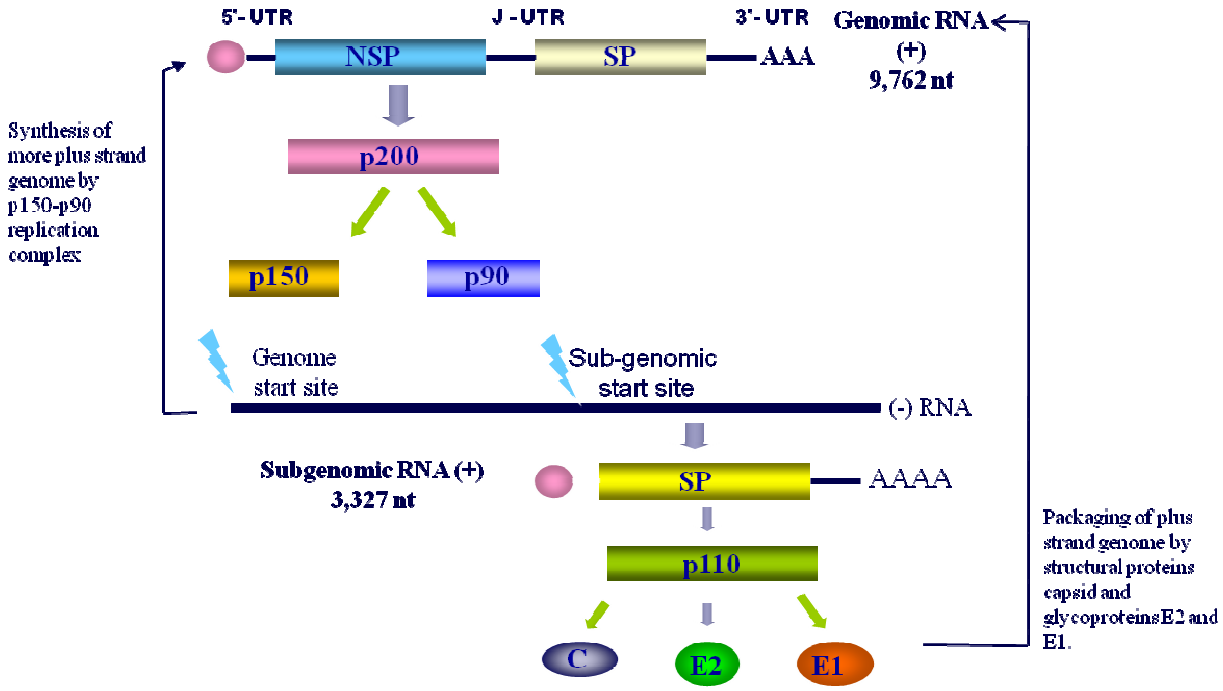

Figure 1.1. Schematic of RUBV virus life cycle.
RUBV virus enters its host via receptor mediated endocytosis. Upon entry into the host cell, diassembly of capsid occurs, releasing the plus strand RNA genome into the cytoplasm. The viral plus strand genome acts as an mRNA, which then is translated to produce the virus non-structural polyprotein (NSP). The NSP is processed by the viral protease to produce separate proteins referred to as P150 and P90 (RNA dependent RNA polymerase). Together, the proteins P150 and P90 form a replication complex that goes on to synthesize the minus strand RNA intermediate and more plus strand RNA. Following transcription at the sub-genomic promoter of the minus strand RNA, structural proteins (SP) are produced. SP is then processed by cellular proteases to form the mature structural proteins, capsid protein, and glycoproteins E2 and E1. These proteins function in packaging the plus strand genome to produce mature RUBV virus particles.

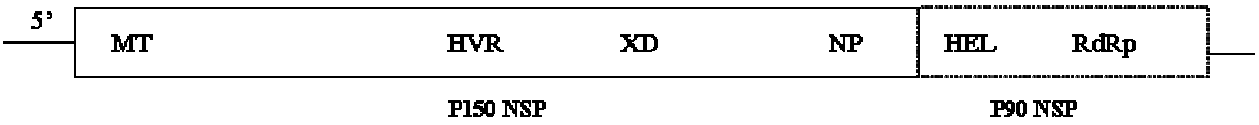

Figure 1.2. Motifs within RUBV P150 and P90 nonstructural proteins.
Various domains present within the P150 nonstructural protein (1301 aa) are: MT (methyltransferase), aa 63-132; HVR (hypervariable region), aa 693-799; XD (X domain/ADP phophatase like motif), aa 817-985 and NP (nonstructural protease), aa 1000-1299. Domains present within the P90 nonstructural protein (aa 1302-2116) are: HEL (helicase), aa 1334-1585; RdRp (RNA dependent RNA polymerase), aa 1595-2115.

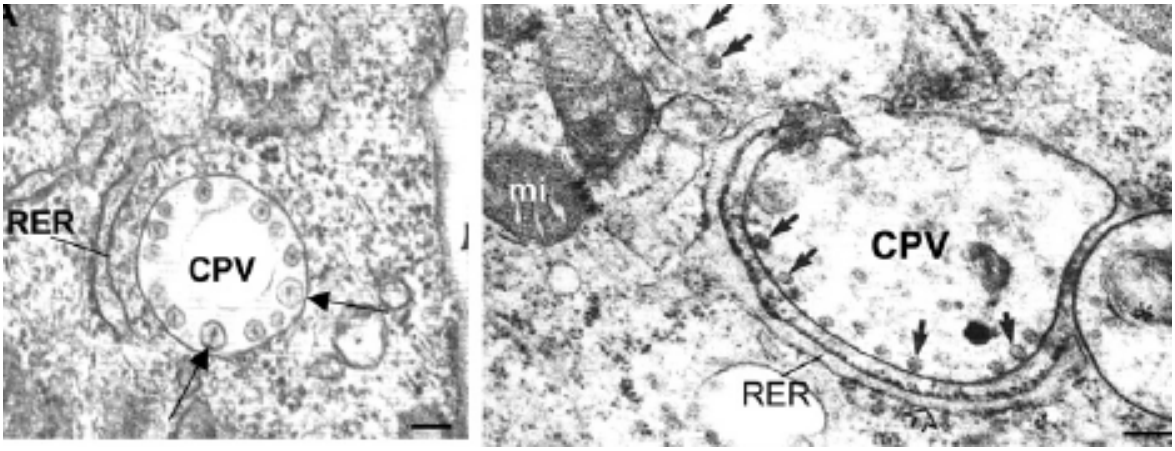

Figure 1.3. Presence of cytopathic vacuoles (CPV) in RUBV infected cells.
Cells infected by RUBV appear to have modified endosomes and lysosomes termed cytopathic vacuoles or CPV. CPVs are 0.6 to 2 μm in size and form 50 nm spherules that line the vacuole membranes at regular intervals. The above images are from a review published by Risco et. al. [44]. The arrows indicate the presence of spherules within CPVs. The CPVs are often surrounded by cisternae of rough endoplasmic reticulum (RER) and mitochondria (mi).

CHAPTER 2

Specific aim 1: Investigating the interaction of host cellular factors with RUBV non-structural replicase protein P150

Introduction

Positive strand RNA viruses have long been known to form RNA replication complexes (RCs) in association with intracellular membranes in the host cell, a subject that has been extensively reviewed [1, 2]. These so-called "virus factories" are formed in association with various intracellular membranes. The viral factories for different virus families are associated with different intracellular membranes. Viruses from the Family *Flaviviridae*, such as hepatitis C virus (HCV) and yellow fever virus (YFV), form RCs that are contiguous with or derived from the rough endoplasic reticulum (RER) and Golgi apparatus [2, 4], while viruses from the Family *Togaviridae*, such as RUBV and Sindbis virus (SINV), form RCs within so-called cytopathic vacuoles (CPVs) that are modifications of late endosomes and lysosomes [2, 5-7]. The association of the RC with an intracellular membranous structure has been suggested to be important for the following reasons. Firstly, intracellular membranes provide a surface for the anchoring of RC. The anchoring of RCs to membranes is usually achieved by the attachment of the RC to the membrane through hydrophobic domains of virus replicase proteins. This mechanism has been shown for the non-structural protein nsP1 of Semliki Forest virus (SFV), a togavirus that was found to anchor the viral RCs to membranes of endocytic organelles via its hydrophobic domain [8]. The assembly and anchoring of the RC to membrane structures can be directed by host factors. As an example, it was found that replication of brome mosaic virus (BMV) was blocked when mutation of the yeast gene YDJ1 was made [10]. YDJ1 was shown to be important in early steps in the BMV virus replication cycle which included targeting of virus

non-structural proteins to the membrane and stabilization of RC. Another piece of evidence showing the importance of host membranes in establishing RCs was obtained in a study that involved mutations of the OLE1 gene in yeast cells that harbour brome mosaic virus (BMV) [11]. OLE1 encodes Δ9 fatty acid desaturase and is important for the formation of membranous structures. Mutation of this gene in BMV infected yeast cells affected early viral replication steps preceding the synthesis of virus negative strand RNA. From these finding, it is quite evident that intracellular membranes do play a viral role in the formation of viral factories containing RCs.

Formation of RCs that are located on and even enclosed within membranous structures of host cells are also important in creating a "safe haven" for the replicating RNA virus as the double stranded RNA (dsRNA) intermediates is targets of the host innate immune response [12]. dsRNAs produced as viral replication intermediates are recognized by different host pattern-recognizition receptors (PRRs) [13]. These PRRs recognize conserved molecular motifs called "pathogen-associated molecular patterns" or PAMPs. Two classes of PRRs play a role in recognition of viral dsRNA intermediates, a class of RNA helicases including RIG-I and MDA-5, and a Toll-like receptor (TLR), namely TLR3 [13]. Both of these classes of PRR induce type 1 interferon responses (through different pathways) and pro-inflammatory cytokines that counter virus infection of both the cell and organism. However, the helicases function by recognizing intracellular dsRNA, while TLR3 primarily recognizes exogenous dsRNA.

Although numerous studies have been done that show the association of virus RCs with intracellular membranes, the exact mechanism of targeting and morphogenesis of RCs is mostly unknown. Not much is known either about the host factors that are physically present in active RCs simply because the isolation of such membrane bound complexes while preserving their

enzymatic integrity is difficult to accomplish. In this study, co-immunoprecipitation with tagged RUBV nonstructural replicase protein P150 was employed to identify host proteins interacting with this protein. At first, P150 was immunoprecipitated from a post-nuclear supernatant prepared from lysates of RUBV-infected cells. Subsequently, immunoprecipitation was done from a cell fraction enriched for cytoplasmic organelles (including the endosome and lysosome-derived CPVs) by differential centrifugation [14]. While this modification was initially made to decrease background, we felt it was also more promising for identifying cell proteins directly associated with RCs. This is the first study of host proteins associated with RUBV nonstructural proteins that was done. These studies were performed in RUBV infected cells.

Materials and methods

Cells and virus

Vero cells, a continuous line of African green monkey kidney cells obtained from the American Type Culture Collection, were grown and maintained at 35^{o}C in a humidified atmosphere with 5% CO_2 in Dulbecco's modified Eagle's medium (DMEM) containing 5% fetal bovine serum (FBS) and gentamicin (10 μg/ml). For infection, Vero cell cultures at ~80% confluence were infected at a multiplicity of infection (MOI) of 1 plaque forming unit (pfu)/cell with RUBV derived from the Robo502 infectious cDNA clone (Robo502 virus)[15] as control or Robo502-912 virus, which bears a FLAG-epitope tagged P150, derived from the Robo502-912 infectious cDNA clone (Wen-Pin Tzeng, unpublished data).

Preparation of virus infected cell lysates and immunoprecipitation

Ten 100 mm culture plates of Vero cells that had been infected with Robo502 or Robo502-912 virus for 48 hours were washed twice with ice-cold phosphate buffered saline (PBS) and the cells were lysed with modified RIPA buffer [10 mM Tris-HCl pH 7.4, 100 mM

NaCl, 1 mM EDTA, 1 mM EGTA, 0.1% SDS, 0.5% sodium deoxycholate, 1% Triton X-100 and 1X broad range protease inhibitor (ROCHE)]. The cells in the lysis buffer were incubated on ice for 20 minutes before centrifugation at 12,000 rpm (Beckman coulter, JA 20 rotor) for 5 minutes to remove nuclei and cellular debris. Ten ml of clarified lysate were incubated with 1 ml of prewashed (PBS + 0.1% Triton X-100) anti-FLAG monoclonal antibody-conjugated agarose beads (SIGMA) for 2 hours at 4^0C. The bound beads were washed three times with lysis buffer. and were eluted with 2 ml of a 100 μg/ml solution of FLAG peptide (SIGMA) and the eluted proteins were precipitated by addition of three volumes of ice cold acetone and incubation at -20^{o}C for 1 hour [16]. Precipitated proteins were collected by centrifugation at 12,000 rpm (Beckman coulter, JA 20 rotor), the acetone was removed, and the precipitated protein pellet was allowed to air dry for ~10 minutes. Precipitated proteins were resuspended in 250 μl of 2D rehydration buffer (7M urea, 2M thiourea, 4% CHAPS, 2% Pharmalyte [broad range pH 3-10] and 40mM dithiothreitol; the latter two components were added to the rehydration buffer just before use) and incubated at 30^{o}C for 1 hour. An aliquot was subjected to SDS-polyacrylamide electorphoresis (SDS-PAGE), transferred onto nitrocellulose membrane (Whatman) using 1X transfer buffer (100 ml 10X transfer buffer [250 mM Tris, 1.92M glycine], 200 ml 100% methanol, and 700 ml deionized water) at 100V for 1 hour in a mini-Protean II apparatus (Biorad) and the Western blot probed with anti-FLAG antibodies (Sigma Aldrich) to confirm the presence of FLAG-tagged P150 in the sample.

First dimensional isoelectric focusing (IEF)

A 250 μl aliquot of resuspended immunoprecipitated proteins was applied to a 13 cm Immobiline strip (GE-Healthcare Life Sciences) with a nonlinear pH range of 3-10. The strip was covered with 1 ml of Dry Strip cover fluid (GE-Healthcare Life Sciences) and isoelectric

focusing was done using an IPGphor apparatus (Amersham) as follows: Rehydration for 16 hours at 30V; Increase to 200 V and hold for 1 hour; Increase to 500 V and hold for 1 hour; Increase to 1000 V and hold for 1 hour; Gradient for 30 minutes to 8000V; and Gradient for 32,000 V/hr up to 8000V. After isoelectric focusing, the strips were prepared for second dimension separation by SDS-PAGE.

Second dimensional SDS-PAGE and protein spot isolation

The IEF strips were removed from the IPGphor and washed for 15 minutes each with 10 ml of 1% DTT and 10 ml of 4% iodoacetamide. The strips were then transferred to the top of a 10% SDS-PAGE gel (10% acrylamide, 0.38 M Tris pH 8.8, 0.1% SDS, 0.1% ammonium persulfate). Agarose (0.5%) was used to seal the strips. Following electorphoresis, the gels were stained with Deep Purple Total protein stain (GE-Amersham) and scanned using a Typhoon imager (GE Healthcare) at an excitation length of 528 nm. The scans were analyzed using Image Master Platinum 2.0 software (GE-Amersham) and spots unique to the Robo502-912-infected cells lysate were isolated using an ETTAN spot-picker. Protein plugs were stored in 4^{o}C until analysis was done by trypsin digestion and Matrix Assisted Laser Desorption Ionisation mass spectrometry (MALDI-TOF) (Morehouse School of Medicine).

Concentration of RUBV cytopathic vacuoles (CPV) in cell lysates

A previously described method for concentration of a lysosomal fraction from cell lysates [14] was used to concentrate RUBV CPVs from Robo502 and Robo502-912 virus-infected cell lysates. Ten 100 mm culture plates of Vero cells infected with Robo502 or Robo502-912 virus (MOI ~1 pfu/cell) were harvested at 48 hours post-infection by using a cell scraper after being washed twice with PBS. The detached cells were collected in cold fractionation buffer (10 mM tris(hydroxymethyl)aminomethane/acetic acid pH 7.0, 250 mM sucrose) and washed twice in

fractionation buffer by low speed centrifugation. Cold fractionation buffer was also used in the following procedures. The washed cells were resuspended in 5 ml of buffer containing 1X broad range protease inhibitor (ROCHE) and cells were homogenized by 10 strokes in a 15 ml disposable tissue grinder system (VWR). The cell homogenate was centrifuged at 2000 X g for 2 minutes to remove debris and then at 4000 X g to pellet a combination of nuclei and cell membranes. The supernatant was collected and transferred to Beckman 3.9 ml Quick-Seal centrifuge tubes which were sealed and centrifuged at 100 000 X g for 2 min in a Beckman TLN100 rotor to pellet the mitochondria, endosome and lysosomes, all organelles associated with RUBV CPVs. The resulting pellet (P100) was resuspended in 0.75 ml RIPA buffer (10 mM Tris-HCl pH 7.4, 150 mM NaCl, 3 mM EDTA, 1% Triton X-100, 0.1% SDS, and 0.5% DOC) containing 1X broad range protease inhibitor (ROCHE) at 4^0C to solubilize the CPVs along with associated proteins from the pellet fraction. After centrifugation at 13,000 rpm for 5 minutes (Eppendorf tabletop centrifuge), the solubilized fractions were immunoprecipitated with anti-FLAG monoclonal antibody-conjugated agarose beads (SIGMA) for 4 to 6 hours at 4^oC. The precipitate was then washed 5 times with RIPA wash buffer (10 mM Tris-HCl pH 7.4, 150 mM NaCl, 0.5% Triton X-100, 0.5% DOC, and 3 mM EDTA). Bound proteins were eluted by addition of 2X SDS-PAGE loading buffer (100 mM Tris-HCl pH6.8, 20 mM dithiothreitol, 4% SDS, 0.2% bromophenol blue, and 20% glycerol) and boiling. Eluted proteins were resolved on 6% and 10% SDS-PAGE gels, stained with GelCode Blue (Pierce) and scanned with a Typhoon imager (GE Healthcare) using no filter and an excitation wavelength of 633nm. Lanes containing proteins isolated from Robo502 and Robo502-912 infected cell pulldown samples were compared. Protein bands were excised from the gel using a clean scalpel and sent to the Scripps

Center for Mass Spectrometry, California. Excised protein bands were sent in deionized water, in 1.5 ml eppendorf tubes. Protein identification was performed by the center using nano-LC/MS/MS.

Western blot analysis

Proteins were separated by SDS-PAGE and then electorphoretically transferred to nitrocellulose membranes (Whatman) with a mini Protean II apparatus (Biorad) using 1X transfer buffer (25 mM Tris pH 7.5, 0.192 M glycine, 20% methanol) at 100V for 1 hour. The membrane was blocked overnight with 5% dried milk in TBS (20 mM Tris-HCl, pH 7.5, 175 mM NaCl) and the blot was probed with mouse anti-FLAG monoclonal antibody (Sigma), goat anti-VPS16 polyclonal antibody (IMGENEX), rabbit GU-8 anti-RUBV P90 antibody [17] or rabbit anti-Lamp2 polyclonal antibody (Abcam), each diluted 1:1000 in antibody dilution buffer (1% non-fat milk powder, 0.02% sodium nitrate in TBS buffer [20 mM Tris-HCl, pH 7.5 and 175 mM NaCl]). The proteins were detected using a BCIP/NBT (Roche) colorimetric assay with alkaline phosphatase-conjugated anti-mouse, anti-goat or anti-rabbit alkaline phosphatase conjugated secondary antibody (Promega) (1:5000 dilution).

Electron microscopy of the P100 pellet to detect the presence of CPVs

The P100 pellet fraction from uninfected or Robo502-912-infected Vero cells was fixed in 4% glutharaldehyde-PBS**,** and sent in an eppendorf tube to Dr. Cristina Risco, Center for Biotechnology, Universidad Autonoma, Cantoblanco Campus, Madrid, Spain, for analysis by transmission EM.

Immunofluorescence assay of P100 pellet with dsRNA antibody

Confirmation of the presence of dsRNA in the CPV-concentrated fraction (P100 pellet fraction) (as an indication of the presence of active replication complexes) was done using

antibodies specific for dsRNA in an immunofluorescence assay (IFA). A small amount of the P100 pellet fraction from uninfected or infected cells was smeared onto an 18mm glass coverslip followed by fixation with 4% paraformaldehyde in PBS for 30 min at 4^{o}C. The coverslips were washed with PBS and incubated PBS-0.25% saponin for 10 min at room temperature to permeabilize the membrane bound CPVs. Coverslips were washed again with PBS and blocked with PBS, 2% BSA, 0.25% saponin for 30 min at room temperature. Primary antibody to dsRNA, a monoclonal mouse anti-dsRNA antibody (J2 from Biocenter, Szeged Hungary), was diluted in PBS, 0.1% BSA and 0.25% saponin (1:500 dilution) and added to the coverslips for 1 hour. After three washes in PBS, secondary mouse anti-FITC antibody (SIGMA) diluted in PBS, 0.1% BSA, 0.25% saponin (1:1000) was added followed by incubation for 30 minutes at room temperature. The coverslips were washed with PBS, inverted and mounted onto glass slides with ProLong gold anti-fade reagent (Molecular Probes/Invitrogen). The cells were visualized with a Zeiss Axioplan 2 microscope with epifluorscence capacity using the 20 X objective.

Results

Identification of host proteins co-immunoprecipitating with P150 by 2D gel electrophoresis

The initial strategy employed to identify host cell proteins interacting with the RUBV P150 nonstructural replicase protein was co-immunoprecipitation from cytoplasmic lysates of RUBV-infected cells. Advantage was taken of the development of RUBV constructs with an epitope tagged P150 that exhibit no difference in titer from corresponding constructs without the tag [18]. The proteins encoded by the constructs used in this study are shown in Fig 2.1. Since virus infection alters the infected cell, cells infected with the standard virus without the tag were used as the control rather than uninfected cells. In this way, any host proteins that cross react with the antibody used in immunoprecipitation and are released or relocalized by virus infection

will not be misidentified as proteins co-immunoprecipitating through an association with P150. Infected cells were harvested 48 after infection because it was previously established that maximal levels of P150 expression occur at this time point [17].

Fig. 2.2 describes the protocol used to identify host proteins co-immunoprecipitating with P150 separated by two-dimensional gel electrophoresis (2-DE). The primary limitation in resolving proteins using 2-DE is that the proteins cannot be denatured prior to electrophoresis in the first dimension since this separation is based on isoelectric focusing under high voltage. In total, co-immunoprecipitation followed by isoelectric focusing and separation of immunoprecipitated proteins according to molecular weight was conducted. The pair of gels with the best resolution is shown in Fig. 2.3A. As can be seen, background (ie spots present in both gels) was high. However, the Image Master Platinum 2.0 program that was used to compare protein spots present on "control" and "sample" gels was able to identify 17 protein spots specifically immunoprecipitated by anti-FLAG antibody from Robo502-912-infected cells. Although these spots are all marked in the gels shown in Fig. 2.3A, blow ups of regions containing the spots specific to the Robo502-912 gel are shown in Figures 2.3B through 2.3G. These unique spots were picked and analyzed by trypsin digestion and mass spectrometry. Each protein spot analyzed by mass spectrometry contained more than one possible "hit" or protein prediction. Only proteins that had a score more than 10 were considered valid and the most probable protein hit for each spot is listed in Table 2.1. As can be seen, 13 out of 17 hits had low scores, ie. ~10. Many of these spots had a number of possible hits for protein identities with slightly lower scores than the one listed. The low scores for protein identity hits from these spots could be due to more than one protein in a spot or low abundance of the protein in the spot. In this regard, it should be noted that some of the unique spots were very close to larger spots

present in both the control and experimental gels (e.g. spots 258, 291, 471, 472, and 477; Fig. 2.3A). Out of the 17 protein IDs however, 4 had scores that ranged from 16 through 58 and were considered possible P150 interacting candidates.

Of the four spots that yielded identity hits with scores >10 (**spot 97**, vacuolar protein sorting protein 16 with a score of 16.09; **spot 59,** zinc finger protein 43 with a score of 18.06; **spot 85,** B cell lymphoma CLL/lymphoma 11A isoform with a score of 18.08; and **spot 62,** follistatin-like 5 with score of 58) **v**acuolar protein sorting protein 16 (Vps16, spot 97) was chosen as a candidate protein to test further for association with P150 because its function was consistent with formation of vesicles by the RUBV replication in association with lysosomes and antibody to this protein was commercially available. Vps16 has been characterized as one of the class C Vps genes involved in multiple vesicle transport pathways, particularly involving the biogenesis and stability of lysosomal vesicles. It also serves as the delivery pathway for lysosomal proteins [19, 20]. In the Western blot used to confirm the binding of Vps16 to FLAG-tagged P150, the anti-Vps16 antibody was capable of detecting the protein in cell lysates (indicated by arrow in the Western blot of Fig. 2.4). However, when P150 was immunoprecipitated from lysates of Robo502 or Robo502-912-infected cells, co-immunoprecipitation of Vps16 with FLAG-tagged P150 did not seem to occur (lane 2, Fig. 2.4). There were two protein bands detected in lanes 1 and 2 at a higher molecular weight than the positive control band in lane 3. We do not know what protein these bands represented.

Overall, the strategy of co-immunoprecipitation and 2-DE to detect host proteins interacting with P150 was too cumbersome, not routinely reproducible, and plagued by high background and therefore another approach was chosen to identify proteins associating with

P150, namely concentrating the CPVs in which RNA synthesis occurs prior to co-immunoprecipitation.

Identification of host proteins co-immunoprecipitating with P150 following concentration of CPVs by 1D gel electrophoresis

Fig. 2.5 shows a schematic of the new approach that was used to concentrate CPVs prior to co-immunoprecipiation with FLAG-tagged P150. This approach was adapted from a published protocol used to isolate fractions containing lysosomes and endosomes as well as mitochondria and was shown to work successfully with different types of cell lines [14]. Basically, the protocol involved cell lysis by Dounce homogenization followed by two low speed centrifugations and then a high speed centrifugation. Lysosomes, endosomes and mitochondria remain in the supernatant following the two low speed centrifugations (S1 and S2) and concentrate in the final pellet following the high speed centrifugation (P3). As shown in Figures 2.6 and 2.7, FLAG-tagged P150 in Robo502-912 infected cells was present in equal amounts in the supernatant and pellet following the first centrifugation that cleared unlysed cells and other debris, but subsequently the majority distributed into the post-nuclear supernatant (S2) following the second low speed centrifugation and the pellet (P3) following the high speed centrifugation, as expected. No P150 could be detected by the anti-FLAG antibody in any fractions from cells infected with Robo502, which expresses an untagged P150.

To confirm that the P3 fraction contained lysosomes, a Western blot was probed with antibodies against Lamp2 protein, a lysosomal membrane associated glycoprotein that is used as a lyosomal marker. Results shown in Fig. 2.8 confirmed the presence of Lamp2 in the P3 fraction, but not the S3 fraction. This is pertinent to our goal of isolating RUB P150 associated with replication complexes because RUBV forms replication complexes in vesicles associated

with lysosomes [21]. However, the amount of Lamp2 protein in the Robo502 P3 fraction was lower that the amount in the Robo-502-912 P3 fraction, and is most probably a result of unequal amounts of protein samples being loaded during this one experiment. To further show that replication complexes were isolated using the fractionation protocol, the P3 fraction was fixed and analyzed by electron microscopy (Fig. 2.9) and an immunofluorescence assay (IFA) (Fig. 2.10) to detect dsRNA, a marker of RNA-dependent-RNA synthesis. As shown in Figures 2.9 A, B and C, structures similar to CPVs seen in RUBV-infected cells (Fig. 2.9D) were detected in the P3 fraction from Robo502-912-infected cells, but not in the corresponding P3 fraction from control uninfected cells (Fig. 2.9E). When fixed smears of P3 fractions were probed with an antibody to double stranded RNA (dsRNA), the fraction from Robo-502-912-infected cells contained multiple distinct bright spots not seen in the fraction from control uninfected cells suggesting the presence of dsRNA in the infected samples (Fig. 2.10). Taken together, these data demonstrate that viral replication complexes were present in the P3 fraction.

The P3 fraction from Robo502 and Robo502-912-infected cells was next used for experiments to detect interactions of host cellular factors with P150 by co-immunoprecipitation following the approach diagrammed in Fig. 2.11. First, the P3 fraction was solubilized with various lysis buffers to maximize the recovery of P150 as shown in Fig. 2.12. Maximal recovery was obtained using the RIPA buffer that had been used to produce whole cells lysates in the 2-DE analysis. Maximum recovery was desired to increase the chances of being able to detect the presence of host cellular proteins that may reside in the RC. However, to ascertain that the process yielding maximum recovery did not affect the binding of RUBV P150 with other proteins, the interaction of a the viral P90 which is known to bind P150 was tested. RUBV P90, the functional replicase protein [22], should be present in the replication complex [17] and

therefore should be present in the same fraction as RUBV P150. Fig. 2.13A (lane 4) and Fig. 2.13B (lanes 9 and 10) show that P150 and P90, respectively, were present in the same fraction (supernatant fraction) of RIPA buffer solubilized P3 fraction. As shown in Fig. 2.13B, P90 was detected in solubilized P3 fraction of both Robo502 and Robo502-912-infected cells. P90 was detected in both because the Western blot was probed with GU8, a rabbit polyclonal antisera against bacterially expressed RUBV P90. To determine whether the extraction method perturbed the physical interaction of RUB P150 with RUB P90, immunoprecipitation was done with anti-FLAG antibody followed by Western analysis to detect the presence of both P150 and P90 using mouse anti-FLAG and rabbit anti-GU8 antibodies, respectively (Fig. 2.14 A and 2.14 B, respectively). Lane 2 of Figure 2.14A shows that P150 was successfully immunoprecipitated from the solubilized supernatant of the P3 fraction, while Lane 4 of Fig. 2.14B shows that P90 was co-precipitated with P150. This experiment demonstrated that the interaction of RUBV P150 with a known interacting protein, i.e. RUB P90, was preserved during the preparation of the CPV-containing fraction and subsequent extraction of P150 from the fraction. Therefore it could be postulated that the interactions of other binding partners of P150 would be similarly preserved.

Next, we wanted to see if host cell proteins were immunoprecipitated with RUBV P150 from the CPV fraction. Fig. 2.15 shows SDS-PAGE separation of the proteins that were immunoprecipitated by anti-FLAG antibody from the solubilized P3 fraction from Robo502 (Lane 1) and Robo502-912 (Lane 2) infected cells. As can be seen, the subcellular fractionation and concentration of CPVs substantially reduced the background encountered when immunoprecipitation was done from unfractionated cell lysates (Fig. 2.3). Two protein bands were detected in the Robo502-912 lane that was not present in the Robo502 control lane. One of

these protein bands (CPV1) migrated between the 116 kDa and 202 kDa MW markers while the second (CPV2) migrated slightly more rapidly than did the 98 kDa MW marker. Trypsinization and mass spectrometry nano-LC/MS/MS analysis of CPV1 and CPV2 identified both proteins as the RUBV P90 replicase protein with 95% confidence (Table 2.2). While the M_r of the CPV2 band corresponded with the molecular weight of P90, the M_r of CPV1 did not and was indicative of P150. However, a western blot of an 18x16 cm SDS-PAGE gel similar to the one used to resolve proteins for mass spectrometry analysis probed with mouse anti-FLAG antibody to identify the location of FLAG-tagged P150 showed that the M_r of P150 was very similar, but possibly slightly less, than that of CPV1 (Fig. 2.16). We concluded that CPV1 most likely was a dimer of P90 which would have a M_r of 180 kDa (Fig. 2.16 B, indicated in asterisk). Nevertheless, P90 was the only pairing partner of P150 that was identified with the technique and protein staining reagent that we used for this particular experiment. No other proteins with molecular mass lower that 90 kDa, were found to interact with P150 (data not shown).

Discussion

The goal of this study was to identify host cell proteins that interact with RUBV proteins and play an important role in viral replication. Previous studies on the interactions of host factors with RUBV components identified cellular proteins that bind to the 5' and 3' untranslated regions (UTR's) of the RUBV genomic RNA and to the P90 replicase protein and the C protein. Specifically, La autoantigen bound to the 5' UTR [23] and calreticulin bound to the 3' UTR [24]. These associations were discovered by introducing radiolabeled RNA probes into cell lysates and detecting binding in gel mobility shift assays. Binding of the retinoblastoma protein to P90 was found based on bioinformatics predictions of binding motifs for this protein in the P90 protein while binding of citron kinase to P90 was identified through yeast two-hybrid assays [25,

26]. Finally, binding of mitochondrial p32 to the C protein was discovered using a yeast two-hybrid assay and the binding of polyA binding protein to C protein was discovered by using a GST-capsid fusion protein expressed in mammalian cells and affinity purification of capsid-binding partners (in the transfected cells) on gluthathione agarose beads [27, 28]. Despite follow-up studies, the role that any of these proteins plays in RUBV replication has not been determined. We reasoned that a more promising way of isolating cell proteins directly involved in RUBV replication would be by co-immunoprecipitation with the RUBV replicase from lysates of infected cells in which virus replication was ongoing. We took advantage of the recent successful insertion of an epitope tag into one of the RUBV replicase proteins, P150, without compromising viral RNA infectivity and used a virus expressing a FLAG-tagged P150 in this study. Similar approaches have been taken with other viruses, e.g. the alphavirus Sindbis virus, albeit with a GFP tag [29, 30].

The first approach taken in this Specific Aim was to resolve proteins co-immunoprecipitating with P150 from cytoplasmic lysates of RUBV-infected cells by two-dimensional electrophoresis (2-DE), a method which first resolved proteins first by iso-electric focusing (charge) and then by molecular mass. The primary advantage conferred by this method is a better separation of proteins compared to the traditional one dimensional SDS-PAGE. 2-DE also allows the identification of post-translational modifications such as phosphorylation and glycosylation on a single species of protein. 2-DE was first introduced by P.H. O'Farrel and J. Klose in 1975 [31, 32]. A modification of this original method by Angelika Gorg [33] provided an easier way to separate proteins on the first iso-electric dimension and, as a result, more consistent patterns of proteins were seen. The traditional method relied on a mixture of carrier ampholytes to facilitate the iso-electric focusing of proteins that led to long focusing times and

modifications of pH gradients that caused non-reproducible results. Commercial immobilized pH gradients (IPG) with the modifications of Angelika Gorg overcame some of the limitations posed by the traditional method of iso-electric focusing. Nevertheless, many steps are necessary to prepare the immunoprecipitated samples properly to retain the native conformation for successful resolution in the first dimension. The majority of research that utilizes this method involves detecting differential expression of proteins in cells, for example tumor versus non-tumor cells or infected versus non-infected cells. However, 2-DE has been used as a tool to study protein-protein interactions as well. For example, two studies, from which we derived our approach, were from labs that studied the interactions of host cellular factors with the HCV NS5A replicase and core protein [16, 34].

As a control for detecting non-specific co-immunoprecipitation by the FLAG-monoclonal antibody-conjugated agarose beads from lysates of Robo502-912-infected cells, lysates were used of cells infected with Robo502, which lacked a FLAG epitope. A non-epitope tagged virus was used as a control for changes in intracellular expression and redistribution of cellular factors that may occur as a result of infection. Most researchers doing similar studies have used lysates from uninfected cells as a control [35, 36] and have failed to take into account the changes in cells caused during infection. As a result, these studies yield higher levels of false positives

The 2-DE gels yielded a large number of background spots; however, comparison of proteins immunoprecipitated from lysates with non-tagged and tagged P150 led to the identification of seventeen unique protein spots that were present in the latter. These spots were visible by staining with deep purple (GE-Amerham), a fluorescent stain that detects proteins at concentrations as low as 50 pg. Even though staining by this method increases sensitivity (low

detection limits), it increases background and as a result, produces false positives. The seventeen spots were picked and analyzed though trypsin digestion and MALDI-TOF analysis. However, the end result for most (thirteen) of the spots was more than twenty proteins as a possible identity for each spot with relatively low scores for each, suggesting that the concentration of the proteins in the spot were low and/or contaminated by proteins in nearby background spots. There are several possible reasons for this finding. Firstly, the many steps that were involved before the proteins in the sample could be focused on the first dimension could have led to the loss of important binding proteins. Secondly, the decrease in the amount of real binding proteins led to masking by proteins that were initially present as non-specific proteins. Finally, the high sensitivity of the staining method gave an illusion of abundance when actually low levels of real binding proteins existed to begin with. To add to these factors, when the proteins are processed through trypsin digestion and further repetitious steps for peptide purification using ZipTip (Millipore), the amount of peptides available for identification become even less.

Despite the low confidence in the proteins identified from thirteen of the seventeen spots, the top candidates from the remaining spots had higher scores. Some of the proteins with higher scores were vacuolar protein sorting protein 16 (Vps16) with a score of 16.09, zinc finger protein 43 with a score of 18.06, B cell lymphoma CLL/lymphoma 11A isoform with a score of 18.08 and follistatin-like 5 with score of 58.10. Other than Vps16, not much has been reported in the literature about the functions of the other identified proteins, nor were there any reagents readily available to test their binding to P150. Thus, Vps16 was chosen for further analysis because it functions in protein transport between the Golgi and vacuolar organelles (e.g., endosomes, the sites of RUBV RC assembly) and an antibody was available. However, we were unable to obtain data indicating that Vps16 interacted with P150 by co-immunoprecipitation.

The high background encountered following co-immunoprecipitation from lysates of infected cells along with the problems encountered with 2-DE (amount of effort, lack of reproducibility, and unconvincing protein identities from unique spots) led us to choose another approach to detect proteins interacting with P150, namely a fractionation protocol designed to concentrate endosomes and lysosomes, the precursors of RUBV CPVs that house the RCs. Such a procedure should reduce background which would allow us to use 1-D SDS-PAGE to resolve proteins co-immunoprecipitating with P150 (the method most commonly employed currently in similar studies on other viruses [29, 30]). Additionally, one of the limitations posed by 2-DE method is the under-representation of membrane proteins due to poor solubility and aggregation which makes it difficult for these proteins to enter the second dimension from the IEF strip [33, 37]. This is a significant problem as far as our research is concerned simply because P150 is a membrane-associated protein (unpublished data) and viral RNA replication in RUBV infected cells occurs in association with membranes [2, 38]. Thus, immunoprecipitation of P150 from a CPV-enriched fraction followed by SDS-PAGE, rather than 2-DE, increased the chances of identifying membrane proteins associated with P150. Furthermore, recent studies have shown that only a fraction of SINV non-structural proteins are present in CPVs and the rest are present in the cytoplasmic locations other that the modified lysosomes [6]. Similarly RUBV P150, it has been shown to exist both as punctuate foci in the cytoplasm of infected cells, which likely correspond to CPVs, and in fibrous structures, particularly late in infection when we made our lysates [7]. These different intracellular locations of P150 suggest that the protein is involved in different stages of virus replication at different times post-infection. Therefore our approach of isolating CPVs prior to studying host factors interacting with P150 in the replication complex was more likely to yield information on host factors that participate in virus RNA synthesis.

As discussed in Chapter 1, co-immunoprecipitation was used to identify cell proteins that interacted with two of the nonstructural replicase proteins of the alphavirus, SINV, namely nsP2 and nsP3, both of which were successfully tagged with GFP without compromising virus infectivity. While a plethora of cell proteins were identified as interacting with nsP2 and nsP3, including cytoskeleton proteins, chaperones, elongation factor 1A, heterogeneous nuclear ribonucleoproteins, 14-3-3 proteins, and some of the ribosomal proteins [29, 35, 39], emphasis was placed on G3BP1 and G3BP2 and the the mosquito cell homolog, Rasputin [29, 30]. The association of these proteins with both nuclear pores and stress granules led to the hypothesis that recruitment of these proteins by the SINV nonstructural proteins played a role in shutoff of nuclear transcription and/or reformatting the translational capacity of the cell to favor translation of virus proteins. Overall, these co-immunoprecipitation studies emphasized the complexity of the interaction between virus and cell proteins. However, a definitive role was not established for any of these proteins in virus replication. More convincing was the cell fractionation study that identified hnRNP-K, along with stress response and cytoskeletal proteins, as a protein enriched in membrane fractions harboring active SINV RCs [36]. It was subsequently shown that hnRNP K co-immunoprecipitated with the SINV nonstructural proteins and the subgenomic (but not the genomic) RNA and it was hypothesized that it played a role as part of the RC in regulating the ratio of genomic and subgenomic RNA synthesis and subsequent subgenomic RNA translation.

The architecture of alphavirus CPVs was described as early as 1968 [40, 41] and subsequent literature added to the description, primarily using electron microscopy and immuno-electron microscopy [5, 42]. Active alphavirus RCs form in membrane limiting regions of modified vacuoles and were termed CPV-I. These vacuoles were later shown to be derived from lysosomes. Since lysosomes evolve from endosomes, it was thought that initial formation of RCs

within endosomes resulted from virus entering the cell through receptor mediated endocytosis. However, this idea did not hold water because the multiplicity of infection did not correspond with the number of CPVs that were formed [42]. Additionally, CPVs are formed following transfection of virus RNA, indicating that their formation was a post-translational event not dependent upon initial localization of virions to an endosome or lysosome. CPVs are approximately 0.6-2.0 μm in diameter and the actual sites of RNA synthesis are membrane-bound spherules 50 nm in diameter that line the inner surface of the CPV vacuole at regular intervals. As for RUBV, CPVs resembling those produced by alphaviruses have been visualized in cells following both transfection and infection [2, 3]. The CPVs are derived from lysosomes and the spherules contain dsRNA and both the P150 and P90 replicase proteins. In order to isolate these CPVs, we took advantage of a previously established differential centrifugation method for fractionation of endosomes, lysosomes and mitochondria from a variety of eukaryotic cell lines [14].

When this fractionation method was applied to a post-nuclear supernatant, P150 segregated quantitatively into the subsequent P3 or "P100" pellet fraction expected to be enriched for endosomes, lysosomes, and mitochondria. In confirmation, we showed that this fraction contained the Lamp2 protein, which is a marker for lysosomes. We next sought physical evidence of the presence of CPVs through electron microscopy and indeed the P100 fraction contained vacuolar structures comparable to previously published electron micrograph images of RUBV CPV that were not present in the corresponding P100 fraction from uninfected cells [3]. The presence of replication complexes in the P100 fraction was supported by a novel experiment whereby the P100 fractions of both control as well as infected Vero cells were fixed and stained with antibodies to double stranded RNA; bright green spots in P100 fractions from

infected cells and not from the control cells were observed. Based on all these observations, we concluded that the P100 fraction contained active replication complexes.

The next challenge was to extract P150 from the membranous CPV while maintaining important binding partners. The P100 fraction was solubilized using three different lysis buffers to maximize the extraction of P150. Co-immunoprecipitation of P90 was evaluated as a positive control and also to ensure that the solubilization technique did not disrupt the potential binding partners of P150. Standard RIPA buffer containing both 1% Triton X-100 and 0.5% DOC was the most successful in extracting P150 from the membranous complex. This finding was in agreement with a previously published paper on the successful recovery of functional replication complexes from alphavirus infected cells [43]. In this paper, RIPA buffer in the presence of 1% Triton X-100 and 1% DOC was successfully used to extract replication complexes from a P15 fraction of alphavirus infected cells yielding all of the nonstructural proteins nsP1, nsP2, nsP3, nsP4 and some nsP34, and an unidentified protein (~120 kDa) believed to be a host cellular protein**.**

In our study, after confirming that the solubilized P100 fraction contained both P150 and P90 and that P90 co-immunoprecipitated with P150, we proceeded to use 1-D SDS-PAGE to resolve putative cell proteins co-immunoprecipitating with P150 for subsequent identification by mass-spec analysis. SDS-PAGE analysis of proteins immunoprecipitated by anti-FLAG antibody revealed that cell fractionation substantially reduced the background present following similar immunoprecipitation from unfractionated, cytoplasmic lysates. Two protein bands were found to be immunoprecipitated by anti-FLAG antibody specific for Robo502-912. These two proteins were identified as RUBV P90. While the molecular mass of CPV2 fit that of P90, the identification of CPV1 as P90 was not expected. Further analysis of the protein band in the

CPV1 region, led us to identify an additional band above the one where the presence of P150 was confirmed through Western blot analysis. P150 may not have been identified through mass-spectrometry because the protein band that was excised for analysis may have contained the protein from the higher molecular mass. We hypothesized that the CPV1 protein band that was identified could be a P90 dimer. The high confidence level (95%) of a number of peptides that matched P90 and the molecular mass of the protein, support our hypothesis. However, further analysis needs to be done to confirm this hypothesis.

However, these data do not mean that host proteins are not involved in the replication of virus genome. Host cellular factors have been shown to interact, as described earlier, with the 5' UTR and 3' UTR of a virus genome. Specific template recognition by a virus RdRp is important to ensure that replication occurs properly. Some of the factors that are important in this respect are the sequences and secondary structures present at the 5' end and the 3'end of the genome. Binding of host cell proteins to these RNA sequences/structures and to the RDRP itself could function to direct the RdRp to the template to promote template specifity as well as to form an active replication complex [1, 44, 45]. In the classic example of the replicase of bacteriophage Qβ, the binding of host cellular elongation factors EF-Tu, EF-Ts and ribosomal protein S1 to the Qβ replicase is important for the formation of the holoenzyme and synthesis of plus strand RNA from negative strand template [46]. The binding of another host factor, HF1, a ribosomal protein to the 3' end of this RNA genome is required for negative strand RNA synthesis [47]. An analysis of RCs formed by flock house virus (FHV), a nodavirus that included electron tomography, it was concluded that in the 50 nm spherules formed on the outer mitochondria membranes that comprise the RC that there was little or no room for any other factors other than

viral replicase protein and the virus RNA [48]. The 50 nm spherules that was studied in FHV are similar to the ones found to line the interior of CPVs in RUBV infected cells.

While we found no host cell proteins interacting with P150 in the replication complex, it has to be pointed out that there were caveats to the approach and method that we used to isolate proteins from the RUBV infected cells. Firstly, even though the fractionation procedure reduced the amount of background for the immunoprecipitation experiment specific for Rob0502-912, it also reduced the amount of host proteins that may already have been low in abundance to begin with. As a result, the enrichment of viral proteins led us to detect P150 and P90 that were higher in abundance in that fraction, and not low abundance host proteins that were faintly detected using by GelCode Blue staining reagent. The second caveat to our method was the fractionation procedure itself. The high speed of the final fractionation step that led to the formation of the P3 pellet may have perturbed host-virus protein interactions. Finally, the solubilization technique using denaturing detergents such as DOC and SDS to remove P150 from the P3 fraction may have disrupted important host-virus protein interactions as well. For future studies, analysis of the all the proteins enriched in the P3 fraction of RUBV infected cells could be done in comparison to a P3 fraction from uninfected cells. The entire set of proteins in a P3 fraction can now be analyzed by high performance liquid chromatography followed by peptide identification through tandem mass spectrometry.

In conclusion for this aim, we did not find P150 binding to host cellular proteins in the context of CPVs. As will be seen from the data obtained for the second Specific Aim, P150 does bind to host cellular factors. However this interaction most probably does not occur in the context of P150 within the RC. P150 is located in different places and structures in the cytoplasm of the infected cells where it may have different functions. In its role as a virus

replicase, P150 does not seem to form stable interactions that can be detected with the techniques used. The interaction of host cellular factors with P150 in its non-CPV form is further investigated in the next Specific Aim.

References

1. Ahlquist, P., et al., *Host factors in positive-strand RNA virus genome replication.* J Virol, 2003. 77(15): p. 8181-6.
2. Novoa, R.R., et al., *Virus factories: associations of cell organelles for viral replication and morphogenesis.* Biol Cell, 2005. 97(2): p. 147-72.
3. Fontana, J., et al., *Novel replication complex architecture in rubella replicon-transfected cells.* Cell Microbiol, 2007. 9(4): p. 875-90.
4. Uchil, P.D. and V. Satchidanandam, *Architecture of the flaviviral replication complex. Protease, nuclease, and detergents reveal encasement within double-layered membrane compartments.* J Biol Chem, 2003. 278(27): p. 24388-98.
5. Froshauer, S., J. Kartenbeck, and A. Helenius, *Alphavirus RNA replicase is located on the cytoplasmic surface of endosomes and lysosomes.* J Cell Biol, 1988. 107(6 Pt 1): p. 2075-86.
6. Kujala, P., et al., *Biogenesis of the Semliki Forest virus RNA replication complex.* J Virol, 2001. 75(8): p. 3873-84.
7. Kujala, P., et al., *Intracellular distribution of rubella virus nonstructural protein P150.* J Virol, 1999. 73(9): p. 7805-11.
8. Peranen, J., et al., *The alphavirus replicase protein nsP1 is membrane-associated and has affinity to endocytic organelles.* Virology, 1995. 208(2): p. 610-20.
9. Tzeng, W.P., J.D. Matthews, and T.K. Frey, *Analysis of rubella virus capsid protein-mediated enhancement of replicon replication and mutant rescue.* J Virol, 2006. 80(8): p. 3966-74.
10. Tomita, Y., et al., *Mutation of host DnaJ homolog inhibits brome mosaic virus negative-strand RNA synthesis.* J Virol, 2003. 77(5): p. 2990-7.
11. Lee, W.M., M. Ishikawa, and P. Ahlquist, *Mutation of host delta9 fatty acid desaturase inhibits brome mosaic virus RNA replication between template recognition and RNA synthesis.* J Virol, 2001. 75(5): p. 2097-106.
12. Ahlquist, P., *RNA-dependent RNA polymerases, viruses, and RNA silencing.* Science, 2002. 296(5571): p. 1270-3.
13. Kawai, T. and S. Akira, *Innate immune recognition of viral infection.* Nat Immunol, 2006. 7(2): p. 131-7.
14. Schroter, C.J., et al., *A rapid method to separate endosomes from lysosomal contents using differential centrifugation and hypotonic lysis of lysosomes.* J Immunol Methods, 1999. 227(1-2): p. 161-8.
15. Tzeng, W.P. and T.K. Frey, *Complementation of a deletion in the rubella virus P150 nonstructural protein by the viral capsid protein.* J Virol, 2003. 77(17): p. 9502-10.
16. Choi, Y.W., et al., *Proteomic approach identifies HSP27 as an interacting partner of the hepatitis C virus NS5A protein.* Biochem Biophys Res Commun, 2004. 318(2): p. 514-9.

17. Forng, R.Y. and T.K. Frey, *Identification of the rubella virus nonstructural proteins.* Virology, 1995. 206(2): p. 843-53.
18. Tzeng, W.P., et al., *Rubella virus DI RNAs and replicons: requirement for nonstructural proteins acting in cis for amplification by helper virus.* Virology, 2001. 289(1): p. 63-73.
19. Kim, B.Y., et al., *Identification of mouse Vps16 and biochemical characterization of mammalian class C Vps complex.* Biochem Biophys Res Commun, 2003. 311(3): p. 577-82.
20. Richardson, S.C., et al., *Mammalian late vacuole protein sorting orthologues participate in early endosomal fusion and interact with the cytoskeleton.* Mol Biol Cell, 2004. 15(3): p. 1197-210.
21. Magliano, D., et al., *Rubella virus replication complexes are virus-modified lysosomes.* Virology, 1998. 240(1): p. 57-63.
22. Wang, X. and S. Gillam, *Mutations in the GDD motif of rubella virus putative RNA-dependent RNA polymerase affect virus replication.* Virology, 2001. 285(2): p. 322-31.
23. Duncan, R.C. and H.L. Nakhasi, *La autoantigen binding to a 5' cis-element of rubella virus RNA correlates with element function in vivo.* Gene, 1997. 201(1-2): p. 137-49.
24. Chen, M.H. and T.K. Frey, *Mutagenic analysis of the 3' cis-acting elements of the rubella virus genome.* J Virol, 1999. 73(4): p. 3386-403.
25. Forng, R.Y. and C.D. Atreya, *Mutations in the retinoblastoma protein-binding LXCXE motif of rubella virus putative replicase affect virus replication.* J Gen Virol, 1999. 80 (Pt 2): p. 327-32.
26. Atreya, C.D., S. Kulkarni, and K.V. Mohan, *Rubella virus P90 associates with the cytokinesis regulatory protein Citron-K kinase and the viral infection and constitutive expression of P90 protein both induce cell cycle arrest following S phase in cell culture.* Arch Virol, 2004. 149(4): p. 779-89.
27. Beatch, M.D. and T.C. Hobman, *Rubella virus capsid associates with host cell protein p32 and localizes to mitochondria.* J Virol, 2000. 74(12): p. 5569-76.
28. Ilkow, C.S., et al., *Rubella virus capsid protein interacts with poly(a)-binding protein and inhibits translation.* J Virol, 2008. 82(9): p. 4284-94.
29. Cristea, I.M., et al., *Tracking and elucidating alphavirus-host protein interactions.* J Biol Chem, 2006. 281(40): p. 30269-78.
30. Gorchakov, R., et al., *Different types of nsP3-containing protein complexes in Sindbis virus-infected cells.* J Virol, 2008. 82(20): p. 10088-101.
31. Klose, J., *Protein mapping by combined isoelectric focusing and electrophoresis of mouse tissues. A novel approach to testing for induced point mutations in mammals.* Humangenetik, 1975. 26(3): p. 231-43.
32. O'Farrell, P.H., *High resolution two-dimensional electrophoresis of proteins.* J Biol Chem, 1975. 250(10): p. 4007-21.
33. Gorg, A., W. Weiss, and M.J. Dunn, *Current two-dimensional electrophoresis technology for proteomics.* Proteomics, 2004. 4(12): p. 3665-85.
34. Kang, S.M., et al., *Proteomic profiling of cellular proteins interacting with the hepatitis C virus core protein.* Proteomics, 2005. 5(8): p. 2227-37.
35. Frolova, E., et al., *Formation of nsP3-specific protein complexes during Sindbis virus replication.* J Virol, 2006. 80(8): p. 4122-34.

36. Burnham, A.J., L. Gong, and R.W. Hardy, *Heterogeneous nuclear ribonuclear protein K interacts with Sindbis virus nonstructural proteins and viral subgenomic mRNA.* Virology, 2007. 367(1): p. 212-21.
37. Santoni, V., M. Molloy, and T. Rabilloud, *Membrane proteins and proteomics: un amour impossible?* Electrophoresis, 2000. 21(6): p. 1054-70.
38. Lee, J.Y., J.A. Marshall, and D.S. Bowden, *Characterization of rubella virus replication complexes using antibodies to double-stranded RNA.* Virology, 1994. 200(1): p. 307-12.
39. Atasheva, S., et al., *Development of Sindbis viruses encoding nsP2/GFP chimeric proteins and their application for studying nsP2 functioning.* J Virol, 2007. 81(10): p. 5046-57.
40. Grimley, P.M., I.K. Berezesky, and R.M. Friedman, *Cytoplasmic structures associated with an arbovirus infection: loci of viral ribonucleic acid synthesis.* J Virol, 1968. 2(11): p. 1326-38.
41. Friedman, R.M., et al., *Membrane-associated replication complex in arbovirus infection.* J Virol, 1972. 10(3): p. 504-15.
42. Peranen, J. and L. Kaariainen, *Biogenesis of type I cytopathic vacuoles in Semliki Forest virus-infected BHK cells.* J Virol, 1991. 65(3): p. 1623-7.
43. Barton, D.J., S.G. Sawicki, and D.L. Sawicki, *Solubilization and immunoprecipitation of alphavirus replication complexes.* J Virol, 1991. 65(3): p. 1496-506.
44. Lai, m.M.M., *Cellular factors in the transcription and replication of viral RNA genomes: A parallel to DNA-dependent RNA transcription.* Virology, 1998. 244: p. 1-12.
45. Dijk, A.A.v., E.V. Makeyev, and D.E. Bamford, *Initiation of viral RNA-dependent Rna polymerazation.* J of Gen. Vir., 2004. 85: p. 1077-1093.
46. Blumenthal, T. and G.G. Carmichael, *RNA replication: function and structure of Qbeta-replicase.* Annu Rev Biochem, 1979. 48: p. 525-48.
47. Barrera, I., et al., *Different mechanisms of recognition of bacteriophage Q beta plus and minus strand RNAs by Q beta replicase.* J Mol Biol, 1993. 232(2): p. 512-21.
48. Kopek, B.G., et al., *Three-dimensional analysis of a viral RNA replication complex reveals a virus-induced mini-organelle.* PLoS Biol, 2007. 5(9): p. e220.

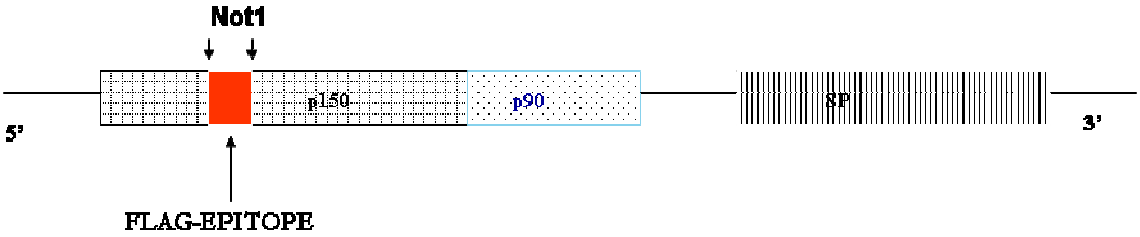

Figure 2.1. Genomic diagram of Robo502-912.
Robo502-912, the experimental virus used in this study, contains a FLAG epitope inserted in a Not I site (nt 1684 and 1685) in the nonstructural replicase protein P150 gene allowing detection of P150 produced by this virus by commercially available FLAG reagents. Insertion of the FLAG epitope tag did not affect the efficiency virus replication and virus titers obtained from this construct was comparable to those produced from the wild type Robo502 virus parent. The Robo502-912 construct was developed by Dr. Wen-Pin Tzeng [9].

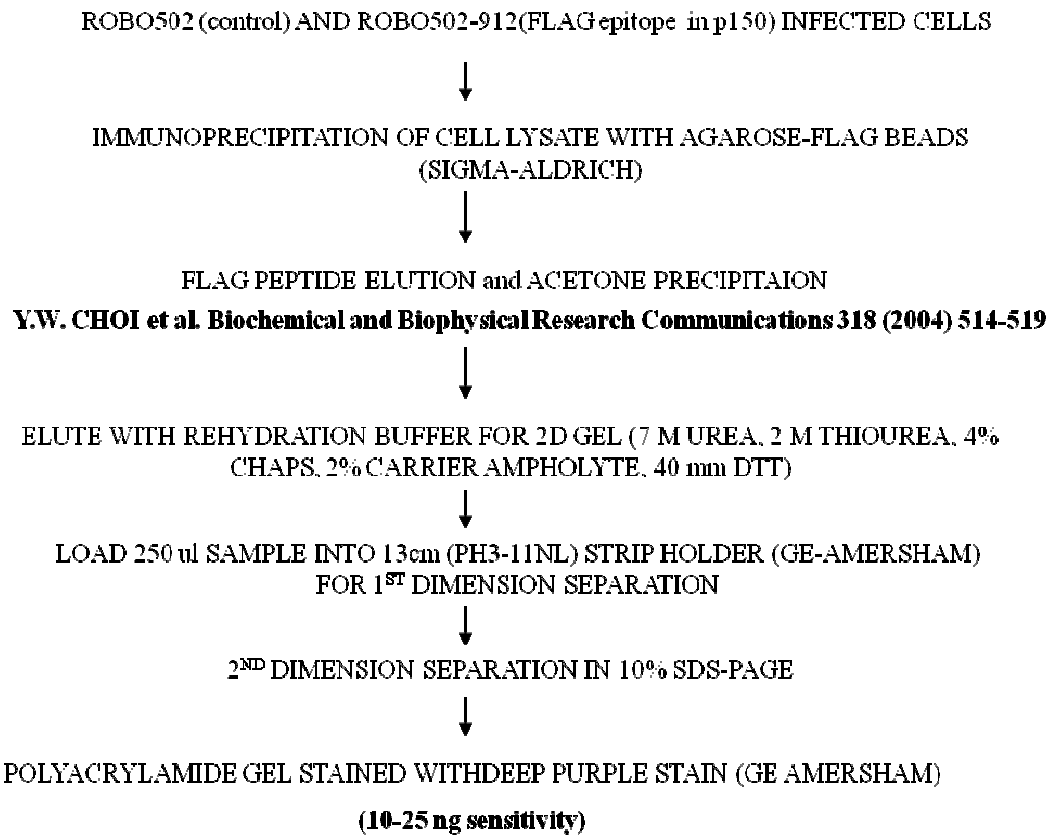

Figure 2.2. Schematic showing the procedures used to identify host cell proteins binding to RUBV P150.

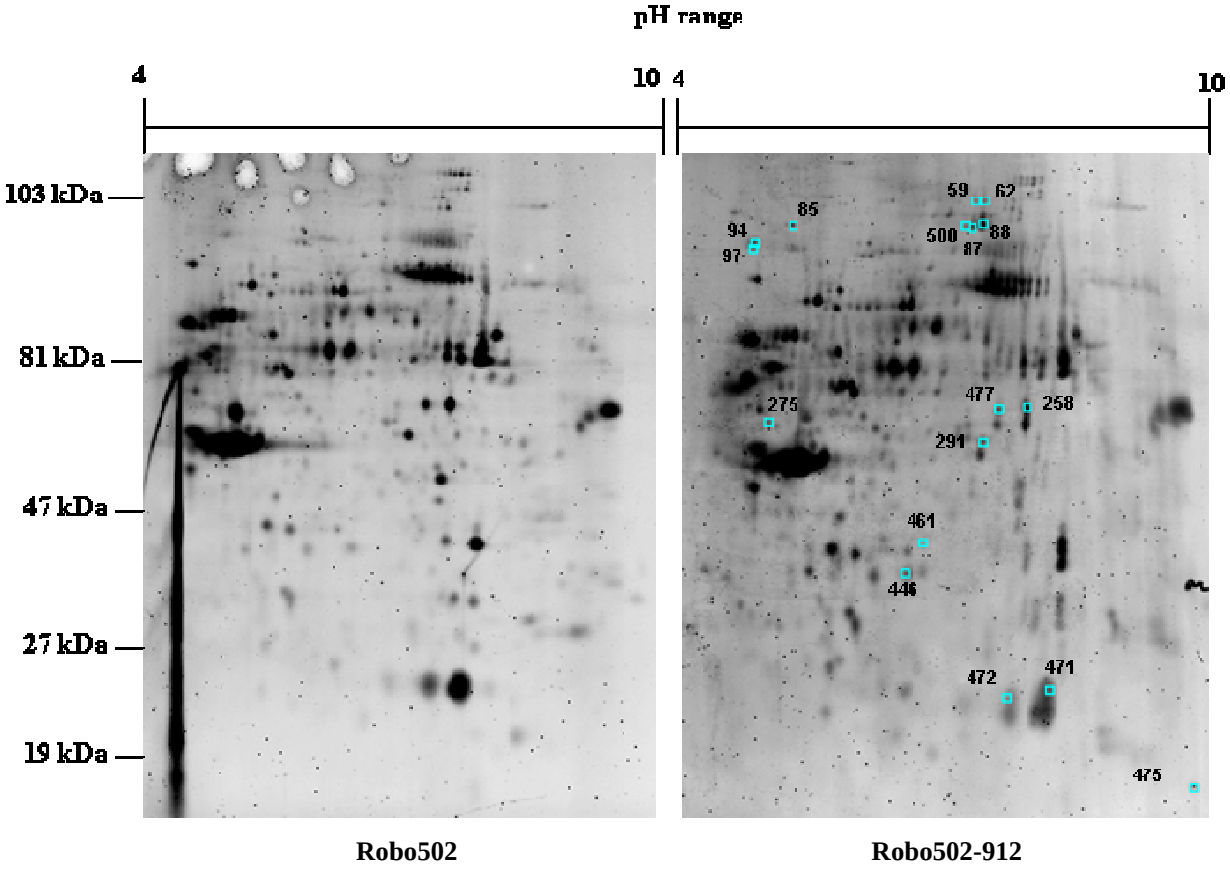

Figure 2.3A. Two-dimensional gel electrophoresis analysis of proteins immunoprecipitating with RUBV P150.
Robo502-912- (FLAG-tagged P150) and Robo502-infected cell lysates were immunoprecipitated using anti-FLAG antibody-conjugated agarose beads and resolved by 2-DE analysis. Proteins were focused on 13 cm Immobiline strips (pH 3-10 non linear range) for the first dimension separation (horizontal), followed by second dimension separation (vertical) by 10% SDS-PAGE. The gel on the left is the control sample (Robo502 infected cells) while the one on the right is the experimental sample (Robo 502-912 infected cells). The gels were stained with deep purple fluorescence stain (GE-Amersham) and viewed with a typhoon imager (GE-Amersham). A total of 17 protein spots were identified using ImageMaster Platinum software (GE-Amersham). Protein spots unique to Robo502-912 infected cells are enclosed within white boxes and the corresponding numbers were assigned by the software. Blow ups of regions of the gel containing unique spots are shown in Figs. 2.3B through 2.3G.

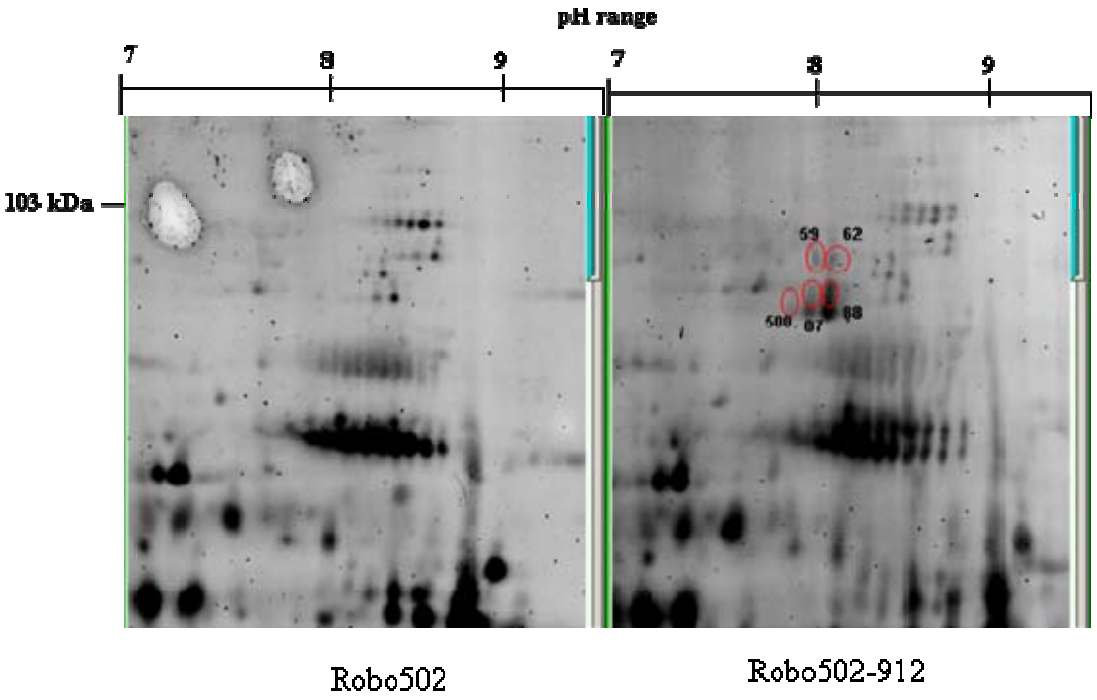

Figure 2.3B. Close-up of 2-DE gel shown in Figure 2.3A.
Protein spots unique to Robo502-912 infected cells are enclosed within circles.

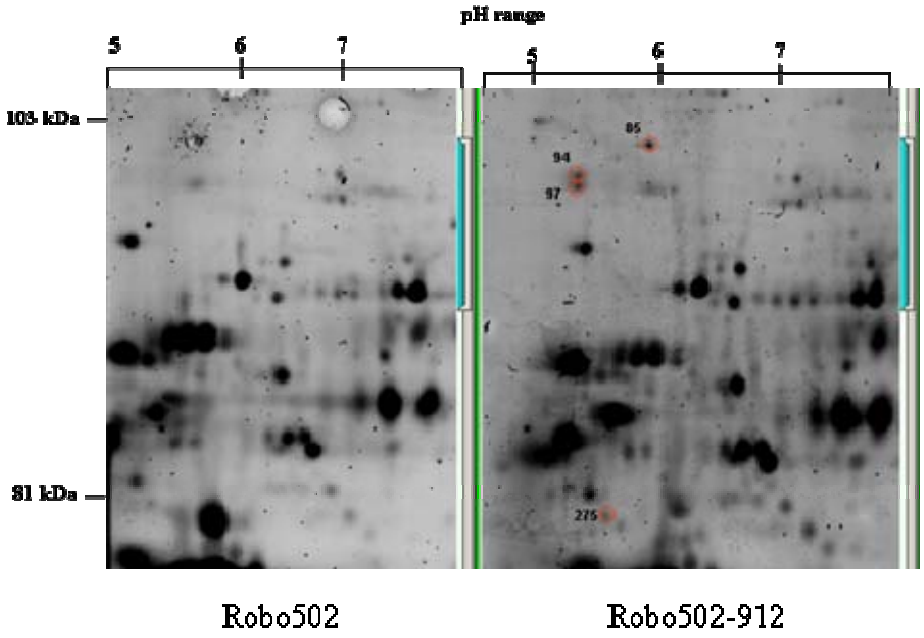

Figure 2.3C. Close-up of 2-DE gel shown in Figure 2.3A.
Protein spots unique to Robo502-912 infected cells are enclosed within circles.

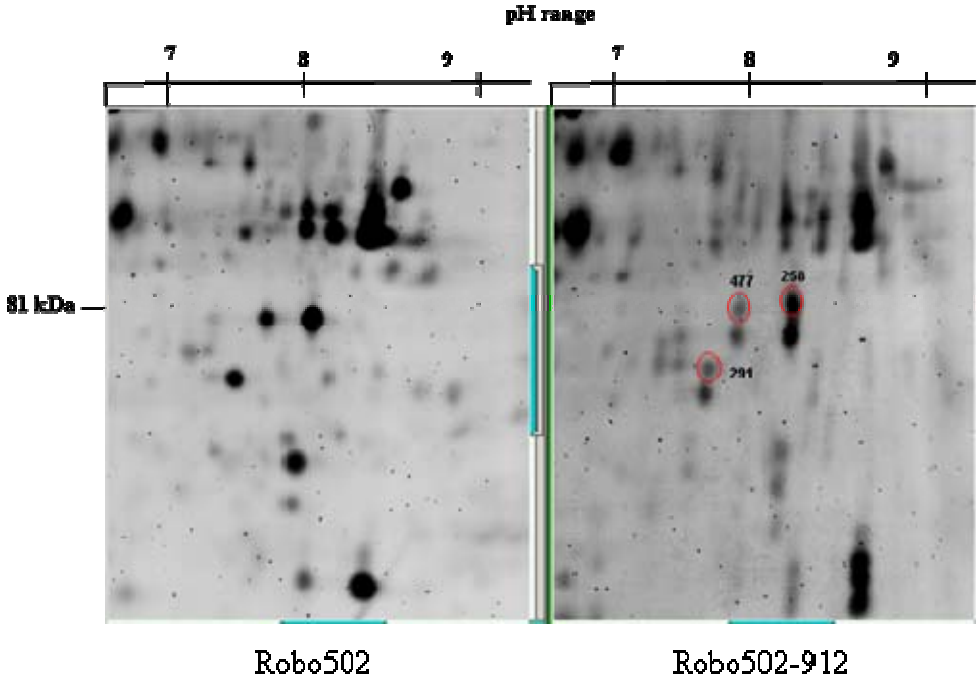

Figure 2.3D. Close-up of 2-DE gel shown in Figure 2.3A.
Protein spots unique to Robo502-912 infected cells are enclosed within circles.

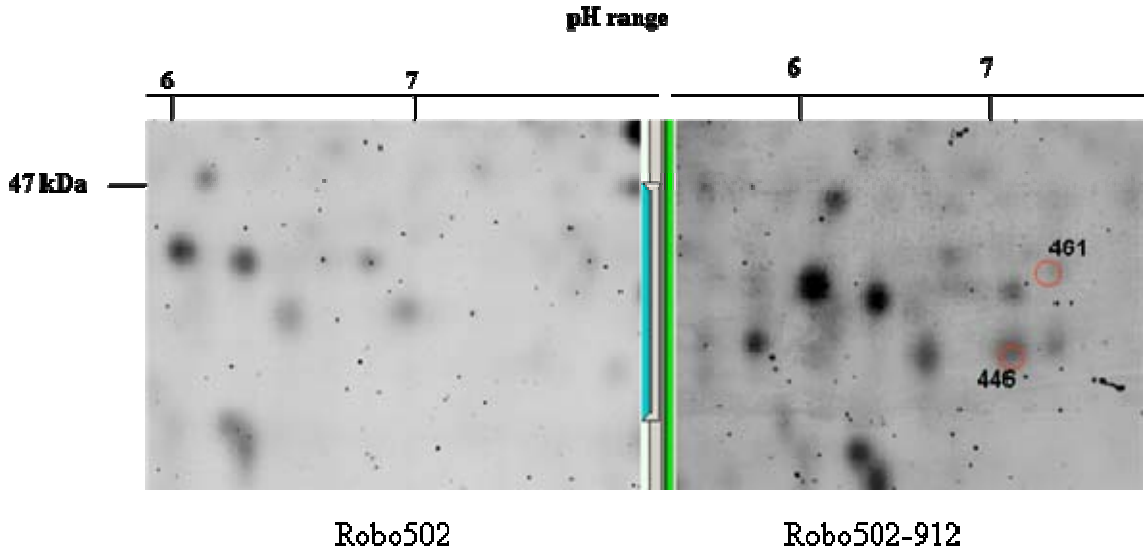

Figure 2.3E. Close-up of 2-DE gel shown in Figure 2.3A.
Protein spots unique to Robo502-912 infected cells are enclosed within circles.

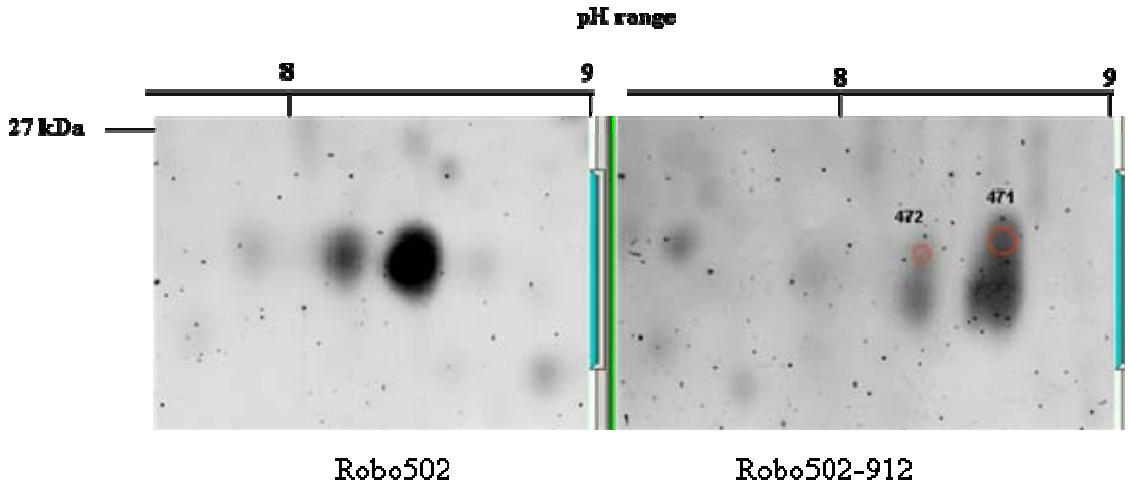

Figure 2.3F. Close-up of 2-DE gel shown in Figure 2.3A.
Protein spots unique to Robo502-912 infected cells are enclosed within circles.

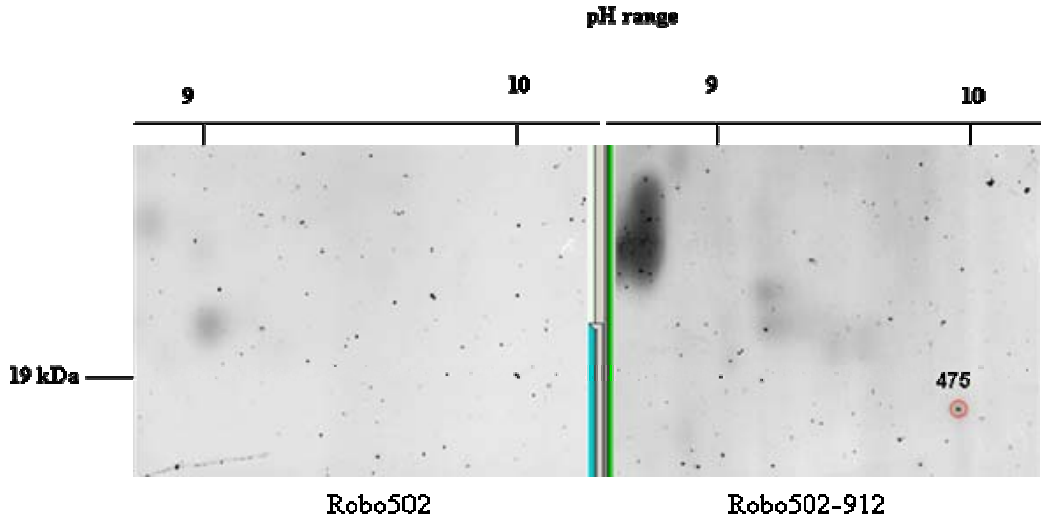

Figure 2.3G. Close-up of 2-DE gel shown in Figure 2.3A.
Protein spots unique to Robo502-912 infected cells are enclosed within circles.

Table 2.1. Mass-spectrometry identification of spots picked from a 2D gel (Fig. 2.3A)
Proteins shown were identified as the top candidates for each of the spots.
**VPS16 was chosen as a candidate protein to confirm interaction and test confidence levels of mass-spectrometry data.*

SPOT NUMBER	IDENTIFIED PROTEIN (ACCESSION NUMBER)	pI	MW	SCORE
59	Zinc finger protein 43 (4508027)	10.07	93426.4	18.06
62	Follistatin-like 5 (28376619)	6.00	95676.2	58.10
85	B-cell CLL/lymphoma 11A isoform 1 (20336305)	6.00	91139.5	18.08
87	Hypothetical protein LOC285513 (33093557)	8.33	82378.8	10.08
88	Excision repair cross complementing rodent repair deficiency, complementation group 4 (4885217)	6.00	104120.4	10.05
94	Predicted: similar to RIKEN cDNA (51471003)	6.00	100184.6	10.05
97	*Vacuolar protein sorting 16 isoform 1 (17978479)	6.00	94633.7	16.09
258	Predicted:hypothetical protein (41149873)	7.17	13248.6	10.06
275	Glycosyltransferase-like 1B (33285008)	8.33	81763.6	10.08
291	PCAF associated factor 65 beta (7657439)	5.13	66113.7	10.07
446	Zinc finger protein 485	10.53	45827.6	10.08
461	Predicted: similar to RIKEN cDNA (51474933)	4.25	50759.8	10.06
471	Brain-specific protein p25 alpha (5902018)	10.53	23679.2	10.09
472	Similar to Protein kinase C, eta type (51493255)	10.53	21150.8	10.07
475	Mitochondrial ribosomal protein L23 (27436904)	10.10	17800.1	10.06
477	Similar to ankyrin repeat domain 30A (51467343)	8.33	81480.2	10.10
500	Hypothetical protein FLJ10466 (8922436)	6.00	73973.7	10.06

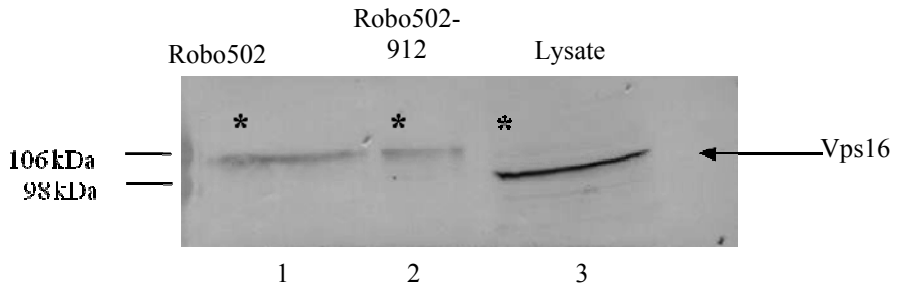

Figure 2.4. Lack of co-immunoprecipitation of Vps16 with P150 antibody.
To test for association between Vps16 and P150, post nuclear fractions of Vero cells infected with Robo502 (lane 1, negative control) or Robo502-912 (lane 2, experimental sample) were immunoprecipitated with anti-FLAG antibody followed by SDS-PAGE and Western blot probed with anti-Vps16 antibody. Lane 3 contains uninfected Vero cell lysate to detect the presence of Vps16 protein. The absence of Vps16 in lane 2 indicates that FLAG tagged P150 does not specifically interact with this cell protein. The asterisks represent unknown protein bands that were immunoprecipitated by Robo502 and Robo502-912 (lanes 1 and 2). There appears to be a very faint protein band at the same location in lane 3 as well. This background protein band could have been enriched in the immunoprecipitated sample.

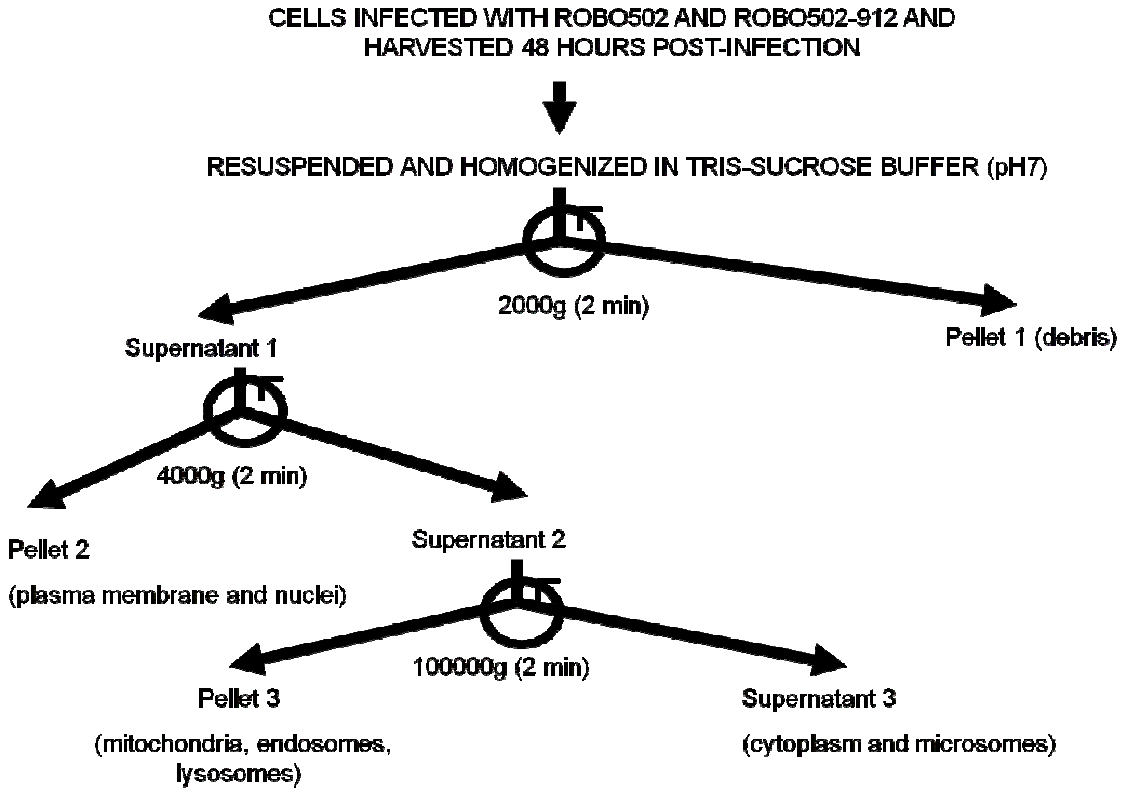

Figure 2.5. Schematic showing the procedures used to fractionate cell lysates to produce a fraction enriched for membranous organelles such as endosomes, lysosomes, and mitochondria plus, putatively, RUBV-induced CPVs.

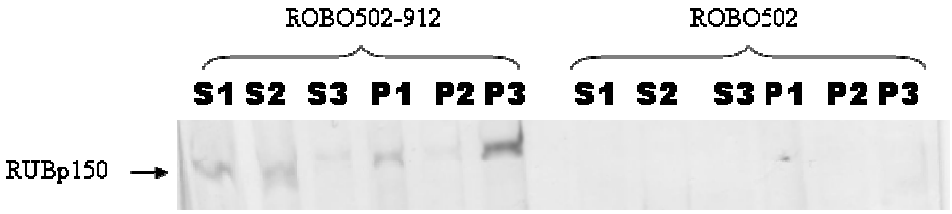

Figure 2.6. P150 distribution in subcellular fractions.
Lysates of Robo502-912 and Robo502-infected Vero cells were fractionated following the procedure outlined in Fig. 2.5. A 1% aliquot (percentage value based on starting material) of each fraction (pellets were solubilized in SDS-PAGE sample buffer) was resolved by 6% SDS-PAGE gel followed by Western blotting probed with mouse anti-FLAG antibody.

Figure 2.7. P150 distribution in high-speed centrifugation fractions.
After the final high speed centrifugation in the fractionation procedure outlined in Fig. 2.5 for lysates of Robo502- and Robo502-912-infected Vero cells, proteins in the supernatant fraction were concentrated by acetone precipitation and resolubilized in SDS-PAGE sample buffer. The P3 pellet was also solubilized in the same amount of SDS-PAGE sample buffer. Equal aliquots were then resolved by 6% SDS-PAGE followed by Western blotting probed with mouse anti-FLAG antibody.

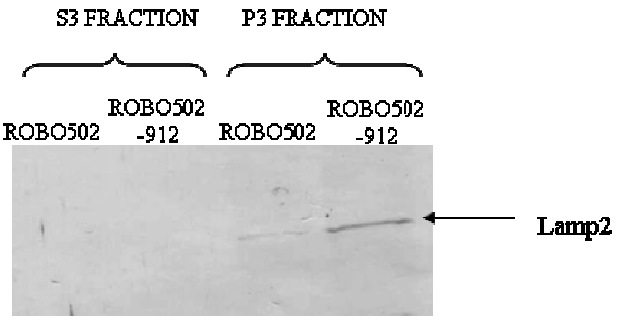

Figure 2.8. Presence of Lamp2 lysosomal marker in high-speed centrifugation fractions. After the final high speed centrifugation in the fractionation procedure outlined in Fig. 2.5 using lysates of Robo502- and Robo502-912-infected Vero cells, the supernatant fraction was concentrated by acetone precipitation and resolubilized in SDS-PAGE sample buffer. The P3 pellet was also solubilized in the same amount of SDS-PAGE sample buffer. Equal aliquots were then resolved by 6% SDS-PAGE followed by Western blotting probed with rabbit anti-Lamp2 polyclonal antibody. The amount of Lamp2 P3 fraction of Robo502 appears less than amounts present in P3 fraction of Robo502-912. This is most probably a result of unequal amounts of protein samples present in each aliquot during this one experiment.

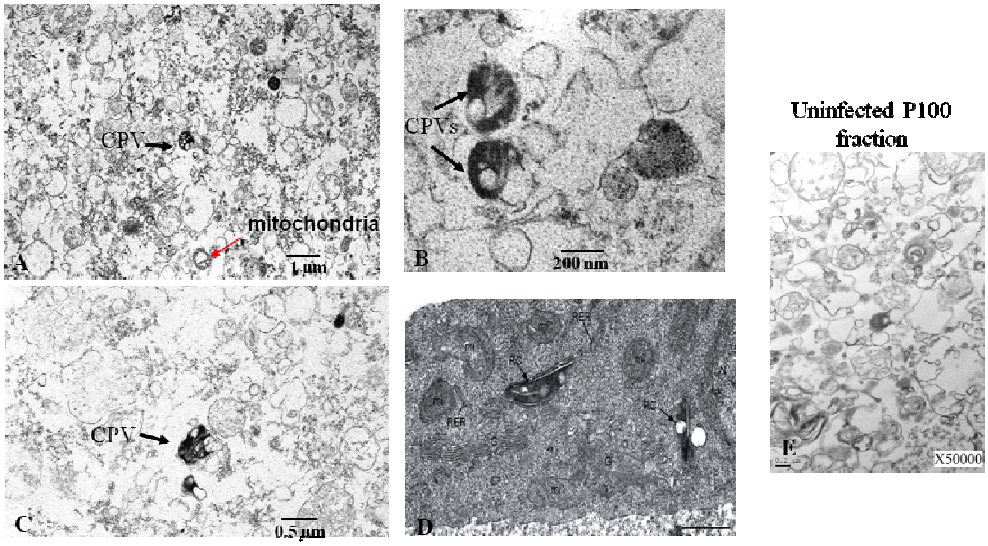

Figure 2.9. Electron micrographs of subcellular structures present in the P3 pellet fraction. Following the fractionation procedure shown in Fig. 2.5, the P3 pellet fractions from uninfected and Robo502-912 infected Vero cells were fixed with 4% glutharaldehye in PBS and sent for transmission EM analysis to Dr Cristina Risco (Centro Nacional de Biotecnologia, Madrid, Spain). Panels A, B and C show micrographs from Robo502-912-infected cells while Panel E shows a micrograph from uninfected cells. CPVs in the infected cells are indicated by arrows. As a comparison, an electron micrograph showing the presence of cytopathic vacuoles (CPV) in RUBV-infected cells is shown in Panel D [3].

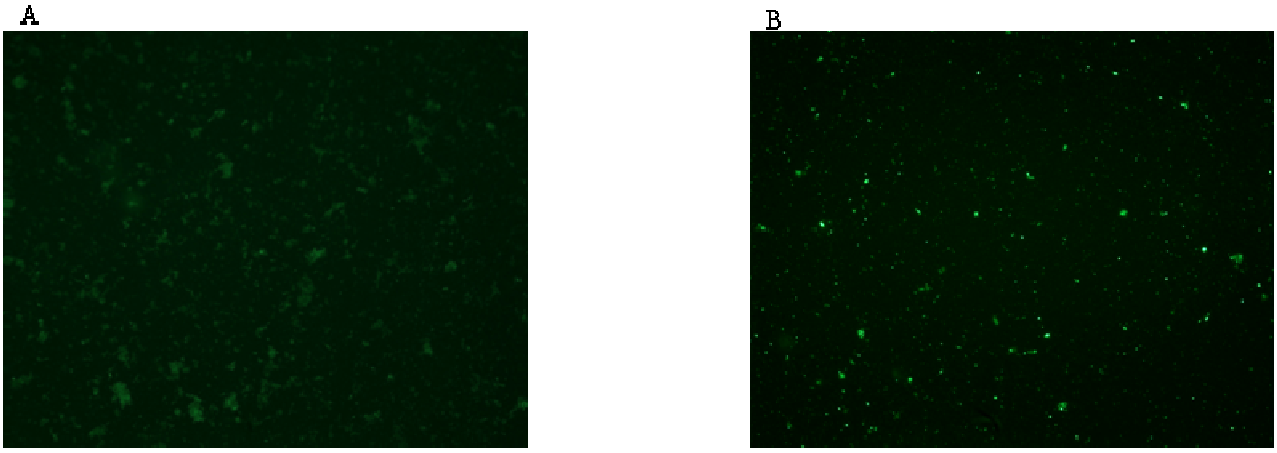

Figure 2.10. Immunoflurescence assay to detect the presence of dsRNA in the P3 pellet fraction.
Following the fractionation procedure outlined in Fig. 2.5, a small amount of the P3 pellet fraction from uninfected (A) or Robo502-912-infected (B) Vero cells was smeared onto an 18 mm glass coverslip and fixed with paraformaldehyde. To detect dsRNA, a replicative intermediate indicative of viral RNA replication, primary antibody to dsRNA, a monoclonal mouse anti-dsRNA antibody, was added followed by secondary anti-mouse FITC labeled antibody. The coverslips were mounted onto glass slides with ProLong gold anti-fade reagent (Molecular Probes/Invitrogen) and visualized with a Zeiss Axioplan 2 microscope with epifluorscence capacity using the 20 X objective.

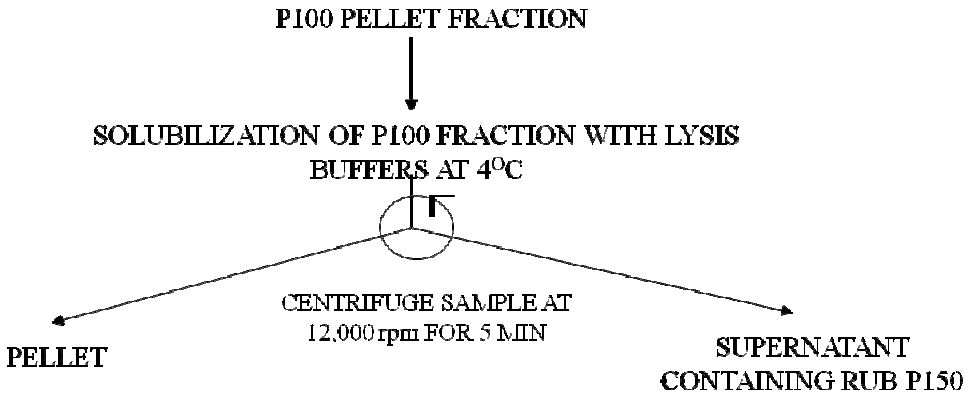

Figure 2.11. Schematic showing the procedure to optimize solubilization of the P3 fraction prior to immunoprecipitation of P150.

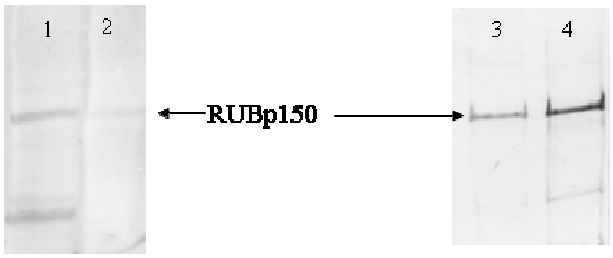

Figure 2.12. Solubilization of the P3 pellet with different lysis buffers.
Following the procedure outlined in Fig. 2.11, the P3 pellet from Robo502-912-infected Vero cells was solubilized with RIPA buffer (Lanes 1 and 4), RIPA buffer lacking SDS and DOC (lane 2) or a buffer containing 2% CHAPS and 2% SB 3-10 (lane 3). After solubilization, equal volumes of the solubilized supernatants were resolved by 6% SDS-PAGE followed by Western blotting probing with mouse anti-FLAG antibody. As can be seen, RIPA buffer gave the best yield.

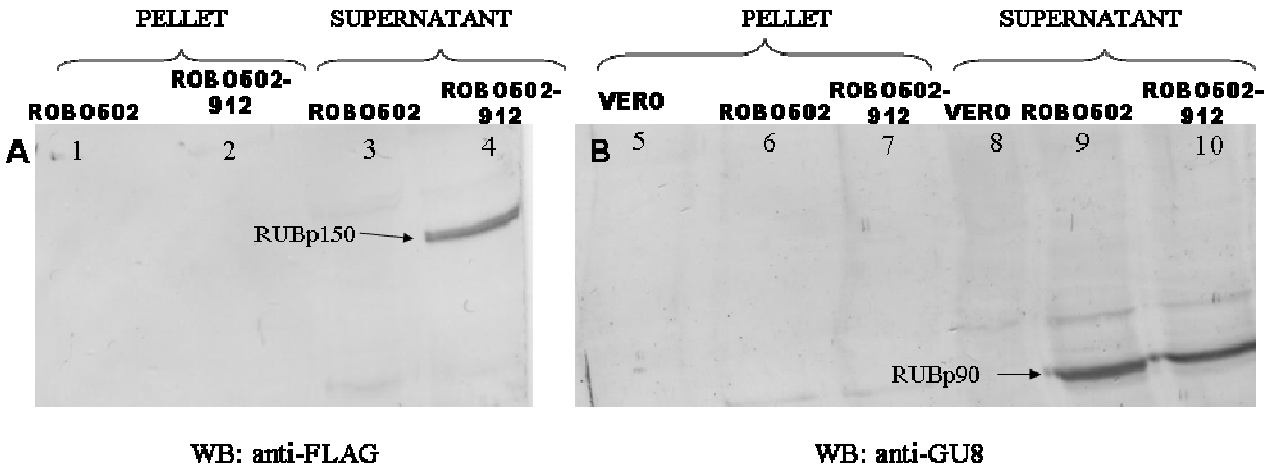

Figure 2.13. Distribution of P150 and P90 following solubilization of P3 fraction with RIPA buffer.
The P3 pellet fraction from uninfected Vero cells or Robo502- or Robo502-912-infected Vero cells was solubilized with RIPA buffer and the resulting supernatants and pellets (see Fig. 2.11) were resolved by 6% SDS-PAGE followed by probing with mouse anti-FLAG antibody (to detect P150, lanes 1-4) or rabbit polyclonal anti-P90 antibody (detects P90 synthesized by either Robo502 or Robo502-912, lanes 5-10). As can be seen, both P150 and P90 were efficiently liberated from the pellet by RIPA buffer.

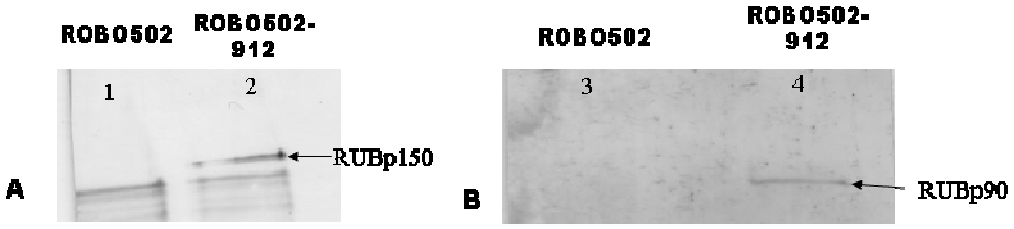

Figure 2.14. Co-immunoprecipitation of P150 and P90 following solubilization of the P3 pellet.

Following solubilization of the P3 fraction from Robo502- (lanes 1 and 3) or Robo502-912- (lanes 2 and 4) infected cells with RIPA buffer (see Fig. 2.11), the supernatants were immunoprecipitated with anti-FLAG antibody to pull-down FLAG-tagged P150. The immunoprecipitated proteins were resolved by 6% SDS-PAGE followed by probing with mouse anti-FLAG antibody (to detect FLAG-tagged P150, Panel A) or rabbit polyclonal GU-8 antibodies (to detect P90, Panel B). As can be seen, P90 co-immunoprecipitated with P150 following lysis of the P3 pellet with RIPA buffer.

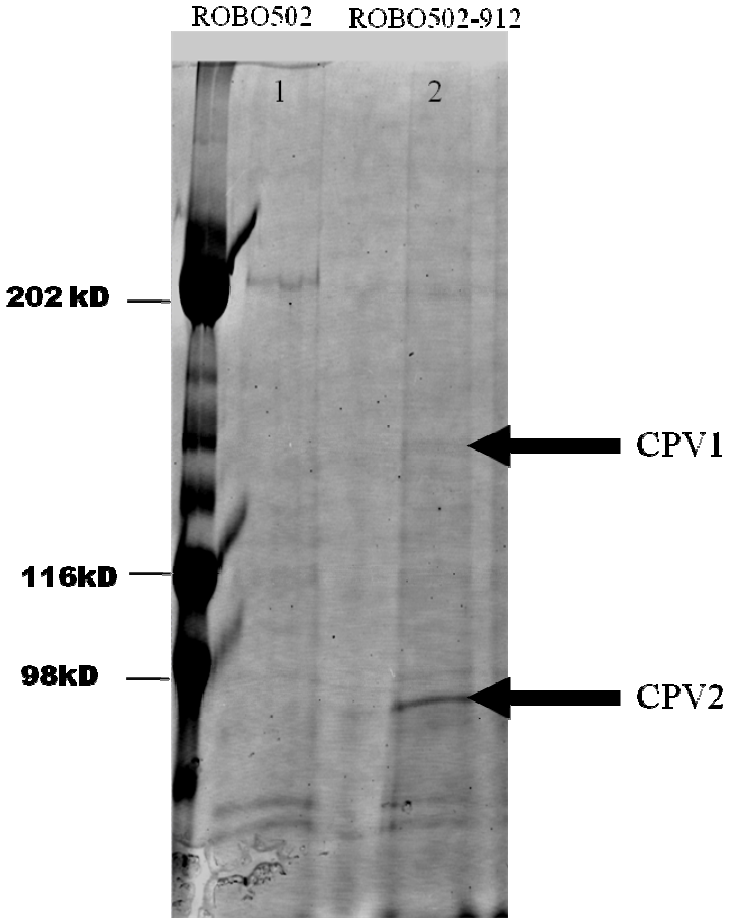

Figure 2.15. 1D SDS-PAGE of proteins immunoprecipitated with P150 in the P3 fraction of RUBV-infected cells.
P3 pellet fractions from Robo502- and Robo502-912-infected Vero cells that had been solubilized with RIPA buffer were immunoprecipitated using mouse anti-FLAG antibody-conjugated agarose beads and the immunoprecipitated proteins were resolved using 6% SDS-PAGE on a 18 X 16 gel format. The gel was stained using GelCode blue and visualized using a Typhoon imager without any filters. Two bands present in the Robo502-912-infected cell lysate, but not in the Robo502-infected cell lysate, designated CPV1 and CPV2, were excised from the gel and sent for identification by trypsin digestion and mass spec.

Table 2.2. Mass-spectrometry identification of proteins co-immunoprecipitated with P150 following cell fractionation to enrich for CPVs.

BAND DESIGNATION	IDENTIFIED PROTEIN	CONFIDENCE
CPV1	RUBELLA VIRUS (p90)	95%
CPV2	RUBELLA VIRUS (P90)	95%

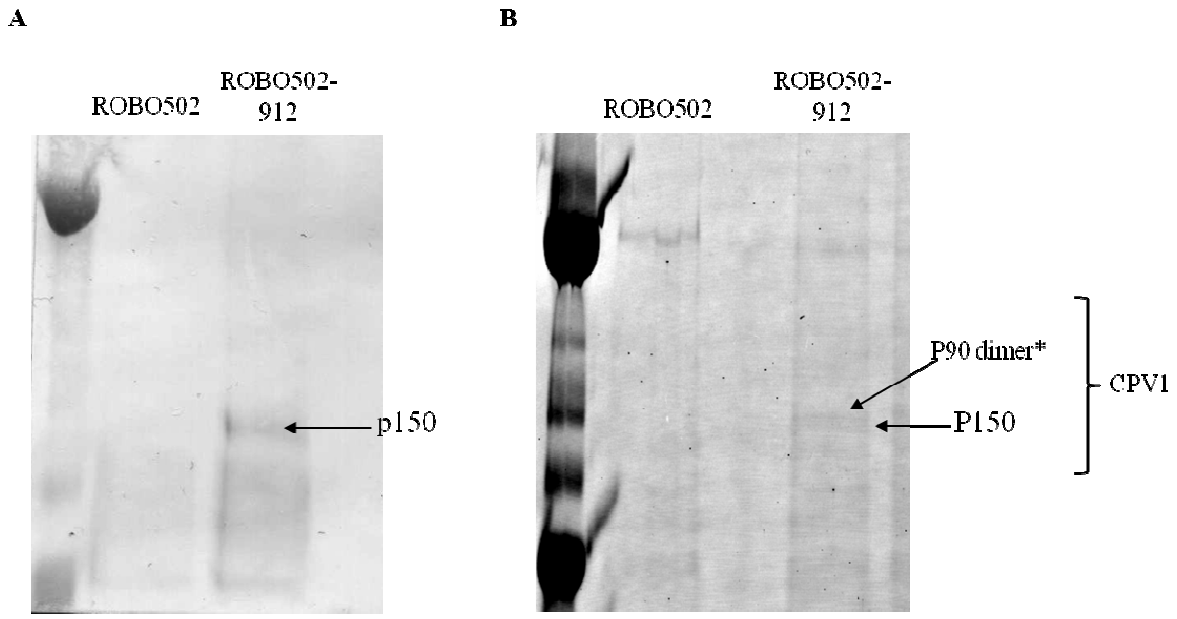

Figure 2.16. Comparison of SDS-PAGE of P150 and CPV1.
To compare the M_r's of P150 and the CPV1 protein band, proteins immunoprecipitated with anti-FLAG antibody from P3 fractions prepared from Robo502- and Robo502-912-infected cells were resolved by 6% SDS-PAGE using the 18 cm X 16 cm format. The area in the region expected to contain P150 was excised and subjected to Western blotting probed with mouse anti-FLAG antibody (Panel A). In comparison with the gel from which CPV1 was identified (Panel B), the presence of two bands in the CPV1 region was evident. During the process of excising protein band for mass-spectrometry analysis, the lower band (representing P150) may have been excluded leaving the upper band (possibly representing P90 dimer) to be excised instead and identified.

CHAPTER 3

Specific aims 2 and 3: To investigate the importance of two SH3 binding domains within the RUBV P150 nonstructural protein in the virus life cycle and identify cell proteins with which they bind

Introduction

Proteins with SH3 domains often bind to ligands containing PxxP motifs in their amino acid sequence [1]. SH3 domains are 50 to 70 amino acids in length and are usually present in proteins in eukaryotic cells involved in signal transduction [2]. Similar SH3 structures have been identified in bacteria [3, 4] and are thought to play a role in bacterial pathogenesis upon infection of a eukaryotic host [5-7]. In addition to signal transduction, SH3 domains in eukaryotes are thought to play a role in directing cell compartmentalization [8, 9]. This hypothesis is based on the finding that SH3 domains are present in various cytoskeletal proteins.

SH3 domains are composed of five β-strands and a single turn of helix [10]. This topology allows formation of two triple-stranded, anti-parallel β–sheets at right angles relative to one another creating hydrophobic pockets that bind PxxP motifs. The mechanism of PxxP binding to SH3 domains has been characterized [11-13]. PxxP motifs form a left handed helical structure with three residues per turn known as polyproline type II (PPII) helix. The PPII helix lacks intramolecular hydrogen bonds, allowing carbonyl groups to form intermolecular hydrogen bonds with target proteins. There are three binding pockets within an SH3 domain. Two of these bind the Px or xP element in the PxxP motif while the third binds to a flanking residue, usually an arginine, that is either before (RxxPxxP) or after (PxxPxR) the PxxP consensus sequence. The twofold pseudosymmetry of the PPII structure allows it to bind to target SH3 domains in two

different orientations, ie in an N- to C-terminal orientation or vice versa. This allows flexibility in binding to a protein with an SH3 domain and may also contribute to the same binding partners having two different functions. Proline is also unique in comparison to other amino acids because it possesses a five-member ring fused onto the nitrogen, making it a secondary amine. This feature allows other proteins to bind to the carbon fused to nitrogen without having to make contact with the rest of the side chain and as a result allows for specific, low affinity interactions to occur [1]. All these features make P-X-X-P domains, and the proline rich region of proteins that contain them, excellent candidates for specific yet weak binding by other proteins [1], a necessity for proteins involved in signal transduction as a quick and readily reversible, yet specific, response is required.

PxxP consensus sequences present in viral proteins have been shown to bind host proteins with SH3 domains [13-17]. Examples of viral proteins with a PxxP consensus sequence that have been found to interact with known cell protein SH3 domains are human immunodeficiency virus (HIV) Nef protein, bovine leukemia virus (BLV) gp30 transmembrane protein, influenza A NS1 protein and hepatitis C virus (HCV) NS5A protein. The interaction of these viral proteins with host proteins containing SH3 domains has been shown to be important for virus replication as well as pathogenicity [14-17]. RUBV has a proline rich region (PRR) in its P150 non-structural replicase protein, stretching from amino acids 716 to 782 of the protein (which contains 1301 aa in total) (Fig. 3.1). Of the eleven PxxP motifs found in this region, three of the motifs fulfill the criteria for the class II binding ligand involving SH3 domains, i.e. PxxPxR. Based on previous findings that proline rich domains of other viral proteins have the ability to interact with host cellular factors that possess SH3 domains, with the result of modulating cell signaling [13, 15, 16, 18] it would not be unexpected to find that the P150 PRR

engages in similar interactions. The goal of this study was to investigate whether the putative SH3 binding domains in the RUB P150 PRR are of significance in the virus replication cycle. If so, it would be a novel finding in the Togaviridae family.

Materials and methods

Cells and virus

The 293-T line of transformed human embryonic kidney cells (HEK) (ATCC) was grown and maintained at 37^{o}C with 5% $CO_{2,}$ in Dulbecco's modified Eagle's medium (DMEM) supplemented with 10% fetal bovine serum (FBS) and penicillin-streptomycin (100 μg/ml). The Vero line of African green monkey kidney cells was grown and maintained at 35^{o}C with 5% CO_2 in DMEM containing 5% FBS and gentamicin (10μg/ml). Two RUBV strains were employed: F-Therein, a wild-type strain, will be referred to as "RUBV" while "Robo502 virus" and its mutants are derived from an infectious cDNA clone.

Mutagenesis of the Robo502 infectious cDNA clone

Site-directed mutagenesis was done to change both prolines in a P-X-X-P-X-R motif to alanines in the Robo502 infectious clone [19]. There are three of these motifs in the proline hinge region, termed Motif 1, Motif 2, and Motif 3, and the following primers were used to create proline to alanine mutations in each motif:

Motif 1 mutation: 5' CAC CCG GCG ACG CCC CGC CGG CGC GCC GCG CAC 3'

Motif 2 mutation: 5' CGG CAC TCC GGC CCC CGC GGC TGC GCG CGA CC 3'

Motif 3 mutation: 5' CCG CCC CCA GCG CGC CCG CGG CAC CCC GCG C TG 3'

These mutagenic primers were combined with forward (5'CGC ATA CGT AGC CTT CCG CGC GTG G 3'; SnaBI site underlined) and reverse (5' GTG GGG GCG GTC CGA GAC GC 3'; Rsr II site underlined) primers in a protocol described previously [20] that introduces

mutations using two rounds of PCR amplification in a single reaction tube. The amplification reaction included: *50-100* ng linearized Robo502 template, 1.0 pmol internal mutagenic forward primer (i.e. Mut1, Mut2, or Mut3),, 0.05 pmol reverse primer, 4 ul 2.5 mM dNTPs, 5 ul 10X Ex-taq buffer (Takara), 10 ul 5X Q solution (Qiagen), 0.5 ul Ex-taq polymerase (Takara) and 29 ul dH_2O . Briefly, the first round of PCR in which mutagenic and reverse primers were added, was done with using the following PCR parameters: 5 cycles of 95^0C for 1 minute, 60^0 C for 30 sec, 72^0 C for 2 min followed by a final incubation at 72^oC for 35 minutes. Following the final 35 minute incubation step, 1 µl of 125 ng/µl forward primer was added and the reaction continued using the following protocol: 25 cycles of 96^0 C for 1 min, 65^0 C for 30 sec, 72^0 C for 2 min followed by 72^0 C for 10 min**.** The extended 35 minute incubation step in the first round of PCR helps the utilization of reverse and mutant primers so that only completed mutagenic megaprimers are present in the final step of the PCR reaction. PCR products were purified by phenol/chloroform extraction, precipitated with ethanol, and digested using Rsr II and SnaBI 1 restriction enzymes (NEB). The resulting fragments were gel purified (Qiagen gel extraction kit) and reintroduced into Robo502 digested with the same restriction enzymes to replace the corresponding wt fragment. Mutagenesis was confirmed by sequencing the entire length of the mutagenized fragment (done by the GSU core facility). The mutant constructs were named Mut1-Robo502, Mut2-Robo502 and Mut3-Robo502 for mutations made in the Motifs 1, 2 and 3 respectively. To make constructs with mutations in motifs 1 and 2 or Motifs 1, 2, and 3 in combinations, a single mutant construct was used as the DNA template and mutations in the other motifs were made sequentially using the protocol described above. These constructs were named Mut1+2-Robo502 and MutX-Robo502 (triple mutant).

Construction of RUBV proline-hinge-GST fusion constructs

The putative SH3-binding domain in P150, between nucleotides 2189 through 2461 of the RUBV genome (between amino acid sequence 716 and 782), was amplified from the Robo502 template using forward and reverse primers that contain BamH I and Cla I restriction sites respectively: 5'**GGA TCC** TCC GCG GCC GCG TCA CCG CCA 3' and 5' **ATC GAT** GTC GCT GTC TGG GTC TGC CCT 3'. The amplified PCR product was digested with BamH I and Cla I (NEB), gel purified (Qiagen gel extraction kit) and ligated into a pEBG mammalian expression vector (provided by Dr Tom Hobman, U. Alberta) that was digested with the same enzymes, creating a construct termed GST-PRR/RUB. A pEBG-Mut 1+2 construct was created using the strategy described above with the GST-PRR/RUB construct as the template, the forward and reverse primers used to amplify the sequence introduced into PRR/RUB, and the Mut1 and Mut2 mutagenic primers. The mutation was confirmed by sequencing. This construct was named GST-PRR/RUB MUT 1+2.

Analysis of PRR mutations created in Robo502

Ten ug of Robo502, Mut1-Robo502, Mut2-Robo502, Mut3-Robo502, double mutant Mut1+2-Robo502, and triple mutant MutX-Robo502 were linearized with EcoR I. The linearized templates were purified by phenol/choloroform extraction and precipitated by addition of 0.1 volume of 3M ammonium acetate and 2.5 volume of ethanol. The precipitated DNA was dissolved initially in 40 μl of deionized water and after determination of the DNA concentration spectrophotometrically ($O.D._{260}$), the volume was adjusted to a final concentration of 250 ng/μl. Each template was used in the following *in vitro* transcription reaction: 5 μl of 5X transcription buffer (40 mM Tris-HCl [pH 7.5], 6 mM $MgCl_2$, 2 mM spermidine) (Epicentre, Madison, Wis), 2.5 μl of 100 mM DTT, 1.0 μl of RNasin ribonuclease inhibitor (Promega), 1.0 μl of 25 mM

NTPs (Amersham), 5.0 μl of 10 mM cap analogue [$m^7G(5')ppp(5')G$] (New England BioLabs), 1 μl of SP6 DNA dependent RNA polymerase (25U; Epicentre, Madison, Wis.), 2 μl of 250 ng/μl linearized template, and deionized water to make a final volume of 25 μl. The reactions were incubated for 1 hour at 37^oC and the quality of the product was ascertained by agarose gel electrophoresis and ethidium bromide staining. Reaction mixtures were used directly for transfection. Sixty mm culture plates of 100% confluent Vero cells were transfected with 30 μg of an RNA transcript from the wild type or mutant constructs using Lipofectamine 2000 following the manufacturer's recommended protocol (GIBCO BRL, Lifetechnologies). The cells were incubated with the transfection mixture for at least 4 hours after which transfection mixture was removed and replaced with Dulbecco's modified Eagle's medium (DMEM) supplemented with 5% fetal bovine serum (FBS) and penicillin-streptomycin (100 μg/ml). The transfected cells were observed microscopically daily for development of cytopathic effect (CPE) and the medium was collected one week post-transfection; this was designated Passage 0 or P0. Titers of virus in the P0 medium were determined by plaque assay [21]. P0 medium was subsequently passaged by infecting 60 mm plates of Vero cell lines (P1) at a multiplicity of infection (MOI) of 1 pfu/cell. Seven days post infection, the P1 medium was collected. An aliquot of the P1 medium was titered by plaque assay and total intracellular RNA was extracted from the infected cells using Tri-Reagent (Molecular Research Center, Inc) according to the manufacturer's protocol. To produce a cDNA template for sequencing, reverse transcription was done using the following protocol: 5 μl of RNA solution was boiled for 5 minutes and then incubated on ice for 5 minutes. One μl of reverse primer (5' ATC GAT GTC GCT GTC TGG GTC TGC CCT 3': nt 2440-2467), 3 μl of deionized water, and 4 μl of 2.5 mM dNTPs were added followed by incubation at 65^oC for 8 minutes. The reaction was cooled in ice and 4 μl of 5X first strand

buffer (Invitrogen), 1 μl of 0.1 M DTT, 1 μl of RNasin RNase Inhibitor (Promega), and 1 μl of Superscript III RNase H Reverse transcriptase (Invitrogen; 200U/μl) were added to make a total reaction volume of 20 μl. The reaction was incubated at 55^{o}C for 1 hour and the cDNA product was subsequently used for PCR amplification. The 50 μl PCR reaction contained: 2 μl of cDNA template, 1 μl of 200 ng/μl forward and reverse primers (5'CGC ATA CGT AGC CTT CCG CGC GTG G 3' and 5' GTG GGG GCG GTC CGA GAC GC 3'; recognizing nt 1204-1229 and 3877-3897, respectively), 4 μl of 2.5 mM dNTP's, 25 μl of GC buffer (Takara), and 0.5 μl of Ex-Taq DNA polymerase (Takara; 5U/μl). The PCR protocol was as follows: 25 cycles of 96^{o}C for 1 min, 65^{o}C for 30 sec, and 72^{o}C for 2 min followed by and incubation at 72^{o}C for 10 min. The PCR product was gel purified (0.7% agarose) using a Qiagen gel extraction kit. The PCR product was sequenced by the GSU Core Facility.

Analysis of PRR mutant RNA and DNA synthesis

Mutations in motifs 1, 2, and 1+2 were introduced into the Robo502-903 infectious clone that yields viruses which express P150 with an HA epitope tag. Mutations were done with mutagenic primers for motifs 1 and 2 (shown earlier) using an asymmetric 3 round PCR protocol as described previously [22]. These manipulations were done by Dr. Wen-Pin Tzeng.

Northern blot analysis of viral genomic and subgenomic RNA produced by wild type and mutant infectious clones was performed as described previously [23]; this analysis was performed by Dr Wen-Pin Tzeng. RNA was extracted from cells transfected with wild type and mutant infectious clones using Tri-Reagent (Molecular Research Center, Inc) according to the manufacturer's protocol. For Northern gel analysis, equivalent amounts of RNA were denatured with Glyoxal Sample Loading Dye (Ambion, Austin, TX) for 30 min at 55°C and placed on ice immediately. The denatured RNA was electrophoresed in a 1% agarose gel made in

NorthernMax-Gly Gel Preparation/Gel Running Buffer (Ambion). After electrophoresis, the RNAs were transferred to a nylon membrane (0.45-mm pore diameter; MSI, Magnagraph, Westboro, MA) by capillary action for 2 hours using NorthernMax Transfer Buffer (Ambion) as the transfer medium. After transfer, the nylon membrane was irradiated with a 254-nm UV Crosslinker Lamp (Fisher Scientific, Pittsburgh, PA). The membrane was heat-sealed in a plastic bag containing NorthernMax Prehyb/Hyb Buffer (Ambion) and prehybridized for 2 hours at 65°C. Nick-translated VR-C-E2-E1 probe (0.5 to 1 mg), which encodes the viral structural ORF was radiolabeled by nick translation using a Nick Translation System Kit (Promega, Madison, WI) and 50 μCi of [α-^{32}P]dCTP (3000 mCi/mmol; New England Nuclear, Boston, MA). Half of the nick-translated DNA probe was denatured in 50% formamide at 100°C for 5 min and added to the blot in Prehyb/Hyb Buffer and hybridization was allowed to proceed at 65°C overnight. After hybridization, the membrane was washed at room temperature once in Low-Stringency Wash Solution 1 (Ambion) for 10 min and twice in High-Stringency Wash Solution 2 (Ambion) for 15 min at 42°C. Washed membranes were wrapped in plastic wrap and exposed to Kodak X-ray film at -70°C between two Cronex Lightning Plus intensifying screens.

Vero cells transfected with the wild type and mutant Robo502 constructs were also analyzed for P150 expression at 6 hours and 3 days post-transfection. Briefly, cells were harvested 6 hours and 3 days post-transfection using RIPA buffer (10 mM Tris-HCl pH 7.4, 150 mM NaCl, 3 mM EDTA, 1% Triton X-100, 0.1% SDS, and 0.5% DOC). An equal volume of the post-nuclear fraction from wild type and mutant construct transfected lysates was mixed with 2X SDS loading buffer (100 mM Tris-HCl pH6.8, 20 mM dithiothreitol, 4% SDS, 0.2% bromophenol blue, and 20% glycerol) and resolved by electrophoresis on 6% SDS polyacrylamide gels (6% acrylamide, 0.38 M Tris pH 8.8, 0.1% SDS, 0.1% ammonium

persulfate). Proteins were transferred onto nitrocellulose membrane (Whatman) using 1X transfer buffer (100 ml 10X transfer buffer [250 mM Tris, 1.92M glycine], 200 ml 100% methanol, and 700 ml deionized water) at 100V for 1 hour in a mini-Protean II apparatus (Biorad). Following transfer, the membranes were blocked overnight with 5% non-fat milk powder in TBS (20 mM Tris-HCl, pH 7.5 and 175 mM NaCl). The blot was probed with mouse anti-HA monoclonal antibody (Roche) (1:1000 dilution) in antibody dilution buffer (1% non-fat milk powder, 0.02% sodium nitrate in TBS buffer [20 mM Tris-HCl, pH 7.5 and 175 mM NaCl]). After addition of primary antibodies, membrane was washed three times for 10 minutes each with 0.05% T-TBS (0.05% Tween-20 sorbitol in 1X TBS). Secondary anti-mouse antibody (Promega) conjugated with alkaline phosphatase, diluted in antibody dilution buffer (1:7500) was used to detect the presence of HA epitope tagged P150. Once again, membrane was washed 3 times for 10 minutes each with 0.05% T-TBS and bound antibodies were detected with a BCIP/NBT (Roche) colorimetric assay.

Transfection with pEBG constructs and identification of interacting cell proteins

Sixty mm dishes of confluent 293-T cells were transfected with pEBG constructs using Lipofectamine 2000 (Invitrogen) according to the manufacturer's protocol. Briefly, each plate was transfected with 5-10 μg of DNA and the transfection mixture was left on the cells for at least 4 hours before being replaced with Dulbecco's modified Eagle's medium (DMEM) supplemented with 10% fetal bovine serum (FBS) and penicillin-streptomycin (100 μg/ml). Three days post-transfection, the cells were washed twice with lysis wash buffer (1% Nonidet P-40, 150 mM NaCl, 50 mM Tris-HCl pH 7.4, 2 mM EDTA and 150 mM sodium salicylate) and lysed with 1% NP40 buffer (1% NP40, 150 mM NaCl, 50 mM Tris-HCl pH 7.4 and 2 mM EDTA) and GST fusion proteins were isolated from the lysate using gluthathione sepharose 4B

beads (Amersham Pharmacia Biotech. Inc). Briefly, 0.5 ml gluthathione sepharose 4B beads (GST beads) were prewashed with 5 ml of phosphate buffered saline (PBS) containing 0.1% Triton X-100, collected by low speed centrifugation and resuspended in final volume of 5 ml PBS containing 0.1% Triton X-100. Before incubation of transfected cell lysates with the GST beads, the lysates was precleared with an equal volume of unconjugated sepharose beads (Sigma). Following the preclearing step, 0.5 ml gluthathione beads were incubated with 5 ml of lysate for 3 hours at 4^{o}C, after which the beads were washed seven times with lysis buffer (1% NP40, 150 mM NaCl, 50 mM Tris-HCl pH 7.4 and 2 mM EDTA), and adherent proteins were eluted with 2X SDS gel loading buffer (50 mM Tris-HCl, pH 6.8, 100 mM DTT, 2% SDS, 0.1% bromophenol blue and 10% glycerol). The proteins were resolved by 6% or 10% SDS-PAGE and proteins were visualized by GelCode blue staining reagent (Piercenet). Proteins of interest (ie. those that bound to GST-PRR/RUB but not GST-PRR/RUB MUT1+2 or the GST control) were excised with a scalpel and sent for trypsin digestion and mass-spectometry analysis to the facility at the Morehouse School of Medicine or the Scripps Institute (TSRI Center for Mass Spectrometry). Protein plugs were maintained in 4^{o}C until transferred to these facilities.

Construction of hemagglutinin (HA) and c-myc epitope tagged p32 protein

The simian p32 gene in a pCB6 [24] vector was kindly provided by Dr. Tom Hobman (University of Alberta). Two p32 constructs were made, one, with HA and c-myc epitope tags on the N- and C- termini, respectively, and the other with a c-myc epitope on the C-terminus. The PCR primers used to create the first construct were 5' CGA GCT AGC CCA TGT ACC CAT ACG ACG TCC CAG ACT ACG CTA TGC TAC CTC TGC TGC GCT GC 3' (forward primer) and 5' CGA GAA TTC CTA CAG ATC TTC TTC AGA AAT AAG TTT TTG TTC CTG GCT CTT GAC AAA ACT C 3' (reverse primer) and to create the second construct were 5' CTA

GCT AGC CCA TGC TAC CTC TGC TGC GCT GCG 3' (forward primer) and 5' CGA GAA TTC CTA CAG ATC TTC TTC AGA AAT AAG TTT TTG TTC CTG GCT CTT GAC AAA ACT C 3' (reverse primer). Nhe I and Eco RI restriction sites (underlined) were introduced for the forward and reverse primers, respectively. Fifty μl PCR reactions contained 1 μl of pCBP6-p32 DNA template, 1 μl each of 200 ng/μl forward and reverse primers, 4 μl of 2.5 mM dNTPs, 10X buffer (Takara), and 0.5 μl of Ex-Taq DNA polymerase(Takara; 5U/μl). The PCR protocol was as follows: 25 cycles of 96^{o}C for 1 min, 65^{o}C for 30 sec, and 72^{o}C for 1 min followed by an incubation at 72^{o}C for 10 min. The PCR product was gel purified (0.7% agarose) using a Qiagen gel extraction kit. The PCR product was sequenced by the GSU Core Facility. The PCR products were digested with Nhe I and EcoR I, gel purified (Qiagen gel purification kit), and ligated into the pcDNA expression vector (Invitrogen) digested with the same enzymes. The resulting constructs were named "pcDNA-HA-p32-myc" and pcDNA-p32-myc", respectively.

Immunoprecipitation and Western blot analysis

Vero cells infected with Robo502-912 (with FLAG tagged P150 as described in the first Specific Aim) and transfected with pcDNA-HA-p32-myc were lysed with RIPA buffer (10 mM Tris-HCl pH 7.4, 150 mM NaCl, 3 mM EDTA, 1% Triton X-100, 0.1% SDS, and 0.5% DOC in the presence of 1X mini complete protease inhibitor [Roche]). Another set of co-transfections was done to investigate the interaction of p32 with P150 without the presence of the RUBV capsid protein. To this end, a plasmid expressing HA-tagged P150 (CMV-P150-HA; provided by Dr. Wen-Pin Tzeng) was employed to transfect Vero cells either alone or with pcDNA-p32-cmyc. Two days post-transfection, cells were harvested and 250 μl of lysate was used for immunoprecipitation studies. Briefly, 1 μl of mouse anti-HA, anti-c-myc monoclonal antibody (Roche) or rabbit anti-C1QBP polyclonal antibody (CeMines) was added as appropriate. Lysate

was incubated with the appropriate antibodies for 2 hours at 4^{o}C. Thirty µl of agarose A beads (Roche) were added to the mixture and incubated for an additional hour. The beads were washed five times with lysis wash buffer (10 mM Tris-HCl pH 7.4, 150 mM NaCl, 0.5% Triton X-100, 0.5% DOC, and 3 mM EDTA) and proteins were eluted by boiling with 60 µl 2X SDS gel-loading buffer (100 mM Tris-HCl pH6.8, 20 mM dithiothreitol, 4% SDS, 0.2% bromophenol blue, and 20% glycerol). Samples were resolved using 6% or 10% SDS-PAGE (6% or 10% acrylamide, 0.38 M Tris pH 8.8, 0.1% SDS, 0.1% ammonium persulfate). Proteins were transferred onto nitrocellulose membrane (Whatman) using 1X transfer buffer (100 ml 10X transfer buffer [250 mM Tris, 1.92M glycine], 200ml 100% methanol, and 700 ml deionized water) at 100V for 1 hour in a mini-Protean II apparatus (Biorad). Following transfer, the membranes were blocked overnight with 5% non-fat milk powder in TBS (20 mM Tris-HCl, pH 7.5 and 175 mM NaCl). The blot was probed with mouse anti-HA monoclonal antibody (Roche) (1:1000 dilution), mouse anti-FLAG monoclonal (Sigma)(1:1000 dilution) or rabbit anti-p32 antibody (CeMines)(1:1000) in antibody dilution buffer (1% non-fat milk powder, 0.02% sodium nitrate in TBS buffer [20 mM Tris-HCl, pH 7.5 and 175 mM NaCl]). After addition of primary antibodies, membrane was washed three times for 10 minutes each with 0.05% T-TBS (0.05% Tween-20 sorbitol in 1X TBS). Secondary anti-mouse antibody (Promega) conjugated with alkaline phosphatase, diluted in antibody dilution buffer (1:7500) was used to detect the presence of HA epitope tagged P150. Once again, membrane was washed 3 times for 10 minutes each with 0.05% T-TBS and bound antibodies were detected with a BCIP/NBT (Roche) colorimetric assay.

Immunofluorescence assay

The intracellular localization of HA-tagged P150 and c-myc-tagged p32 was analyzed by immunofluorescence (IFA) as described previously [25]. Briefly, Vero cells were plated on 18 mm glass coverslips placed in 35 mm plates (1:25 ml dilution). Cells were transfected with pcDNA-p32-myc and co-transfected with CMV-P150-HA or infected with Robo502-930 (expressing an HA-tagged P150). Forty eight hours post transfection, the cells were fixed with 4% paraformaldehyde in PBS for 30 min at 4^{o}C and permeabilized with PBS-0.25% saponin for 10 min at room temperature. The coverslips were removed from the culture dishes, washed again with PBS, and blocked by incubation with PBS, 2% BSA, 0.25% saponin for 30 min at room temperature. Primary antibodies diluted 1:500 in PBS, 0.1% BSA, 0.25% saponin were placed on the coverslip and incubated for 1 hour at room temperature. The primary antibodies used were mouse anti-HA monoclonal antibody (Roche), mouse anti-c-myc monoclonal antibody (Roche) or rabbit anti-C1QBP (CeMines) polyclonal antibody (all in 1:500 dilution). After washing three times in PBS, secondary mouse anti-FITC antibody and rabbit anti-TRITC antibody diluted 1:1000 in PBS, 0.1% BSA, 0.25% saponin were added and incubated for 30 minutes at room temperature. 1:1000 dilution of Hoechst was added in the reaction during the last 2 minutes of incubation. Following washing with PBS, the coverslips were mounted on glass slides using ProLong gold anti-fade reagent (Molecular Probes/Invitrogen). The cells were visualized using a Zeiss Axioplan 2 imaging system at 100X magnification.

RUBV replication in cells overexpressing p32

Vero cells were either mock transfected or transfected with pcDNA-p32-myc as described above. One day post-transfection, both cultures were infected with wt RUBV at an MOI of 1. The cells were examined daily by microscopy for development of CPE and the medium was collected each day through four days post-infection and subsequently titered by plaque assay [21].

Results

Effect of mutagenesis of the putative SH3 binding domain in P150 on virus replication

Fig. 3.1A shows a schematic diagram of the domains within RUBV P150, including the proline rich region (PRR) of interest. The PRR is located between amino acid residues 716 through 782 of P150. This region is also known as the hypervariable region or, HVR as it is the most variable region of the RUBV genome among natural RUBV isolates [26]. Analysis of the PRR using ScanProsite software (Expasy Proteomics Server) led to the identification of 3 putative Class II SH3 binding motifs with the consensus amino acid sequences "P-x-x-P-x-R". Fig. 3.1B shows the sequence of the PRR with the three putative SH3 binding motifs in color. These putative SH3 binding motifs are referred to as motifs 1, 2 and 3, from the N- to C-terminus of the PRR respectively. An alignment of sequences of the PRR from viruses of 7 genotypes showed that all three motifs were highly conserved (Fig. 3.2), with the exception of the Anam5_KOR96 strain of RUBV that had a serine instead of a proline in motif 1 (S-x-x-P-x-R instead of P-x-x-P-x-R). However, this strain of virus had the ability to replicate to levels that were similar to other strains of virus with conserved PxxPxR sequences (personal data communication). The presence of conserved PxxPxR sequences in motif 2 of the Anam5_KOR96 strain may possibly compensate for the lack of such conservation in motif 1.

This may also help explain the importance of repeated PxxPxR sequences being present in one small region of the proline rich domain.

To analyze the importance of the PxxPxR motifs in RUBV replication, proline to alanines mutations were made in the critical proline residues of each motif, i.e. P-x-x-P-x-R to A-x-x-A-x-R, in the RUBV infectious cDNA clone, Robo502 [19]. Mutations in the individual motifs were named Mut1-Robo502, Mut2-Robo502 and Mut3-Robo502. In addition, combination mutations were made in motifs 1 and 2 as well as in all three motifs and these constructs were named Mut1+2-Robo502 and Mut-X-Robo502, respectively. *In vitro* transcripts synthesized from these constructs were used to transfect Vero cells and the transfected cell medium was collected seven days post-transfection. Cytopathic effect (CPE) is usually observed in cells transfected with transcripts from wt Robo502 at three days post-transfection. Plaque assays done on medium harvested from the Mut1-, Mut2-, and Mut3-Robo502 transfected cells (passage 0 or P0) revealed that the Mut3-Robo502 transcripts produced a titer and plaque morphology that were the same as for wt Robo502 transcripts. Also, CPE were observed on day 3 post-transfection with wt and Mut3-Robo502 transcripts. However, cells transfected with Mut1- and Mut2-Robo502 transcripts yielded lower virus titers (1-4x10^4 pfu/ml) and a small plaque morphology (see Fig 3.3). We further investigated the relative importance of these first two domains with the combination mutants. Mut 1+2-Robo502 transcripts produced low virus titers (1x10^4 pfu/ml) with a small plaque morphology, although CPE were observed on day 3 post-transfection. Mut-X-Robo502 failed to show evidence of replication.

P0 medium was subsequently passaged once in Vero cells. As shown in Fig 3.4, the P1 titer and plaque morphology as well as the development of CPE were similar for all five mutants and wild type virus. These data suggested that reversion of the mutations in the SH3 binding

domain may have occurred and we investigated this possibility by sequencing the virus from infected cells. The results are shown in Table 3.1. The mutant Motif 1 present in the Mut1-, Mut1+2, and MutX-Robo502 constructs reverted to the wt sequence and the mutant Motif 2 present in the Mut2- and MutX-Robo502 constructs reverted to the wt sequence. Interestingly, the mutant Motif 2 in the Mut1+2-Robo502 construct did not revert. The mutant Motif 3 in either Mut3- or MutX-Robo502 did not revert as expected from the wt phenotype exhibited by the Mut3-Robo502 construct.

We next wanted to see if the Motif 1 or Motif 2 mutations affected synthesis of either P150 or viral RNA. Fig. 3.5 A and B show Western blots to detect P150 at 6 hours and 3 days post-transfection. P150 levels at 6 hours represents translation from input transcripts (a control indicative that the construct is functional) and 3 days translation is from replicated transcripts. One of the two Mut1+2-Robo502 clones that were tested was nonfunctional. This is one of the reasons for the 6 hr post-transfection screening. As for the other Robo-502 mutant clones, little difference between wt and either the single mutants or double mutant was detected. The difference that was noted was that the translation levels of P150 from the Mut1-Robo502 clones were slightly lower than from the wt construct. However, levels of P150 translation for the wt and all the mutant clones were similar 3 days post transfection. A Northern blot shown in Fig 3.5C shows that levels of RNA, 3 days post transfection for the single or the double mutations, were similar in levels to the wt. We cannot conclude that the levels of genomic and subgenomic RNA were not affected by the mutations because reversions seem to occur rapidly and could have accounted for the majority of RNA present.

Identification of host proteins that bind to Motifs 1 and 2 in the P150 PRR

We next wanted to investigate the host proteins that bind to the PRR within P150. Since mutations of Motifs 1 and 2 suppressed virus yield and also reverted to wt sequences, we concentrated on these motifs. To do so, we made a GST fusion expression construct in which GST was fused to the PRR. Fig. 3.6 shows a schematic diagram of the wild type construct, GST-PRR/RUB. Another construct containing mutations in both motifs 1 and 2, GST-PRR/RUB Mut1+2 was also constructed. Fig. 3.7 shows the strategy employed to identify the host factors that specifically bound to the PRR. Basically, proteins binding to the wt GST-PRR/RUB, but not the GST-PRR/RUB Mut1+2 with mutations in motifs 1 and 2 were considered as candidates (see Fig.3.8). When this strategy was employed, a total of 4 putative host proteins were identified, termed PRR-1, PRR-2, PRR-3, and PRR-4 (Fig. 3.8). The first protein that was identified, PRR-4, (by Dr Powell of Morehouse School of Medicine) is p32 (score:46.11), which was previously shown to bind to the RUBV capsid protein and for which constructs and reagents were readily available. The other three proteins that were identified by the Mass Spec facility at the Scripps Research Institute were PRR-1: human Mdn1 protein (Q9NU22), PRR-2: Gcn1L protein (Q92616), and PRR-3: nucleopore complex protein Nup205 (Q92621). More than 2 peptides were identified at 95% confidence for all three of these proteins. There are no commercially available reagents for any of these three proteins, whose functions will be discussed later. Therefore, further characterization was confined to p32. As shown in Fig. 3.9, a Western blot probed with anti-p32 antibodies confirmed the binding of p32 to GST-PRR/RUB (wt) but not GST-PRR/RUB-MUT 1+2 or the GST control.

Confirmation of the binding of host protein p32 to RUBV P150

To confirm that p32 binds to P150 as well as the GST-PRR/RUB fusion protein, a plasmid construct expressing an HA tagged P150 was used to transfect Vero cells. Immunoprecipitation was then performed with either anti-HA antibody, a control for pull-down of expressed HA tagged P150, or anti-p32 antibody, to detect a P150-p32 interaction. Fig. 3.10 shows a Western blot of immunoprecipitated proteins probed with anti-HA antibody to detect HA-tagged P150. Lane 3 shows the positive control while Lane 4 demonstrates that P150 was co-immunoprecipitated with p32. This result indicated that the binding of P150 was authentic.

We next explored the interaction between P150 and expressed p32. For this purpose, two p32 expression constructs were generated, one tagged on its N-terminus with an HA epitope and on its C-terminus with a c-myc epitope (pcDNA-HA-p32-myc) and one tagged only on its C-terminus with the c-myc epitope (pcDNA-p32-myc). Vero cells were transfected with pcDNA-HA-p32-myc and co-infected with Robo502-912, which carries a FLAG epitope on P150 (this infectious clone was used in Specific Aim 1). The Fig. 3.11 Western blot shows that FLAG-tagged P150 expressed from virus co-immunoprecipitated with the plasmid expressed HA-p32-myc. In an experiment that employed the expressed p32-myc in cells co-transfected with HA-p32-myc and CMV-P150-HA plasmid, reciprocal immunoprecipitation was demonstrated (Fig. 3.12). Specifically, HA-tagged P150 was co-immunoprecipitated by c-myc antibodies which react with p32-myc (Panel A) while c-myc-tagged p32 was co-immunoprecipitated by anti HA antibodies which react with HA-tagged P150. An additional protein band present above p32-c-myc in lane 4, Panel B (Fig. 3.12), may represent a modified p32 protein.

Interaction between the two proteins was also explored by immunofluorescence. As shown in Fig. 3.13, Panel B, plasmid expressed HA-tagged P150 (red) co-localized with expressed p32 (green) in perinuclear foci. The same observation was made when cells were infected with Robo502/912 which expresses an HA-tagged P150 (Fig 3.13, Panel A) and thus interaction occurs whether P150 is expressed in a plasmid or virus context.

Finally, in light of our earlier results that mutations in motifs 1 and 2 in the GST-PRR/RUB fusion abolished the binding of p32, the finding that led to identification of p32 as a P150 pairing partner, we introduced the same motif 1 and 2 mutations into the CMV-P150 expression contruct. Vero cells were co-transfected with pcDNA-p32-myc and either CMV-P150 or CMV-P150-MUT1+2 vector DNA. As shown in Fig. 3.14, anti-c-myc antibody co-precipitated P150 expressed by CMV-P150 (Lane 4) but not mutant P150 expressed by CMV-P150-MUT1+2 **(**Lane 6**)**. Thus, P150-p32 binding is mediated by the PRR region of P150.

Investigation of the function of p32 in the RUBV life cycle

Evidence obtained with virus that had mutations in the PxxPxR motifs in the PRR indicated that while this region was not necessary for virus RNA synthesis and concomitant protein production, these mutations suppressed virus titers and revertants were rapidly generated. We thus wanted to look at the physiological relevance of the p32-P150 interaction as means of further studying this phenotype. Previous attempts in our lab to knockdown p32 using siRNA were unsuccessful (H. Mousa, unpublished observations) and another lab also did not have success (T. Hobman, personal communication). We therefore tested the effect of overexpression of p32 on RUBV replication [27]. Vero cells transfected with pcDNA-p32-myc were co-infected with RUBV. Approximately 80% of cells were successfully transfected (data not shown). As shown in Fig. 3.15, p32-myc expression was maintained through 4 days post-transfection,

whether the cells were infected or not, and the localization of expressed p32-myc by immunofluorescence (Fig. 3.16) was comparable to endogenous p32 as shown in Fig. 3.13. However, as shown in Table 3.2 the increased levels of p32 in the transfected cells mildly increased the levels of virus replication in the first two days post infection, compared to mock-transfected cells. These data taken together would suggest that p32 may be involved in the ability of the virus to replicate because the presence of an increased amount of host factor did lead to an increase in the amount of virus production, especially early times of infection.

Discussion

In this study, we investigated the PRR region of RUBV P150, spanning from amino acids 716 to 782, that contained a putative SH3 binding domain. We wanted to know if the three P-X-X-P-X-R consensus Class II SH3 binding motifs of interest that were predicted in this region and that were conserved despite the variability of the region among viral isolates, were of any consequence to the RUBV life cycle. In order to do this, we made proline to alanine mutations, ie P-X-X-P-X-R to A-X-X-A-X-R, in the three putative SH3 binding motifs (we called these Motifs 1, 2 and 3) in the RUBV infectious clone, Robo502. After transfection of Vero cells, it was apparent that the Motif 1 and 2 mutants negatively affected virus replication. First, the cells transfected with these mutants did not exhibit CPE. Usually, CPE occurs on day 3 following transfection with wt Robo502. Secondly, viral RNA mutated in either of the first two motifs produced virus titers that were at least 2 logs lower compared to wild type RNA. Thirdly, the Motif 1 and 2 mutants produced small plaque morphology. In contrast, mutations made in the third predicted SH3 binding motif yielded a phenotype similar to wild type, indicating that this predicted motif was not of importance to the replication of the virus. A double mutant of motifs

1 and 2 exhibited a phenotype similar to the individual motif 1 and 2 mutants while a triple mutant of all three motifs produced neither CPE nor plaques following transfection.

Culture medium from transfection plates was passaged to see if revertants would arise. P1 medium from infections with viruses with mutations in motif 1, motif 2, or motifs 1+2 displayed a similar titer and plaque morphology as did wild type virus. Virus with the triple mutation also displayed a wild type phenotype after the first passage. These observations prompted us to analyze the sequences of the passage 1 viruses. As expected, we found that individual mutations made in motifs 1 and 2 had reverted to the wild type sequence as had both these motifs in the triple mutant. In the double motif 1+2 mutant, only motif 1 reverted to wild type. However, mutations made in motif 3, either in the individual mutant or in the triple mutant, did not revert to the wild type sequence. These data strongly suggested that the motifs 1 and 2 of the predicted SH3 binding domain were under positive selection pressure and were important for the virus life cycle.

Next, we looked at translation of P150 following transfection to see if the mutations in the region of interest affected levels of protein translation using Western blot analysis of lysates collected 6 hours and 3 days post-transfection with the individual motif 1 or motif 2 mutants or the double mutant. The first time point represents translation of the input transcript while the second time point represents translation from replicated transcripts. As mentioned in the results, levels of P150 translation of viral RNA with mutation in motif 1 was lower compared to wt at 6 hours post-transfection. However, the result of the 3 day time point indicated wt-level replication for the genome RNA. Also, Northern blot analyses of the intracellular genomic and subgenomic RNA levels showed no differences between the mutants and wt. These data do not necessarily indicate that the mutations had no effect on the production of subgenomic or genomic RNA. As

revertants seem to occur rapidly, it is possible that by 3 days post-transfection, the majority of the genomic and subgenomic RNA accumulated were apparently reverted (wt). To accurately evaluate the effects of mutations on levels of viral genomic and subgenomic RNA production, the experiment has to be approached in two ways. One way is to look at RNA levels at times that are earlier than 3 days post-transfection, having an appropriate control for the decay of input transfected infectious clone RNA. Secondly, instead of point mutations, proline rich sequences of interest could be deleted to avoid the occurrence of revertants. Such experiments would provide an accurate assessment of the effect of the PxxPxR sequences of P150 RUBV on virus replication.

The role of proline rich domains in the proteins of other viruses has been associated with virus maturation and release [28, 29] as well as pathogenicity [17]. The C-terminus of the Gag protein of HIV, for example, has a proline rich region (PxxP motif), called the P6 domain that has been shown to play an important role in virus budding and release [30]. Mutations made in this region resulted in a 20 fold decrease in virus production. The process of virus budding and release is known to occur through interaction of virus components with a variety of host proteins mediated by PxxP motifs. A protein called Tsg101 is a host protein involved in the sorting of proteins via the endosomal sorting complex required for transport (ESCRT) [31]. Binding of Tsg101 to the PxxP (Pro-Thr-Ala-Pro) domain of HIV-1 Gag protein has been shown to be critical for the proteolytic processing of Gag and virus particle release [32, 33]. The Ebola virus Vp40 matrix protein (EbVp40) was also shown to contain a PxxP motif that is important for virus particle egress through interaction with Tsg101 [34]. We know from previous studies that RUBV P150 interacts with the capsid structural protein. It is possible that the PRR domain within P150 mediates the interaction with capsid protein via host cellular factors (e.g. p32 binds

to both) so that virus assembly and release can occur. The disruption of this interaction by mutagenesis of the P150 PxxP motifs could have caused the observed decrease in virus release. Alternatively, a host factor binding to P150 may be important in transport of the newly replicated virus RNA to the site of virion assembly.

Viral SH3 binding domains are also important in regulating signaling pathways that promote virus replication. For example, in a recent study involving influenza A virus, SH3 binding domains were found in the NS1 nonstructural protein [18], an important virulence factor. An association of the NS1 SH3 binding domain with Crk/CrkL proteins was found. These proteins contain SH3 domains and have been implicated in a variety of signaling pathways, including the PI3K pathway involved in cell survival. In this study, the researchers found through mutagenesis of the NS1 region responsible for binding to the Crk/CrkL proteins that interferon suppression mediated by NS1 was not affected, but rather PI3K signaling was not enhanced. Activation of PI3K signaling had been previously shown to enhance influenza A virus replication and decrease apoptosis in infected cells [15]. Therefore, this study provides a mechanism that is mediated through the SH3 binding domain of NS1 protein that is important for the replicative capacity of the virus and similar interactions between P150 and signaling pathways could be important in the RUBV life cycle.

Aside from interaction with host cellular factors that affect virus maturation via assembly and release or cell signaling pathways that promote virus replication, it has been extensively shown that PxxP motifs and their interaction with SH3 domains play a role in the development of virus pathogenesis. The HIV Nef protein is one such example of a virus protein that contains a PxxP consensus sequence. Nef is important for several functions. Firstly, it is important for enhancing infectivity of virus particles [14, 35, 36]. Secondly, it has a role in the regulation of

CD4 and MHC I expression on the plasma membrane [37, 38]. Thirdly, it has been shown to be involved in cellular signaling [39]. Nef protein is important for the pathogenesis of the virus as it is required for the development of AIDS in humans and rhesus macaques [40, 41]. In one study on the Nef PxxP consensus sequence, it was found that it binds to a member of the Src kinase family, Hck protein, a form of tyrosine kinase which is involved in cellular signaling [13, 42]. The interaction of Nef protein with Hck was found to be important for the infectivity of HIV-1.

Hepatitis C virus (HCV) nonstructural protein NS5A also has class II PxxP consensus sequences in its C-terminus. NS5A is an important virus protein involved in IFN-α resistance [43, 44] and replication in general [45-47]. The PxxP sequence of NS5A was shown to bind Amphiphysin II (Bin1) in two different studies [48, 49]. This interaction was mediated through an SH3 domain present in the C-terminus of the Bin1 protein. Bin1 is a nucleocytoplasmic c-myc interacting protein associated with apoptosis [50] and clathrin mediated endocytosis [51]. According to these studies, mutations in the SH3 binding domain of NS5A resulted in a virus that was not infectious in chimpanzees and also not able to overcome Bin1 induced apoptosis. These data point to the importance of this particular SH3 binding domain in viral pathogenesis.

The importance of the viral SH3 binding domains in pathogenesis of a virus was also shown in studies of the PxxP motif of the gp30 protein of bovine leukemia virus (BLV) [17]. In this study, infection of sheep with viruses having mutations in the PxxP motif of the BLV gp30 transmembrane protein did not lead to tumorigenesis while sheep infected with the wild type virus died of leukemia and lymphoma. Although all of the animals seroconverted at approximately the same time, only those transfected with the wild type virus developed tumors, revealing the importance of the SH3 binding domain in the development of tumors in animals infected with this virus. Data from other viruses suggest that there is a possibility that RUB P150

through interaction with host factors via its SH3 domain is important for the development of pathogenesis of the virus. However, the lack of an animal model for RUB would make it difficult to further study this hypothesis.

Since we had shown that the predicted SH3 binding domains 1 and 2 of RUB P150 are of importance to the virus life cycle, we next wanted to identify the potential binding partners of these domains. Binding experiments using the PRR of P150 fused to GST as bait led to identification of four putative host cellular interacting proteins, namely the p32 protein (gC1qR), human Mdn1 protein, Gcn1L protein and nucleopore complex protein Nup205. The human Mdn1 protein is a homolog of the yeast Rea1 protein that is involved in ribosome biogenesis [52], Gcn1L protein has protein binding and ribosome binding domains that are involved in regulation of translation [53] and the Nup205 protein is part of the nuclear pore complex and, like other members of the nuclear pore complex, is involved in regulating permeability of the nuclear membrane [54]. Interestingly, studies have shown that some RNA viruses target members of the nuclear pore complex to disrupt normal trafficking of host RNA and proteins [55], a mechanism that probably targets host cell protein synthesis. In this regard, RUBV does not exhibit a marked shutdown of either cell RNA or protein synthesis [56]. The interaction of these three host factors with P150 was not investigated as there were no commercially available reagents to do so. We decided to investigate the interaction of p32 with RUB P150 as there was precedence for the binding of this protein to RUB capsid protein [24, 57] as well as to proteins of other viruses [58-60]. It was therefore quite plausible that the p32 host protein in conjunction with both P150 and capsid (both p32 interacting partners) is involved in the regulation of the viral life cycle. Furthermore, reagents for p32 were commercially available to facilitate our

studies. These reagents were first used to confirm that p32 bound to wt GST-PRR/RUBV, but not GST-PRR/RUV MUT 1+2.

We next wanted to ensure that p32 bound to the complete P150 protein and did so by expressing P150 in Vero cells and showing that it was co-immunoprecipitated by anti-p32 antibodies. Finally, an immunofluorescence assay using anti-p32 antibodies showed co-localization of P150, either in virus-infected cells or cells transfected with the P150 expression construct, with endogenous p32. In virus infected cells, the foci of P150 colocalized with p32, but there were also cytoplasmic punctae of p32 not associated with P150. In P150-transfected cells, P150 fibers were formed and colocalization of p32 with these fibers was observed.

For subsequent experiments, we expressed p32 protein from a pcDNA expression vector with epitopes at the N and/or C termini of the protein. The construct design was based on the precursor form of p32 (282 amino acids in length) that had 73 amino acids at the N-terminus containing a mitochondrial targeting sequence [61]. We designed two constructs, one that had a HA epitope at the N-terminus and a c-myc epitope at its C-terminus and one that only had the c-myc epitope at the C-terminus. Anti-HA antibodies were used to co-immunoprecipitate P150 in lysates of virus-infected cells co-transfected with the HA-p32-myc construct. However, the amount of P150 that was pulled down was low. Three factors could have contributed to this observation. Firstly, there were low levels of RUB P150 present in these cells because it was expressed from the virus; secondly, an HA epitope at the N terminus of p32 could be masking the interaction site for RUB P150; and thirdly, the retargeting of p32 to a different site in the cytoplasm because of the presence of a tag on the N terminus that contains the mitochondrial targeting signal. P32 in this new site may not be easily accessible for the binding to RUB P150. The retargeting of p32 to a site other than its usual one due to the addition of an epitope tag at

the N-terminus was shown by a group of cell biologists in the UK [62]. Thus, we used C-terminally c-myc-tagged p32 construct for the remainder of the experiments. Immunofluorescence assay of this construct showed localization that was comparable to the distribution of endogenous p32 as was described by other researchers [62, 63]. We first used the pcDNA-p32-myc construct to demonstrate reciprocal co-immunoprecipitation between p32 and P150 in cells co-transfected with CMV-P150 and pcDNA-p32-myc.

In order to try to understand the role that p32 is playing in the RUBV life cycle, we looked at the effects of p32 overexpression on virus titer based on an earlier report that overexpression of p32 in Vero cells enhanced RUBV replication [27]. In that study, researchers overexpressed p32 in Vero cells and looked at the levels of RUBV capsid protein as an indication of levels of infection because they were not able to measure production of virus by plaque assay. They found that cells overexpressing p32 had significantly higher levels (about 75% higher that control cells not overexpressing p32) of RUBV capsid as evident through Western blot and IFA analysis. Their analysis was done 3 days post-infection. For our studies, Vero cells were first transfected with pcDNA-p32-*myc* and then infected the following day with RUBV. Culture medium was collected each day post-infection for four days and virus titer was determined. A mild increase (about ½ log) in viral titers were observed between Vero cells and pcDNA-p32-myc transfected cells, especially on days 1 and 2 post-infection. The expression of p32 over the duration of the experiment was further confirmed by Western blot. Based on our findings, we cannot make comparisons with the earlier report [27] because RUBV replication in that report was measured by accumulation of intracellular capsid protein, not plaque assay. While higher viral titers during the first 2 days of virus infection in cells overexpressing p32 could be related to the finding that RUBV capsid is increased in amount, further studies need to

be done especially at earlier infection times, before we can draw those conclusions. Another observation that was made in infected cells overexpressing p32, was that CPE was somewhat stronger than in the RUBV-infected Vero cells. RUBV-induced CPE in Vero cells is due to induction of apoptosis [64, 65] and a propidium iodide-based assay to detect apoptotic cells indicated an increase of sub-G0 phase cells in p32 transfected vs the untransfected Vero cell cultures infected with RUBV (data not shown). It has been shown that p32 is associated with induction of apoptosis [66, 67].

Our results do not prove that the phenotype of viruses with mutations in Motifs 1 and 2 in the P150 PRR (ie. little effect on RNA synthesis or NSP expression, but reduced titer and rapid reversion) are due to abrogated binding of p32 and thus the function of p32 in the RUBV life cycle, if any, is not clear, but potential functions may be speculated on based on our findings and previous work on p32 and its association with other viruses. The p32 protein is known by other names: gC1Qr (globular heads of the C1q protein receptor) and HABP (the hyaluronic acid-binding protein). The diversity in the names of this protein are an indication of the multiple functions that this protein is thought to have. Historically, the p32 protein was isolated as part of the ASF/SF2 human splicing factor complex in the nucleus of HeLa cells [68]. In a later study [69], it was suggested that p32 regulated the activity of the ASF/SF2 complex by acting as an inhibitor to control RNA binding activity. This was shown to be achieved through inhibition of ASF/SF2 phosphorylation. In addition to its function in the nucleus, p32 was later shown to be a resident of the mitochondria [63] and in this study it was found that p32 was primarily a resident in mitochondria. Additionally, mutations of genes homologous to p32 in yeast showed that p32 was involved in maintaining oxidative phosphorylation. Aside from this study, earlier work on p32 showed that it functioned as a phosphate translocator in mitochondria [70, 71]. Another

report that supports the localization of p32 in the mitochondria was one that showed the binding of mitochondrial precursor proteins to p32 [61]. These researchers showed that proteins destined for the mitochondria were bound to p32 through a mitochondrial signal sequence which allowed p32 to act as an import receptor. It was later shown that p32 does indeed contain a 73 amino acid mitochondrial targeting sequence at the N-terminus that is efficiently removed by proteolytic processing [63]. P32 was also identified as a potential binding partner for a variety of proteins that would have to bind p32 at the cell surface. Examples of some of these proteins are C1 complement component protein, C1g [72], and other extracellular plasma proteins involved in coagulation such as kininogen [73], and factor XII [74]. All these findings suggests that p32 is a multifunctional protein.

The interaction of p32 with proteins from a variety of viruses, and even bacteria, has been documented. For instance, the interaction of p32 with the HIV Tat and EBV EBNA-1 proteins was shown to be important for enhancement of transcriptional activity [58, 75]. Additionally, p32 was shown to bind to the HIV Rev protein [60], which facilitates nucleus to cytoplasm transport of unspliced HIV RNA, and also to the adenovirus core protein that potentially mediate the shuttling of adenoviral DNA into the nucleus [59, 76]. From these studies it seems that p32 is involved in two main kinds of function: RNA-related regulatory functions and shuttling of RNA. One interaction of particular interest to us is the interaction between p32 and the RUBV capsid protein [24, 57]. This interaction was hypothesized to be involved in the reorganization and distribution of [25] mitochondria to cluster around CPVs, which is a unique hallmark of RUBV infection [25] . This reorganization of mitochondria was thought to perhaps serve as a source of energy for the RNA synthesis process. It was also hypothesized that the reorganization of mitochondria by capsid may facilitate the incorporation of cardiolipin into the

mature virion [77]. In addition, disruption of the p32 binding site on the capsid protein leads to decreased levels of virus production, as measured by plaque assay, and a specific decrease in the synthesis of the subgenomic RNA [57]. However, the binding sites that were mutated were two arginine clusters that have also been shown to bind the viral RNA. The capsid protein is important in both modulating the ratio of genomic to subgenomic RNA [57] and in capsid formation and thus these capsid mutations could have affected these functions independent of binding p32.

As for the association of p32 with RUB P150, two possible functions that could be mediated by this interaction are virion assembly and virus pathogenesis. Concerning virus assembly, P150 forms a fibrous network in cells [78] that could be involved in helping virus particle movement out of the infected cell and our data indicate that p32 is recruited to this network. As discussed earlier, a variety of host proteins found in the extracellular matrix have been shown to bind to p32. In a study that used immunogold electron microscopy to evaluate subcellular localization of p32 [79] in various culture cell lines, apart from detecting the presence of p32 in the mitochondria, this protein was also found on cell surface of pancreatic acinar cells. P32 was also found in zymogen granules, condensing vacuoles and endoplasmic reticulum. In another experiment that attempted to track the localization of p32 after attaching epitope tags to either the N or C termini of the protein, researchers made the observation that masking the mitochondrial targeting signal (MTS) redirected p32 either to the ER or to the cell surface [62]. They hypothesized that masking the N terminus MTS caused the redirection of the protein to these other locations in the cells, possibly explaining the ambiguity in the variety of locations that p32 is found. It is possible that the binding of p32 to both P150 and capsid protein could functionally be important during virus assembly. However, further studies have to be done

to test this hypothesis. One study that could be done is to look at the effect of P150 PxxP mutants on the localization of P150 and on the co-localization of P150 with p32.

Two recent studies suggests a role for p32 in reducing mitochondrial membrane potential and inducing apoptosis [66, 67]. Our previous studies have shown that P150 is the determinant of cytopathogenicity in Vero cells [21] and recent studies in our lab showed that RUB P150 alone can induce apoptosis. Interestingly, induction of apoptosis is suppressed in the presence of the capsid protein (unpublished data). It is therefore possible that the interaction of P150, capsid protein, and p32 modulates the induction of apoptosis in infected cells.

In conclusion, we found that mutations in the first 2 PxxPxR motifs of P150 led to a 2 log decrease in viral titers after passage 0. Additionally, the mutations in motifs 1 and 2 reverted to wt sequence by the first passage. As for the effects of mutations on levels of genomic and subgenomic RNA, we did not see significant differences 3 days post-transfection of wt and mutant viral RNA. However, with the rapid rate of reversion observed, genomic and subgenomic RNA levels should probably be analyzed at earlier times post-transfection. As for the studies involving host cellular factors that bind to the proline rich region, we confirmed the binding of cellular p32 to motifs 1 and 2 of P150. Overexpression of p32 in cells infected with RUBV led to ½ log increase in viral titers at earlier times post-infection. Further studies need to be done to elucidate the actual role of p32 in the RUBV life cycle. In addition to p32, 3 other cellular proteins were identified, but further analyses of these interactions with P150 were not pursued. More host proteins may associate with the proline region of P150, but our technique of interacting protein detection led to the identification of host proteins that were present in higher abundance.

References

1. Zarrinpar, A., R.P. Bhattacharyya, and W.A. Lim, *The structure and function of proline recognition domains.* Sci STKE, 2003. **2003**(179): p. RE8.
2. Kay, B.K., M.P. Williamson, and M. Sudol, *The importance of being proline: the interaction of proline-rich motifs in signaling proteins with their cognate domains.* FASEB J, 2000. **14**(2): p. 231-41.
3. Falzone, C.J., et al., *Three-dimensional solution structure of PsaE from the cyanobacterium Synechococcus sp. strain PCC 7002, a photosystem I protein that shows structural homology with SH3 domains.* Biochemistry, 1994. **33**(20): p. 6052-62.
4. Ponting, C.P., et al., *Eukaryotic signalling domain homologues in archaea and bacteria. Ancient ancestry and horizontal gene transfer.* J Mol Biol, 1999. **289**(4): p. 729-45.
5. Bilwes, A.M., et al., *Structure of CheA, a signal-transducing histidine kinase.* Cell, 1999. **96**(1): p. 131-41.
6. Pohl, E., R.K. Holmes, and W.G. Hol, *Crystal structure of a cobalt-activated diphtheria toxin repressor-DNA complex reveals a metal-binding SH3-like domain.* J Mol Biol, 1999. **292**(3): p. 653-67.
7. Whisstock, J.C. and A.M. Lesk, *SH3 domains in prokaryotes.* Trends Biochem Sci, 1999. **24**(4): p. 132-3.
8. Bar-Sagi, D., et al., *SH3 domains direct cellular localization of signaling molecules.* Cell, 1993. **74**(1): p. 83-91.
9. Koch, C.A., et al., *SH2 and SH3 domains: elements that control interactions of cytoplasmic signaling proteins.* Science, 1991. **252**(5006): p. 668-74.
10. Musacchio, A., et al., *Crystal structure of a Src-homology 3 (SH3) domain.* Nature, 1992. **359**(6398): p. 851-5.
11. Cohen, G.B., R. Ren, and D. Baltimore, *Modular binding domains in signal transduction proteins.* Cell, 1995. **80**(2): p. 237-48.
12. Feng, S., et al., *Specific interactions outside the proline-rich core of two classes of Src homology 3 ligands.* Proc Natl Acad Sci U S A, 1995. **92**(26): p. 12408-15.
13. Saksela, K., G. Cheng, and D. Baltimore, *Proline-rich (PxxP) motifs in HIV-1 Nef bind to SH3 domains of a subset of Src kinases and are required for the enhanced growth of Nef+ viruses but not for down-regulation of CD4.* EMBO J, 1995. **14**(3): p. 484-91.
14. Aiken, C. and D. Trono, *Nef stimulates human immunodeficiency virus type 1 proviral DNA synthesis.* J Virol, 1995. **69**(8): p. 5048-56.
15. Ehrhardt, C., et al., *Influenza A virus NS1 protein activates the PI3K/Akt pathway to mediate antiapoptotic signaling responses.* J Virol, 2007. **81**(7): p. 3058-67.
16. Linnemann, T., et al., *Interaction between Nef and phosphatidylinositol-3-kinase leads to activation of p21-activated kinase and increased production of HIV.* Virology, 2002. **294**(2): p. 246-55.
17. Reichert, M., et al., *Role of the proline-rich motif of bovine leukemia virus transmembrane protein gp30 in viral load and pathogenicity in sheep.* J Virol, 2001. **75**(17): p. 8082-9.

18. Heikkinen, L.S., et al., *Avian and 1918 Spanish influenza a virus NS1 proteins bind to Crk/CrkL Src homology 3 domains to activate host cell signaling.* J Biol Chem, 2008. **283**(9): p. 5719-27.
19. Tzeng, W.P. and T.K. Frey, *Complementation of a deletion in the rubella virus P150 nonstructural protein by the viral capsid protein.* J Virol, 2003. **77**(17): p. 9502-10.
20. Tyagi, R., R. Lai, and R.G. Duggleby, *A new approach to 'megaprimer' polymerase chain reaction mutagenesis without an intermediate gel purification step.* BMC Biotechnol, 2004. **4**: p. 2.
21. Pugachev, K.V., E.S. Abernathy, and T.K. Frey, *Improvement of the specific infectivity of the rubella virus (RUB) infectious clone: determinants of cytopathogenicity induced by RUB map to the nonstructural proteins.* J Virol, 1997. **71**(1): p. 562-8.
22. Tzeng, W.P. and T.K. Frey, *Mapping the rubella virus subgenomic promoter.* J Virol, 2002. **76**(7): p. 3189-201.
23. Tzeng, W.P., et al., *Rubella virus DI RNAs and replicons: requirement for nonstructural proteins acting in cis for amplification by helper virus.* Virology, 2001. **289**(1): p. 63-73.
24. Beatch, M.D. and T.C. Hobman, *Rubella virus capsid associates with host cell protein p32 and localizes to mitochondria.* J Virol, 2000. **74**(12): p. 5569-76.
25. Fontana, J., et al., *Novel replication complex architecture in rubella replicon-transfected cells.* Cell Microbiol, 2007. **9**(4): p. 875-90.
26. Zhou, Y., H. Ushijima, and T.K. Frey, *Genomic analysis of diverse rubella virus genotypes.* J Gen Virol, 2007. **88**(Pt 3): p. 932-41.
27. Mohan, K.V., B. Ghebrehiwet, and C.D. Atreya, *The N-terminal conserved domain of rubella virus capsid interacts with the C-terminal region of cellular p32 and overexpression of p32 enhances the viral infectivity.* Virus Res, 2002. **85**(2): p. 151-61.
28. Morikawa, Y., *HIV capsid assembly.* Curr HIV Res, 2003. **1**(1): p. 1-14.
29. Freed, E.O., *Viral late domains.* J Virol, 2002. **76**(10): p. 4679-87.
30. Dettenhofer, M. and X.F. Yu, *Proline residues in human immunodeficiency virus type 1 p6(Gag) exert a cell type-dependent effect on viral replication and virion incorporation of Pol proteins.* J Virol, 1999. **73**(6): p. 4696-704.
31. Katzmann, D.J., M. Babst, and S.D. Emr, *Ubiquitin-dependent sorting into the multivesicular body pathway requires the function of a conserved endosomal protein sorting complex, ESCRT-I.* Cell, 2001. **106**(2): p. 145-55.
32. Garrus, J.E., et al., *Tsg101 and the vacuolar protein sorting pathway are essential for HIV-1 budding.* Cell, 2001. **107**(1): p. 55-65.
33. VerPlank, L., et al., *Tsg101, a homologue of ubiquitin-conjugating (E2) enzymes, binds the L domain in HIV type 1 Pr55(Gag).* Proc Natl Acad Sci U S A, 2001. **98**(14): p. 7724-9.
34. Martin-Serrano, J., T. Zang, and P.D. Bieniasz, *HIV-1 and Ebola virus encode small peptide motifs that recruit Tsg101 to sites of particle assembly to facilitate egress.* Nat Med, 2001. **7**(12): p. 1313-9.
35. Chowers, M.Y., et al., *The growth advantage conferred by HIV-1 nef is determined at the level of viral DNA formation and is independent of CD4 downregulation.* Virology, 1995. **212**(2): p. 451-7.
36. Schwartz, O., et al., *Human immunodeficiency virus type 1 Nef increases the efficiency of reverse transcription in the infected cell.* J Virol, 1995. **69**(7): p. 4053-9.

37. Schwartz, O., et al., *Endocytosis of major histocompatibility complex class I molecules is induced by the HIV-1 Nef protein.* Nat Med, 1996. **2**(3): p. 338-42.
38. Garcia, J.V. and A.D. Miller, *Serine phosphorylation-independent downregulation of cell-surface CD4 by nef.* Nature, 1991. **350**(6318): p. 508-11.
39. Marsh, J.W., *The numerous effector functions of Nef.* Arch Biochem Biophys, 1999. **365**(2): p. 192-8.
40. Kestler, H.W., 3rd, et al., *Importance of the nef gene for maintenance of high virus loads and for development of AIDS.* Cell, 1991. **65**(4): p. 651-62.
41. Kirchhoff, F., et al., *Brief report: absence of intact nef sequences in a long-term survivor with nonprogressive HIV-1 infection.* N Engl J Med, 1995. **332**(4): p. 228-32.
42. Lee, C.H., et al., *A single amino acid in the SH3 domain of Hck determines its high affinity and specificity in binding to HIV-1 Nef protein.* EMBO J, 1995. **14**(20): p. 5006-15.
43. Enomoto, N., et al., *Comparison of full-length sequences of interferon-sensitive and resistant hepatitis C virus 1b. Sensitivity to interferon is conferred by amino acid substitutions in the NS5A region.* J Clin Invest, 1995. **96**(1): p. 224-30.
44. Enomoto, N., et al., *Mutations in the nonstructural protein 5A gene and response to interferon in patients with chronic hepatitis C virus 1b infection.* N Engl J Med, 1996. **334**(2): p. 77-81.
45. Brass, V., et al., *An amino-terminal amphipathic alpha-helix mediates membrane association of the hepatitis C virus nonstructural protein 5A.* J Biol Chem, 2002. **277**(10): p. 8130-9.
46. Hijikata, M., et al., *Proteolytic processing and membrane association of putative nonstructural proteins of hepatitis C virus.* Proc Natl Acad Sci U S A, 1993. **90**(22): p. 10773-7.
47. Shirota, Y., et al., *Hepatitis C virus (HCV) NS5A binds RNA-dependent RNA polymerase (RdRP) NS5B and modulates RNA-dependent RNA polymerase activity.* J Biol Chem, 2002. **277**(13): p. 11149-55.
48. Nanda, S.K., D. Herion, and T.J. Liang, *The SH3 binding motif of HCV [corrected] NS5A protein interacts with Bin1 and is important for apoptosis and infectivity.* Gastroenterology, 2006. **130**(3): p. 794-809.
49. Zech, B., et al., *Identification and characterization of amphiphysin II as a novel cellular interaction partner of the hepatitis C virus NS5A protein.* J Gen Virol, 2003. **84**(Pt 3): p. 555-60.
50. Sakamuro, D., et al., *BIN1 is a novel MYC-interacting protein with features of a tumour suppressor.* Nat Genet, 1996. **14**(1): p. 69-77.
51. Wigge, P., et al., *Amphiphysin heterodimers: potential role in clathrin-mediated endocytosis.* Mol Biol Cell, 1997. **8**(10): p. 2003-15.
52. Galani, K., et al., *Rea1, a dynein-related nuclear AAA-ATPase, is involved in late rRNA processing and nuclear export of 60 S subunits.* J Biol Chem, 2004. **279**(53): p. 55411-8.
53. Sattlegger, E. and A.G. Hinnebusch, *Separate domains in GCN1 for binding protein kinase GCN2 and ribosomes are required for GCN2 activation in amino acid-starved cells.* EMBO J, 2000. **19**(23): p. 6622-33.
54. Grandi, P., et al., *Nup93, a vertebrate homologue of yeast Nic96p, forms a complex with a novel 205-kDa protein and is required for correct nuclear pore assembly.* Mol Biol Cell, 1997. **8**(10): p. 2017-38.

55. Gustin, K.E., *Inhibition of nucleo-cytoplasmic trafficking by RNA viruses: targeting the nuclear pore complex.* Virus Res, 2003. **95**(1-2): p. 35-44.
56. Hemphill, M.L., et al., *Time course of virus-specific macromolecular synthesis during rubella virus infection in Vero cells.* Virology, 1988. **162**(1): p. 65-75.
57. Beatch, M.D., et al., *Interactions between rubella virus capsid and host protein p32 are important for virus replication.* J Virol, 2005. **79**(16): p. 10807-20.
58. Wang, Y., et al., *P32/TAP, a cellular protein that interacts with EBNA-1 of Epstein-Barr virus.* Virology, 1997. **236**(1): p. 18-29.
59. Matthews, D.A. and W.C. Russell, *Adenovirus core protein V is delivered by the invading virus to the nucleus of the infected cell and later in infection is associated with nucleoli.* J Gen Virol, 1998. **79 (Pt 7)**: p. 1671-5.
60. Luo, Y., H. Yu, and B.M. Peterlin, *Cellular protein modulates effects of human immunodeficiency virus type 1 Rev.* J Virol, 1994. **68**(6): p. 3850-6.
61. Murakami, H., G. Blobel, and D. Pain, *Signal sequence region of mitochondrial precursor proteins binds to mitochondrial import receptor.* Proc Natl Acad Sci U S A, 1993. **90**(8): p. 3358-62.
62. van Leeuwen, H.C. and P. O'Hare, *Retargeting of the mitochondrial protein p32/gC1Qr to a cytoplasmic compartment and the cell surface.* J Cell Sci, 2001. **114**(Pt 11): p. 2115-23.
63. Muta, T., et al., *p32 protein, a splicing factor 2-associated protein, is localized in mitochondrial matrix and is functionally important in maintaining oxidative phosphorylation.* J Biol Chem, 1997. **272**(39): p. 24363-70.
64. Duncan, R., et al., *Rubella virus-induced apoptosis varies among cell lines and is modulated by Bcl-XL and caspase inhibitors.* Virology, 1999. **255**(1): p. 117-28.
65. Pugachev, K.V. and T.K. Frey, *Rubella virus induces apoptosis in culture cells.* Virology, 1998. **250**(2): p. 359-70.
66. Chowdhury, A.R., I. Ghosh, and K. Datta, *Excessive reactive oxygen species induces apoptosis in fibroblasts: role of mitochondrially accumulated hyaluronic acid binding protein 1 (HABP1/p32/gC1qR).* Exp Cell Res, 2008. **314**(3): p. 651-67.
67. Itahana, K. and Y. Zhang, *Mitochondrial p32 is a critical mediator of ARF-induced apoptosis.* Cancer Cell, 2008. **13**(6): p. 542-53.
68. Krainer, A.R., et al., *Functional expression of cloned human splicing factor SF2: homology to RNA-binding proteins, U1 70K, and Drosophila splicing regulators.* Cell, 1991. **66**(2): p. 383-94.
69. Petersen-Mahrt, S.K., et al., *The splicing factor-associated protein, p32, regulates RNA splicing by inhibiting ASF/SF2 RNA binding and phosphorylation.* EMBO J, 1999. **18**(4): p. 1014-24.
70. Guerin, B., et al., *Mitochondrial phosphate transport. N-ethylmaleimide insensitivity correlates with absence of beef heart-like Cys42 from the Saccharomyces cerevisiae phosphate transport protein.* J Biol Chem, 1990. **265**(32): p. 19736-41.
71. Phelps, A., C.T. Schobert, and H. Wohlrab, *Cloning and characterization of the mitochondrial phosphate transport protein gene from the yeast Saccharomyces cerevisiae.* Biochemistry, 1991. **30**(1): p. 248-52.
72. Ghebrehiwet, B., et al., *Isolation, cDNA cloning, and overexpression of a 33-kD cell surface glycoprotein that binds to the globular "heads" of C1q.* J Exp Med, 1994. **179**(6): p. 1809-21.

73. Herwald, H., et al., *Isolation and characterization of the kininogen-binding protein p33 from endothelial cells. Identity with the gC1q receptor.* J Biol Chem, 1996. **271**(22): p. 13040-7.
74. Joseph, K., et al., *Identification of the zinc-dependent endothelial cell binding protein for high molecular weight kininogen and factor XII: identity with the receptor that binds to the globular "heads" of C1q (gC1q-R).* Proc Natl Acad Sci U S A, 1996. **93**(16): p. 8552-7.
75. Yu, L., et al., *Molecular cloning and characterization of a cellular protein that interacts with the human immunodeficiency virus type 1 Tat transactivator and encodes a strong transcriptional activation domain.* J Virol, 1995. **69**(5): p. 3007-16.
76. Matthews, D.A. and W.C. Russell, *Adenovirus core protein V interacts with p32--a protein which is associated with both the mitochondria and the nucleus.* J Gen Virol, 1998. **79 (Pt 7)**: p. 1677-85.
77. Bardeletti, G. and D.C. Gautheron, *Phospholipid and cholesterol composition of rubella virus and its host cell BHK 21 grown in suspension cultures.* Arch Virol, 1976. **52**(1-2): p. 19-27.
78. Kujala, P., et al., *Intracellular distribution of rubella virus nonstructural protein P150.* J Virol, 1999. **73**(9): p. 7805-11.
79. Soltys, B.J., D. Kang, and R.S. Gupta, *Localization of P32 protein (gC1q-R) in mitochondria and at specific extramitochondrial locations in normal tissues.* Histochem Cell Biol, 2000. **114**(3): p. 245-55.

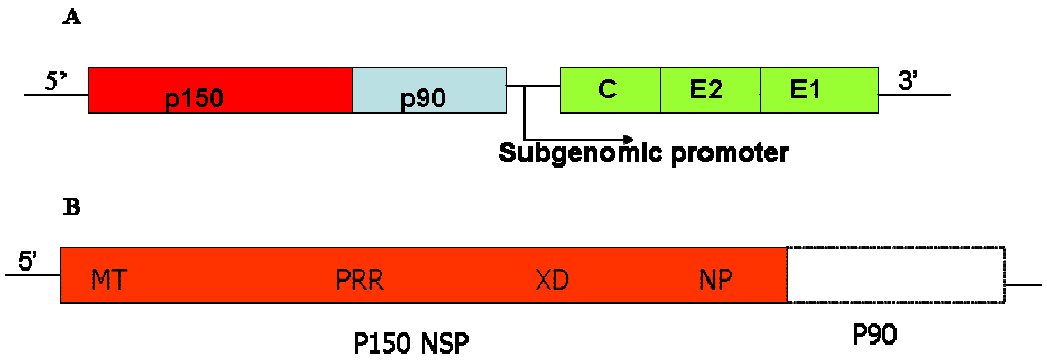

Figure 3.1A. RUBV genomic organization and domains within the P150 nonstructural protein.
A) Rubella virus genome organization showing the two ORFs and five nonstructural and structural proteins encoded by the virus. B) Domains present within the P150 nonstructural protein (1301aa): MT (methyl/guanylyltransferase), nt 230-439 (70aa); PPR (polyproline region), nt 2120-2440 (107aa); XD (X domain, adenosyl-ribose phosphatase), nt 2492-2998 (169aa); NP (nonstructural protease), nt 3041-3940 (300aa).

Figure 3.1B. Predicted consensus SH3 binding motifs within the P150 PRR.
The sequence of the PRR within P150 (aa 716-782) is given. Motifs 1 through 3 are predicted class II SH3 binding domains with PxxPxR consensus sequences.

(SEQUENCES KINDLY PROVIDED BY YUMEI ZHOU)

Figure 3.2. Multiple sequence alignment of proline rich region of RUBV from 7 genotypes. Alignment of 14 different genotypes of RUBV reveals high levels of conservation of the 3 P-x-x-P-x-R sequences (highlighted in green). This alignment was performed by Dr Yumei Zhou.

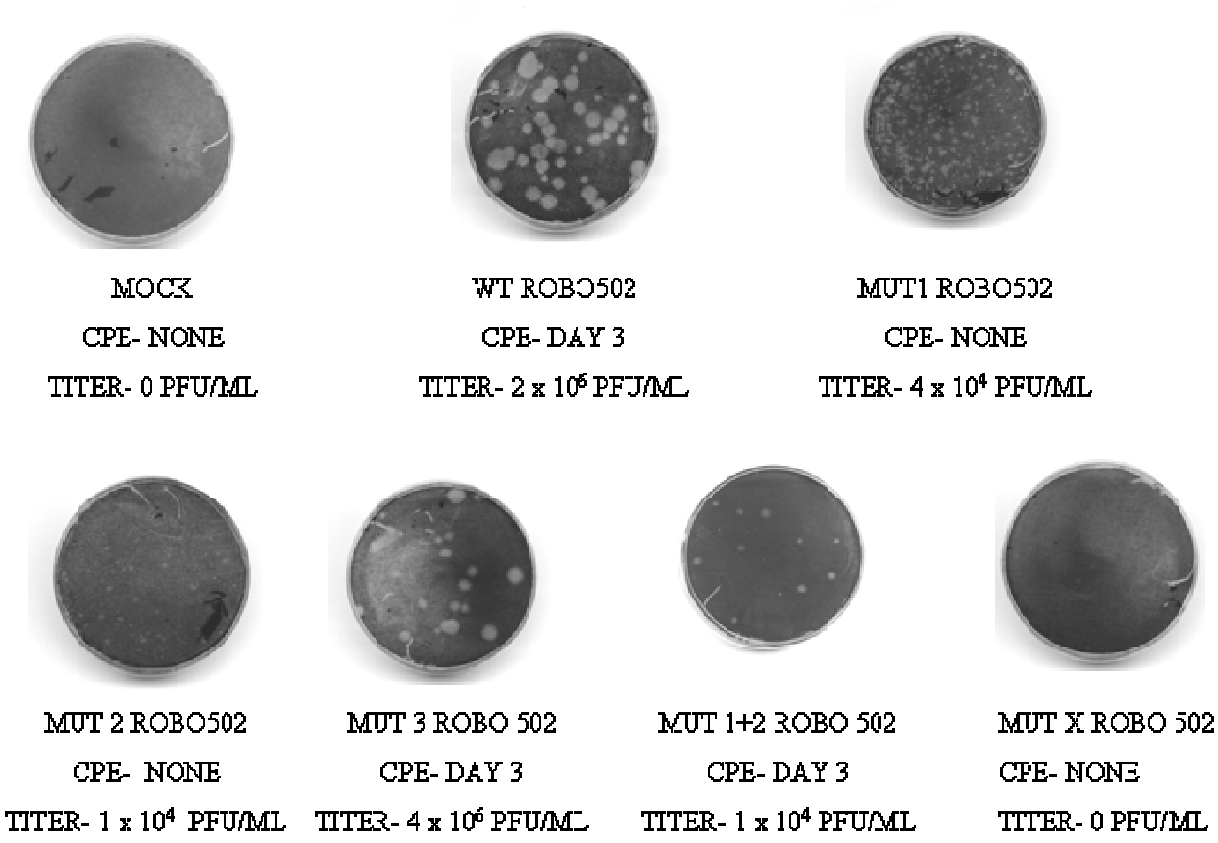

Figure 3.3. Viral titers in culture fluid from transfection plates and plaque morphologies. Vero cells were mock-transfected or transfected with transcripts from the wild type infectious clone (Robo502) or Robo502 derivatives containing proline to alanine mutations in the predicted SH3 binding motifs 1, 2 and/or 3 (the construct with mutations in all three motifs was designated as MutX). The transfected cells were observed daily for CPE (the day on which CPE was first observed is indicated) and the transfected cell medium (designated as "passage 0" or "P0") was collected on day 3 post-transfection and titered by plaque assay. The virus titer in each P0 culture fluid and the highest dilution plate on which plaques were observed is shown for visualization of plaque morphology.

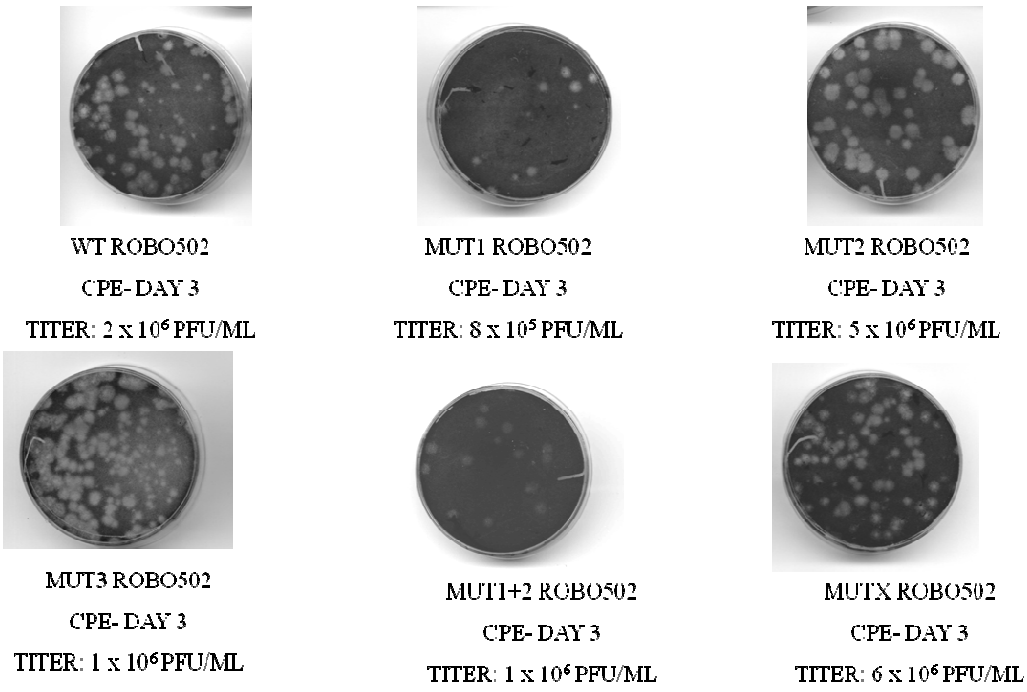

Figure 3.4. Viral titers in culture fluid from infected plates after passage 1 and plaque morphologies.
Vero cells were infected with P0 culture fluids (see Fig. 3.3) and observed daily for CPE (the day on which CPE was first observed is indicated). The culture medium (designated as "passage 1" or "P1") was collected on day 3 post-infection and titered by plaque assay. The virus titer in each P1 culture fluid and the highest dilution plate on which plaques were observed is shown for visualization of plaque morphology.

Table 3.1. Sequence of Robo502 PxxPxR motif mutants after one passage in Vero cells.

Construct[1]	Sequence[1]
Wild type Robo502	Wild type sequence
Robo502-MUT1	Reverted to wild type sequence
Robo502-MUT2	Reverted to wild type sequence
Robo502-MUT3	No revertants; mutation still at motif 3
Robo502-Mut1+2	Motif 1 reverted to wild type sequence
Robo502-MUTX	Motif 1 and 2 reverted to wild type sequence; mutation still at motif 3

[1]Vero cells were transfected with the indicated Robo502 constructs. The transfected culture medium was harvested and passaged once in Vero cells. The PRR domain of passaged virus was sequenced.

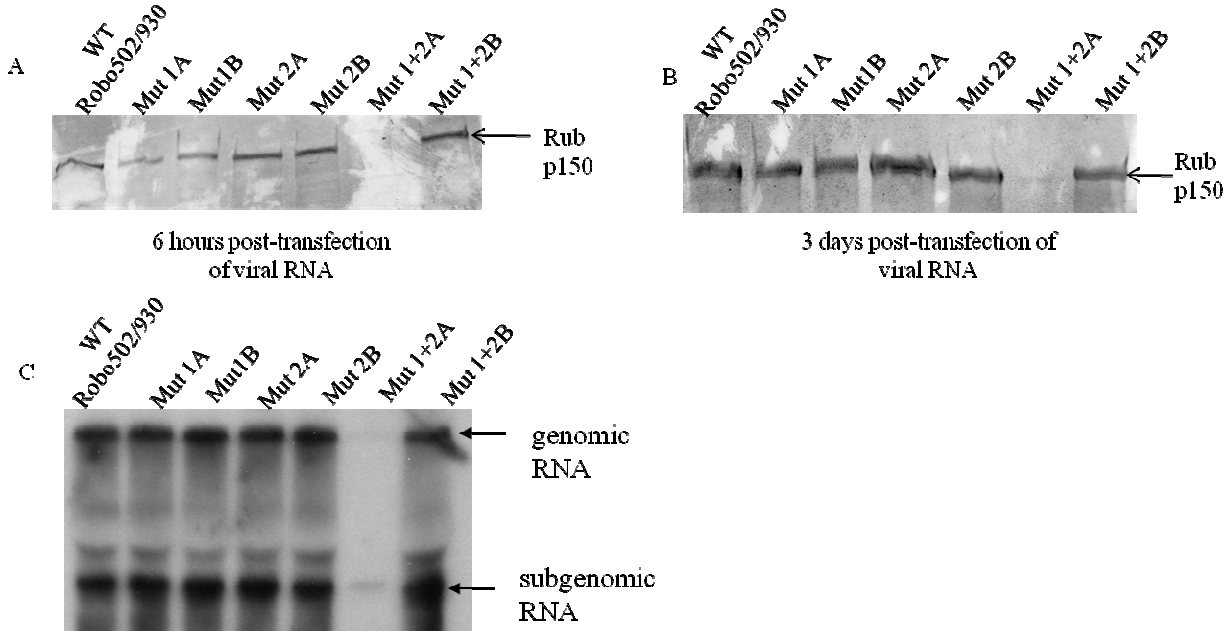

Figure 3.5. P150 and RNA production by Robo502 wt and mutant RNA.
(A and B). Vero cell were transfected with transcripts from the wild type and mutant Robo502 –930 infectious cDNA clones which contain an HA epitope-tagged P150. Viral RNA transcript from 2 clones of each mutant was used. Lysates of the transfected cells were made at 6 hours and 3 days post-transfection. Proteins in the cells lysates were resolved by 6% SDS-PAGE followed by Western blot analysis using mouse monoclonal anti-HA antibody. (C) Vero cells transfected with transcripts from wild type and mutant Robo502-930 infectious cDNA clones were harvested 3 days post-transfection and total cell RNA was extracted and resolved on a 1% agarose gel followed by Northern blotting probed with VR-C-E2-E1 (see Materials and Methods)

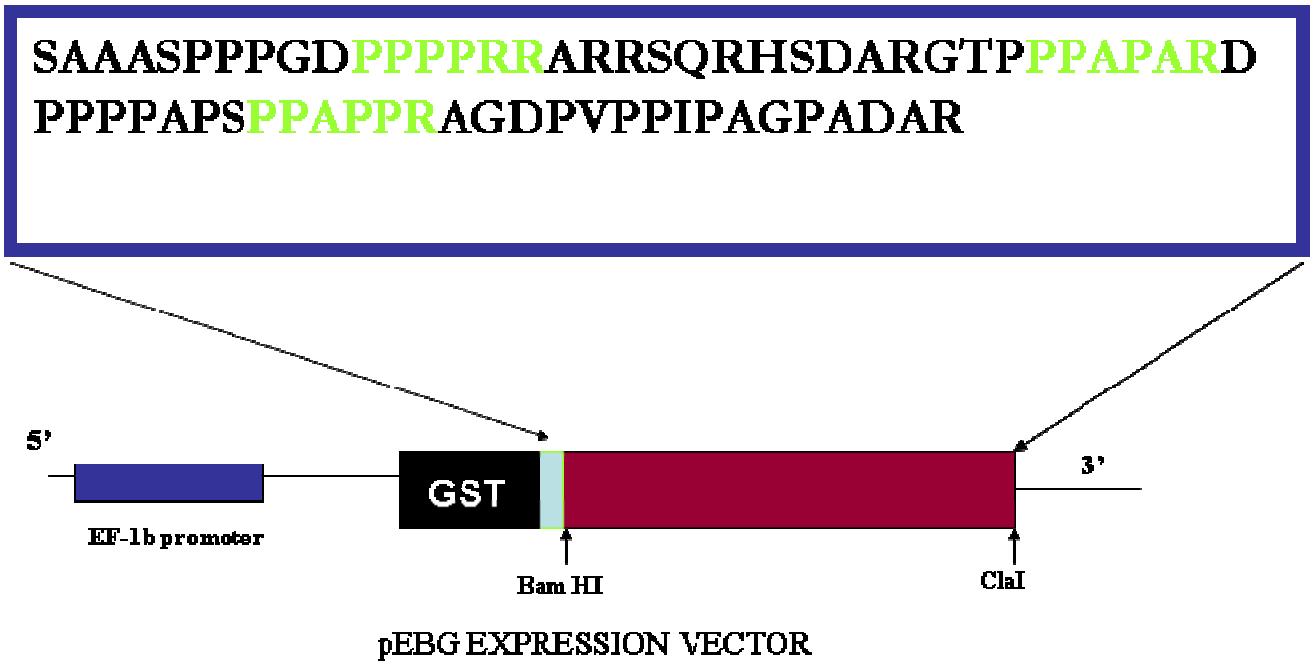

Figure 3.6. GST-PRR expression vector.
The P150 PRR was cloned into the pEBG mammalian expression vector between the Bam HI and Cla I restriction sites as shown to produce a GST-PRR fusion protein when expressed in transfected 293T human embryonic kidney cells.

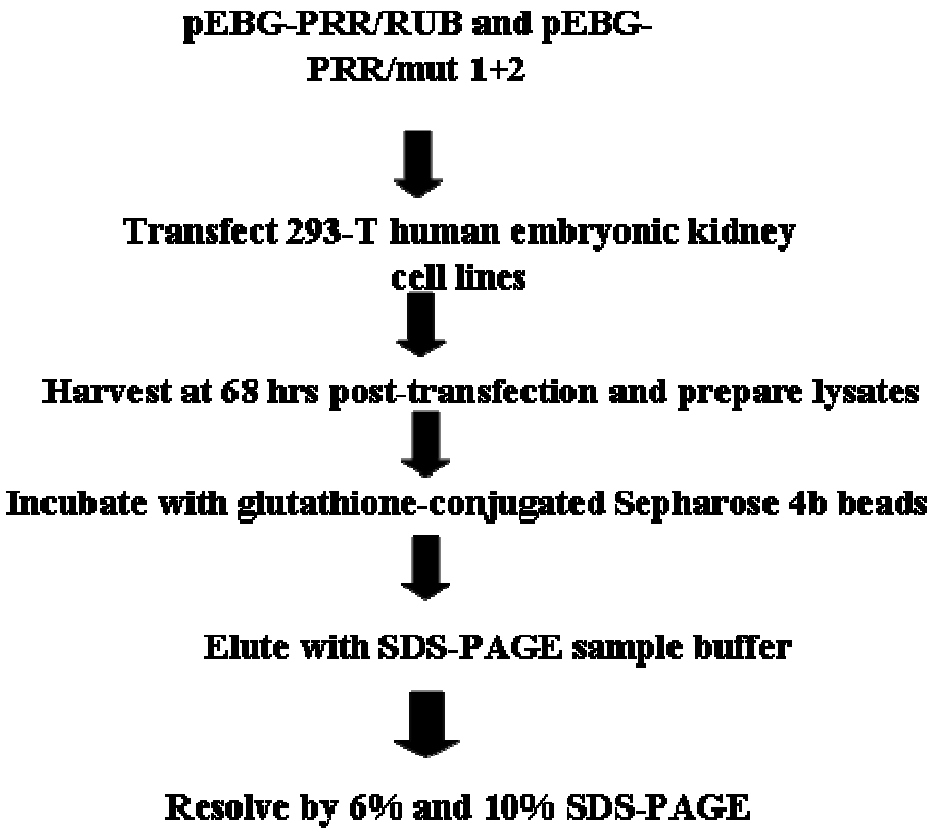

Figure 3.7. Schematic of procedure used to identify proteins interacting with GST-PRR fusion protein.

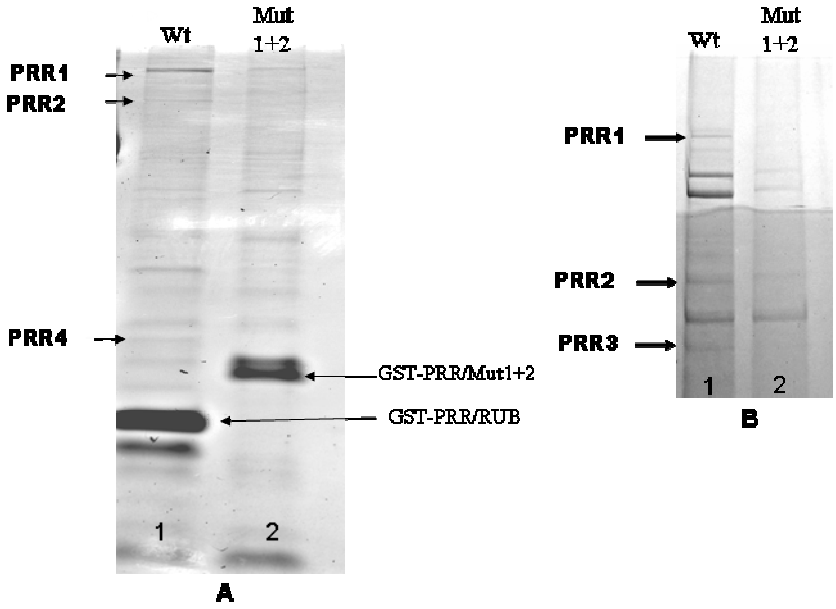

Figure 3.8. Resolution of cell proteins interacting with pGST-PRR and pGST-PRR-MUT 1+2 fusion proteins.
293-T cells were transfected with the wild type (pGST-PRR/RUB (lane 1) or mutant (pGST-PRR/RUB-Mut1+2)(lane 2) GST fusion protein expression constructs and lysates were prepared 68 hours post-transfection and incubated with gluthathione sepharose 4B beads. Bound proteins were eluted and resolved by 10% SDS-PAGE (Panel A) or 6% SDS-PAGE (Panel B). Proteins that bound to the wt fusion protein but not to the mutant fusion protein (PRR1-PRR4) were excised and identified by trypsin digestion and mass spectroscopy.

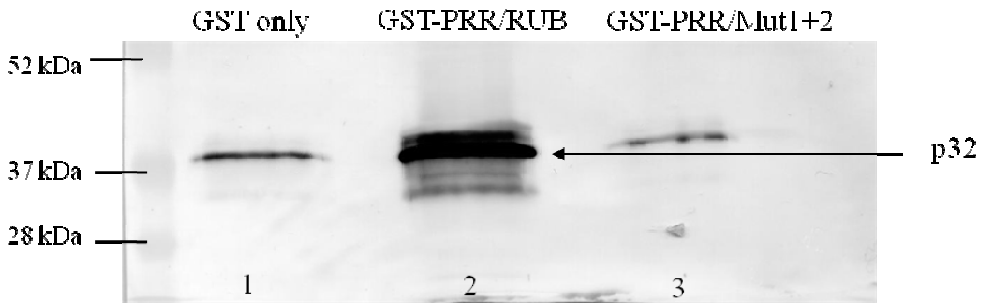

Figure 3.9. Interaction of GST-PRR fusion proteins with host cell protein p32/HABP1/gC1qR.
293-T cell lines were transfected with pEBG, wild type GST-PRR/RUB or mutant GST-PRR/Mut1+2 vector DNA. Three days post-transfection, the cells were lysed, and the GST or GST-PRR proteins and interacting cell proteins were isolated on glutathione sepharose 4B and resolved by 10% SDS-PAGE followed by Western blotting probed with polyclonal rabbit anti-p32 antibody. As can be seen, p32 interacted with the wt GST-PRR/RUB fusion protein, but not the GST-PRR/Mut1+2 fusion protein or the control GST protein. Additional bands below arrow indicating p32 could be degradative products of p32.

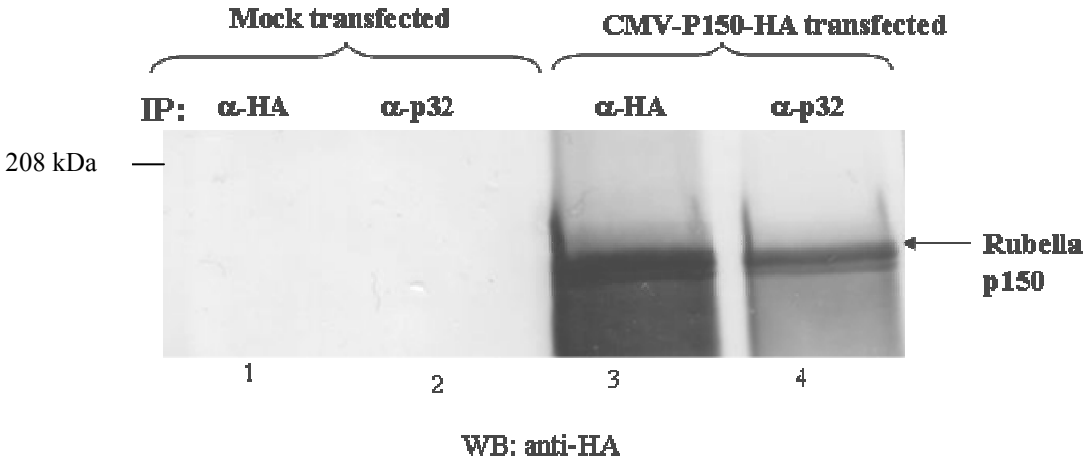

Figure 3.10. Co-immunoprecipitation of expressed P150 with endogenous p32.
Vero cells were either mock-transfected (lanes 1 and 2) or transfected with a plasmid vector (CMV-P150-HA) expressing an HA epitope-tagged P150 (lanes 3 and 4) and lysed two days post-transfection. The lysates were immunoprecipitated with monoclonal mouse anti-HA antibody or rabbit anti-P32 antibody followed by 6% SDS-PAGE and Western blot probed with anti-HA antibody. As can be seen, in the CMV-P150-HA-transfected cells, HA-tagged P150 was immunoprecipitated by both anti HA (control) and anti p32 antibody.

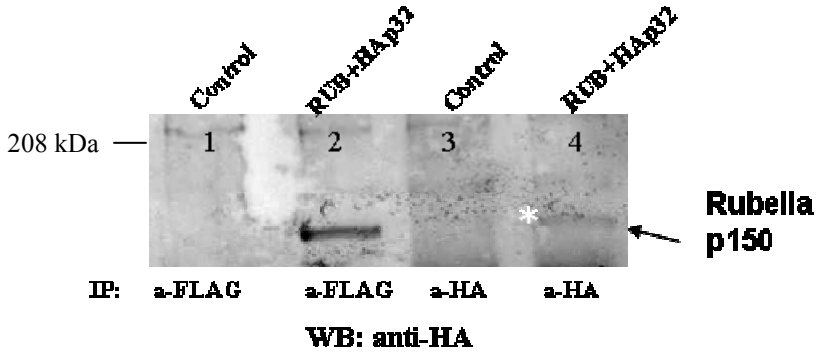

Figure 3.11. Co-immunoprecipitation of expressed p32 and P150 in RUBV-infected cells. Vero cells were mock-transfected (lanes 1 and 3) or infected with Robo502-912 (which expresses a FLAG-tagged P150) and transfected with HA-p32-c-myc (which expresses p32 N- and C-terminally tagged with HA and c-myc epitopes, respectively). Two days post-infection/transfection cells were lysed and samples were immunoprecipitated using monoclonal mouse anti-FLAG or mouse anti-HA antibody followed by 6% SDS-PAGE and Western blot probing with monoclonal mouse anti-FLAG antibody. As can be seen, FLAG-tagged P150 was immunoprecipitated with both anti-FLAG (control) and anti-HA antibody.

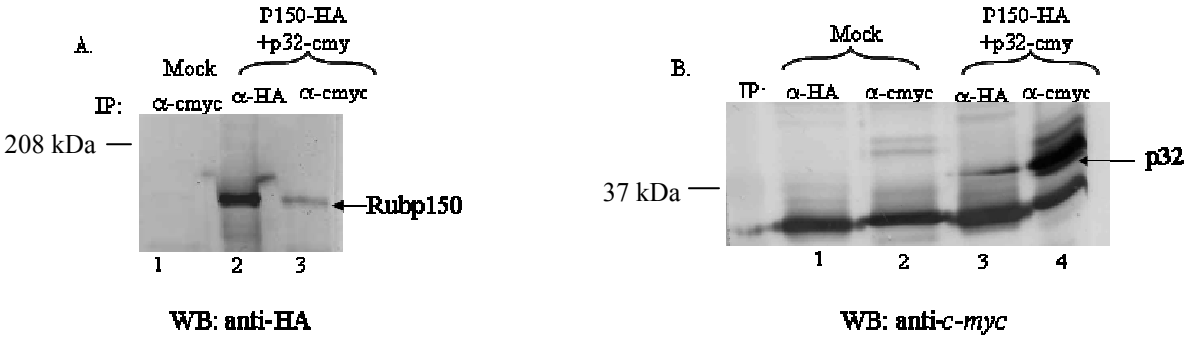

Figure 3.12. Reciprocal co-immunoprecipitation of expressed P150 and p32.
VERO cells were either mock transfected or co-transfected with CMV-P150-HA, which expresses an HA-tagged P150, and p32-c-*myc*, which expresses a C-terminal c-myc tagged p32. Two days post-transfection, the cells were lysed and immunoprecipitated with monoclonal mouse anti-HA or anti-c-myc antibody. Following resolution by 6% and 10% SDS-PAGE, respectively, Western blot analysis was performed using anti-HA (Panel A) or anti-c-myc (Panel B) antibodies. As can be seen, anti HA and anti-c-myc antibodies both immunoprecipiated HA-tagged P150 (Panel A) and, reciprocally, anti c-myc and anti-HA antibodies both immunoprecipitated c-myc tagged p32 (Panel B). Additional band above p32-c-myc in lane 4 may represent a modified p32.

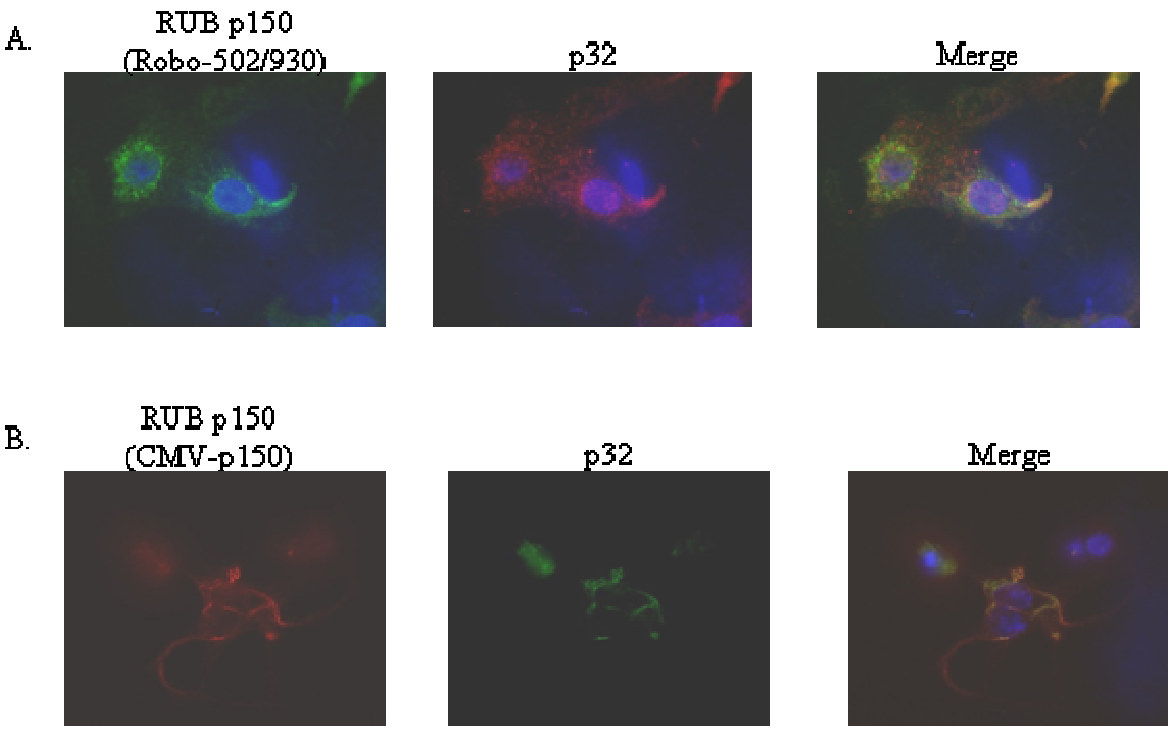

Figure 3.13. Colocalization of endogenous p32 with P150.
A) Vero cells were infected with Robo502-912, which expresses a FLAG epitope tagged P150. Twenty four hours post-infection, the cells were processed for IFA using mouse anti-FLAG antibody (green) and rabbit anti-p32 antibody (red). B) Vero cells were transfected with CMV-P150-HA. Twenty four hours post-infection the cells were processed for IFA using mouse anti-HA antibody (red) and rabbit anti-p32 antibody (green). Hoechst Dye was used to stain nuclear DNA (blue). The cells were visualized using Zeiss Axioplan 2 imaging system at 100X magnification.

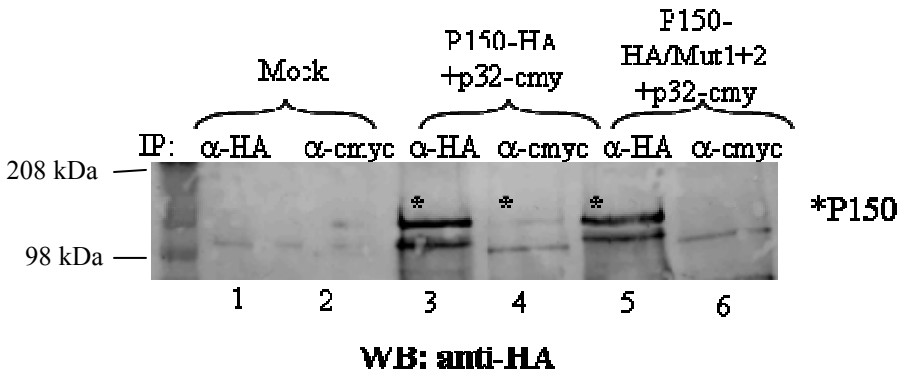

Figure 3.14. Lack of co-immunoprecipitation of p32 with a P150 that has mutated PxxPxR motifs.

Vero cells were mock transfected (lanes 1 and 2), co-transfected with CMV-P150-HA and p32-c-*myc* (lanes 3 and 4) or co-transfected with CMV-P150-HA/Mut1+2 and p32-c-*myc* (lanes 5 and 6). Two days post-transfection, the cells were lysed and the lysates were immunoprecipitated using monoclonal mouse anti-HA (lanes 1, 3, and 5) or mouse anti-c-myc (lanes 2, 4, and 6) antibody. The immunoprecipitated proteins were resolved by 6% SDS-PAGE followed by Western blot analysis probing with anti-HA antibody. As can be seen, wt expressed P150 was co-immunoprecipitated by anti-c-myc antibody while the mutant expressed P150 was not.

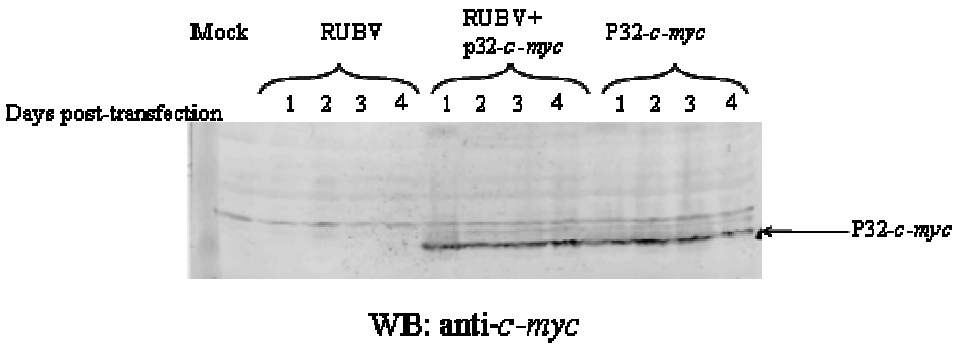

Figure 3.15. Expression of transfected p32-c-myc.
Vero cells were mock transfected or transfected with p32-c-myc and then infected the next day with RUBV, or just transfected with p32-c-myc. On days 1 through post-transfection, cells were lysed and the lysates were resolved by 10% SDS-PAGE followed by Western blot analysis probed with mouse monoclonal anti-c-myc antibody.

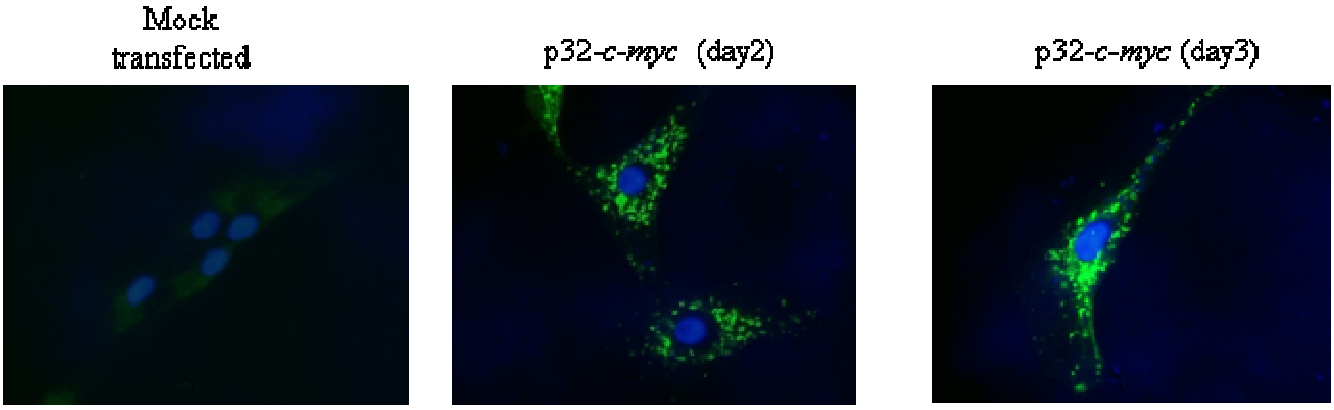

Figure 3.16. Intracellular localization of expressed c-myc tagged p32.
Vero cell lines were mock transfected or transfected with pcDNA-p32-c-*myc*. On days 2 and 3 post-transfection, cells were processed for IFA using anti-c-myc antibody (green). Hoechst Dye was used to stain nuclear DNA (blue). The cells were visualized using a Zeiss Axioplan 2 imaging system under 100X magnification.

Table 3.2. RUBV replication in Vero cells over-expressing p32.

Titer / Experiment	Day 1	Day 2	Day 3	Day 4
RUBV	1×10^5 pfu/ml	1×10^6 pfu/ml	8×10^6 pfu/ml	3×10^6 pfu/ml
RUBV + c-myc-p32	2×10^5 pfu/ml	6×10^6 pfu/ml	8×10^6 pfu/ml	5×10^6 pfu/ml

[1]Vero cells were mock-transfected or transfected with pcDNA-p32-myc and then infected with RUBV (MOI = 1 pfu/cell) the next day. The culture medium was harvested daily and titered by plaque assay. This experiment was done twice and the titers are averaged.